

The Preserve: Lehigh Library Digital Collections

Modeling and process optimization of solder paste stencil printing for micro-BGA and fine pitch surface mount assembly.

Citation

Pan, Jianbiao. *Modeling and Process Optimization of Solder Paste Stencil Printing for Micro-BGA and Fine Pitch Surface Mount Assembly.* 2000, https://preserve.lehigh.edu/lehigh-scholarship/graduate-publications-theses-dissertations/theses-dissertations/modeling-process.

Find more at https://preserve.lehigh.edu/

This document is brought to you for free and open access by Lehigh Preserve. It has been accepted for inclusion by an authorized administrator of Lehigh Preserve. For more information, please contact preserve@lehigh.edu.

INFORMATION TO USERS

This manuscript has been reproduced from the microfilm master. UMI films the text directly from the original or copy submitted. Thus, some thesis and dissertation copies are in typewriter face, while others may be from any type of computer printer.

The quality of this reproduction is dependent upon the quality of the copy submitted. Broken or indistinct print, colored or poor quality illustrations and photographs, print bleedthrough, substandard margins, and improper alignment can adversely affect reproduction.

In the unlikely event that the author did not send UMI a complete manuscript and there are missing pages, these will be noted. Also, if unauthorized copyright material had to be removed, a note will indicate the deletion.

Oversize materials (e.g., maps, drawings, charts) are reproduced by sectioning the original, beginning at the upper left-hand corner and continuing from left to right in equal sections with small overlaps.

Photographs included in the original manuscript have been reproduced xerographically in this copy. Higher quality 6" x 9" black and white photographic prints are available for any photographs or illustrations appearing in this copy for an additional charge. Contact UMI directly to order.

Bell & Howell Information and Learning
300 North Zeeb Road, Ann Arbor, MI 48106-1346 USA
800-521-0600

UMI®

Reproduced with permission of the copyright owner. Further reproduction prohibited without permission.

Reproduced with permission of the copyright owner. Further reproduction prohibited without permission.

Modeling and Process Optimization of Solder Paste Stencil Printing for Micro-BGA and Fine Pitch Surface Mount Assembly

by

Jianbiao Pan

Presented to the Graduate and Research Committee

of Lehigh University

in Candidacy for the Degree of

Doctor of Philosophy

in

Department of Industrial and Manufacturing Systems Engineering

Lehigh University

Feburary 2000

Reproduced with permission of the copyright owner. Further reproduction prohibited without permission.

UMI Number: 9982874

UMI®

UMI Microform 9982874
Copyright 2000 by Bell & Howell Information and Learning Company.
All rights reserved. This microform edition is protected against
unauthorized copying under Title 17, United States Code.

Bell & Howell Information and Learning Company
300 North Zeeb Road
P.O. Box 1346
Ann Arbor, MI 48106-1346

Reproduced with permission of the copyright owner. Further reproduction prohibited without permission.

Approved and recommended for acceptance as a dissertation in partial fulfillment of the requirements for the degree of Doctor of Philosophy.

February 11, 2000

Date

Dr. Gregory L. Tonkay, Associate Professor, Lehigh University,

Dissertation Advisor and Chairman of the Committee

March 10, 2000

Accepted Date

Dr. Mikell P. Groover, Professor, Lehigh University

Dr. Robert H. Storer, Professor, Lehigh University

Dr. Manoj K. Chaudhury, Associate Professor,
Lehigh University

Dr. J. Rene Villalobos, Associate Professor,
Arizona State University

Reproduced with permission of the copyright owner. Further reproduction prohibited without permission.

Acknowledgments

I would like to thank Randy Hume of Visteon and Thomas Green of the National Training Center for Microelectronics at Northampton Community College for the fruitful discussions on the screen printing process and introducing me to the electronics manufacturing industry. Thanks to John Todora of the National Training Center for Microelectronics for his help in using the measurement equipment. I wish to thank Visteon for the partial support of the research project and the use of equipment in conducting the experiments. Special thanks to Ronald M. Sallade and David J. Leandri of Visteon for working with me on the solder paste stencil printing experiment.

I would like to thank Prof. Mikell P. Groover, Prof. Robert H. Storer, Prof. Manoj K. Chaudhury, and Prof. J. Rene Villalobos for their support and suggestions as members of my doctoral committee. Thanks to Prof. Robert H. Storer for valuable discussion on the design and analysis of experiments. A special thanks to Prof. Gregory L. Tonkay, dissertation advisor, for his encouragement, guidance, support and kindly help throughout the project.

Thanks to IMAPS, NSF, Department of Industrial & Manufacturing Systems Engineering of Lehigh University, and Prof. Tonkay for providing travel grants for 4 international conferences.

Finally, I would like to thank my wife Nianpin Cheng for her assistance, endurance, encouragement and devotion throughout the past three and a half years.

Reproduced with permission of the copyright owner. Further reproduction prohibited without permission.

Tables of Content

LIST OF FIGURES ..... **VII**

LIST OF TABLES ..... **X**

ABSTRACT **1**

1 INTRODUCTION **3**

1.1 ELECTRONIC PACKAGING AND ITS TRENDS 3

1.1.1 Packaging for Through-hole Technology *4*

1.1.2 Surface Mount Technology and Fine Pitch *5*

1.1.3 Packaging for Surface Mount Technology *6*

1.1.4 Direct Chip Attach *8*

1.2 EFFECTS OF HIGH DENSITY PACKAGING ON SMT MANUFACTURING PROCESS 9

1.3 SCREEN PRINTING VS. STENCIL PRINTING 10

1.4 OBJECTIVES OF RESEARCH 13

1.5 LIMITATIONS OF RESEARCH 14

2 LITERATURE REVIEW **15**

2.1 THE STENCIL PRINTING PROCESS 15

2.2 EXPERIMENTAL WORK ON STENCIL PRINTING 18

2.2.1 Effects of the Stencil *18*

2.2.2 Effects of the Solder Paste *20*

2.2.3 Effects of the Process Variables *21*

2.2.4 Effects of the Squeegee *22*

2.2.5 Effects of the Substrate *23*

2.2.6 Effects of the Printing Machine *24*

Reproduced with permission of the copyright owner. Further reproduction prohibited without permission.

2.3 THEORETICAL WORK ON THE STENCIL PRINTING PROCESS 24

2.3.1 Rheological Behavior *24*

2.3.2 Streamline Pattern of Paste in Front of the Squeegee *28*

2.3.3 Aperture Filling Process *30*

2.3.4 Release Process *31*

2.4 SUMMARY 32

3 MODELING OF THE SOLDER PASTE STENCIL DEPOSITION PROCESS 33

3.1 NOMENCLATURE 34

3.2 THE HYDRODYNAMICS OF THE PASTE TRAVEL PROCESS 35

3.3 THE APERTURE FILLING PROCESS 39

3.4 PASTE TRANSFER RATIO VS. ASPECT RATIO 41

3.5 PRINTING PERPENDICULAR VS. PARALLEL APERTURES 42

3.6 SUMMARY 45

4 DESCRIPTION OF EXPERIMENTAL PROCEDURE 47

4.1 DESCRIPTION OF THE EXPERIMENT 47

4.2 GAUGE REPEATABILITY & REPRODUCIBILITY STUDY FOR A 3-D SOLDER PASTE INSPECTION SYSTEM 54

4.2.1 Introduction *54*

4.2.2 Gauge Accuracy, Repeatability, and Reproducibility *54*

4.2.3 Absolute Measurement & Relative Measurement *56*

4.2.4 Analysis Method *56*

4.2.5 Triangulation Principle *57*

4.2.6 Gauge Repeatability Analysis of a 3-D Solder Paste Inspection System *60*

4.2.7 Conclusions *65*

5 ANALYSIS AND DISCUSSION OF RESULTS 66

Reproduced with permission of the copyright owner. Further reproduction prohibited without permission.

5.1 RESIDUAL CHECK 66
5.2 ANALYSIS OF THE DATA 77
5.2.1 Effects of Aperture Size and Stencil Thickness *77*
5.2.2 Effects of Aperture Orientation *89*
5.2.3 Effects of Solder Paste and Print Speed *91*
5.2.4 Effects of Board Finish *93*
5.3 CONCLUSIONS 95
6 CONCLUSIONS AND FUTURE RESEARCH 96
6.1 CONCLUSIONS 96
6.2 IMPORTANT CONTRIBUTIONS 98
6.3 FUTURE RESEARCH 100
BIBLIOGRAPHY 101
VITA 107

Reproduced with permission of the copyright owner. Further reproduction prohibited without permission.

List of Figures

FIGURE 1-1 WORLDWIDE IC PACKAGE USAGE TREND 4

FIGURE 1-2 SCHEMATIC DIAGRAM OF THE SCREEN PRINTING PROCESS 12

FIGURE 2-1 SCHEMATIC OF THE STENCIL PRINTING PROCESS 15

FIGURE 2-2 FACTORS THAT INFLUENCE THE STENCIL PRINTING PROCESS 17

FIGURE 2-3 SHEAR STRESS VS. SHEAR RATE FOR DIFFERENT FLUIDS 26

FIGURE 2-4 VISCOSITY VS. SHEAR RATE FOR DIFFERENT FLUIDS 27

FIGURE 3-1 FLOW BETWEEN THE SQUEEGEE AND THE STENCIL 35

FIGURE 3-2 STREAMLINE (A: THE MODEL; B: RIEMER'S MODEL) 37

FIGURE 3-3 APERTURE FILLING MECHANISM 44

FIGURE 4-1 TEST PATTERN OF STENCILS AND FR-4 BOARDS 50

FIGURE 4-2 RHEOLOGY OF SOLDER PASTE TYPE 3 AND TYPE 4 53

FIGURE 4-3 LASER TRIANGULATION 59

FIGURE 4-4 BOARD WARPAGE WITH LOCAL REFERENCE HEIGHTS AND SOLDER PAD 59

FIGURE 4-5 REPEATABILITY OF THE SOLDER DEPOSIT VOLUME 62

FIGURE 4-6 REPEATABILITY OF THE SOLDER DEPOSIT AREA 62

FIGURE 4-7 REPEATABILITY OF THE SOLDER DEPOSIT AVERAGE HEIGHT 63

FIGURE 4-8 REPEATABILITY OF THE SOLDER DEPOSIT VOLUME 63

FIGURE 4-9 REPEATABILITY OF THE SOLDER DEPOSIT AREA 64

FIGURE 4-10 REPEATABILITY OF THE SOLDER DEPOSIT AVERAGE HEIGHT 64

FIGURE 5-1 NORMAL PROBABILITY PLOT FOR RESIDUALS OF QFP SOLDER DEPOSITED VOLUME 67

FIGURE 5-2 PLOT OF RESIDUAL VERSUS PREDICTED VALUES FOR SOLDER DEPOSITED VOLUME OF QFP 67

FIGURE 5-3 PLOT OF RESIDUAL VERSUS EXPERIMENTAL SEQUENCE FOR QFP SOLDER DEPOSITED VOLUME .. 68

FIGURE 5-4 PLOT OF RESIDUAL VERSUS PITCH (APERTURE WIDTH) FOR QFP SOLDER DEPOSITED VOLUME ... 70

FIGURE 5-5 PLOT OF RESIDUAL VERSUS STENCIL THICKNESS FOR QFP SOLDER DEPOSITED VOLUME 70

Reproduced with permission of the copyright owner. Further reproduction prohibited without permission.

FIGURE 5-6 PLOT OF RESIDUAL VERSUS APERTURE SHAPE FOR QFP SOLDER DEPOSITED VOLUME 71
FIGURE 5-7 PLOT OF RESIDUAL VERSUS BOARD FINISH FOR QFP SOLDER DEPOSITED VOLUME 71
FIGURE 5-8 PLOT OF RESIDUAL VERSUS SOLDER TYPE FOR QFP SOLDER DEPOSITED VOLUME 72
FIGURE 5-9 PLOT OF RESIDUAL VERSUS PRINT SPEED FOR QFP SOLDER DEPOSITED VOLUME..... 72
FIGURE 5-10 NORMAL PROBABILITY PLOT FOR RESIDUALS OF BGA SOLDER DEPOSITED VOLUME..... 73
FIGURE 5-11 PLOT OF RESIDUAL VERSUS PREDICTED VALUES FOR SOLDER DEPOSITED VOLUME OF BGA..... 73
FIGURE 5-12 PLOT OF RESIDUAL VERSUS EXPERIMENTAL SEQUENCE FOR BGA SOLDER DEPOSITED VOLUME 74
FIGURE 5-13 PLOT OF RESIDUAL VERSUS PITCH (APERTURE WIDTH) FOR BGA SOLDER DEPOSITED VOLUME 74
FIGURE 5-14 PLOT OF RESIDUAL VERSUS STENCIL THICKNESS FOR BGA SOLDER DEPOSITED VOLUME..... 75
FIGURE 5-15 PLOT OF RESIDUAL VERSUS BOARD FINISH FOR BGA SOLDER DEPOSITED VOLUME 75
FIGURE 5-16 PLOT OF RESIDUAL VERSUS PRINT SPEED FOR BGA SOLDER DEPOSITED VOLUME..... 76
FIGURE 5-17 PLOT OF RESIDUAL VERSUS SOLDER TYPE FOR BGA SOLDER DEPOSITED VOLUME 76
FIGURE 5-18 INTERACTION PLOT OF QFP APERTURE SIZE AND STENCIL THICKNESS..... 80
FIGURE 5-19 INTERACTION PLOT OF BGA APERTURE SIZE AND STENCIL THICKNESS..... 80
FIGURE 5-20 TRANSFER RATIO VS. PITCH FOR QFP APERTURES 85
FIGURE 5-21 TRANSFER RATIO VS. PITCH FOR BGA APERTURES 85
FIGURE 5-22 COMPARISON OF THE MODEL AND EXPERIMENTAL RESULTS (POINTS: THE OVERALL AVERAGE OF EXPERIMENTAL DATA THAT HAVE THE SAME AREA RATIO; LINE: MODEL)..... 87
FIGURE 5-23 COMPARISON OF THE MODEL AND EXPERIMENTAL RESULTS (POINTS: THE AVERAGE OF EXPERIMENTAL DATA THAT HAVE THE SAME AREA RATIO IN DIFFERENT EXPERIMENTAL RUNS AND DIFFERENT QFP APERTURE SHAPES; LINE: MODEL)..... 88
FIGURE 5-24 SOLDER VOLUME VS. APERTURE ORIENTATION 90
FIGURE 5-25 INTERACTION PLOT OF SOLDER TYPE AND PRINT SPEED FOR QFP APERTURES 92
FIGURE 5-26 INTERACTION PLOT OF SOLDER TYPE AND PRINT SPEED FOR BGA APERTURES 92
FIGURE 5-27 TRANSFER RATIO VS. BOARD FINISH FOR QFP APERTURES 94

Reproduced with permission of the copyright owner. Further reproduction prohibited without permission.

FIGURE 5-28 TRANSFER RATIO VS. BOARD FINISH FOR BGA APERTURES 94

Reproduced with permission of the copyright owner. Further reproduction prohibited without permission.

List of Tables

TABLE 1-1 EVOLUTION OF ELECTRONICS PACKAGING 9

TABLE 1-2 INDUSTRY CAPABILITY FOR FINE LINE SCREEN PRINTING 12

TABLE 3-1 PRESSURE AND SHEAR STRESS VS. SQUEEGEE ANGLE 39

TABLE 4-1 INPUT VARIABLES AND THEIR LEVELS 48

TABLE 4-2 APERTURE SIZES OF A STENCIL (UNIT: MIL = 0.0254MM) 48

TABLE 4-3 SOLDER PASTE SPECIFICATION 48

TABLE 4-4 RANDOMIZED 2^4 FACTORIAL DESIGN MATRIX 51

TABLE 4-5 PROCESS VARIABLES 53

TABLE 5-1 ANOVA FOR QFP SOLDER DEPOSITED VOLUME 78

TABLE 5-2 ANOVA FOR BGA SOLDER VOLUME 79

TABLE 5-3 ANOVA FOR QFP SOLDER TRANSFER RATIO 82

TABLE 5-4 ANOVA FOR BGA SOLDER TRANSFER RATIO 83

TABLE 5-5 AREA RATIO (AAR) AND APERTURE VOLUME 84

Reproduced with permission of the copyright owner. Further reproduction prohibited without permission.

Abstract

The need for higher pin count, higher performance, smaller size and lighter weight has driven the development of advanced packages such as Quad Flat Package (QFP), Ball Grid Array (BGA), Chip Scale Package (CSP), and Flip Chip. These high-density electronic packages have had a tremendous impact on board-level assembly. One of the main challenges continues to be the solder paste deposition process and, specifically, controlling the amount of solder paste deposited. Stencil printing is one of the most cost-effective processes for solder paste deposition and it has been widely used in traditional surface mount assembly. However, the solder paste stencil printing process is still not completely understood as indicated by the fact that industry reports 52 - 71% of fine pitch and ultra-fine pitch SMT defects are related to the solder paste stencil printing process.

The objective of this research was to understand and optimize the solder paste stencil printing process. An analytical model was developed using fluid mechanics theory. The paste flow pattern in front of the squeegee was studied and the volume of paste through the aperture was calculated. The relationship between transfer ratio and area ratio was derived. This model explains two experimental phenomena. One is that increasing stencil thickness does not necessarily lead to thicker deposits. The other is that perpendicular apertures print thicker than parallel apertures.

An experiment was designed and conducted to validate the model and to investigate the effects of relevant process parameters on the amount of solder paste

Reproduced with permission of the copyright owner. Further reproduction prohibited without permission.

deposited. The factors selected in the experiment are aperture size, aperture shape, board finish, stencil thickness, solder type, and print speed. The deposited solder paste was measured by an automatic laser-based 3-D triangulation solder paste inspection system. The gauge repeatability & reproducibility (R&R) of the inspection system was evaluated.

The experimental data were analyzed by Analysis of Variance (ANOVA). The critical variables were identified and interactions between process variables were determined. The experimental results are shown to be consistent with the theoretical model. This study will help to accelerate the development and utilization of BGA, CSP and flip chip packages.

Reproduced with permission of the copyright owner. Further reproduction prohibited without permission.

1 Introduction

1.1 Electronic Packaging and its Trends

Electronic packaging can be divided into two categories: the assembly of the Integrated Circuit (IC) or multiple ICs into a package, and the assembly of the IC or packaged IC to the Printed Circuit Board (PCB). Examples of the first category (called chip level packaging) include the dual in-line package (DIP), pin grid array (PGA), chip carrier (CC), small outline (SO), quad flat package (QFP), ball grid array (BGA), multichip modules (MCM), chip scale packages (CSP) and micro ball grid array (mBGA or Micro-BGA, or μBGA). Examples of the latter category (called board level packaging) include through-hole (TH) technology, surface mount technology (SMT), and direct chip attach (DCA).

The major forces driving electronic packaging and interconnection are accelerating demand for lighter weight, smaller size, lower cost, higher performance and higher reliability. The market drivers are computer, telecommunications, consumer products, military and the automotive industry. With a growing need for denser packaging and higher pin count, electronic packaging and interconnection has evolved from through-hole technology to surface mount technology (SMT) and direct chip attach (DCA).

Reproduced with permission of the copyright owner. Further reproduction prohibited without permission.

Figure 1-1 shows recent worldwide electronic package trends [Brathwaite, 1998]. It is predicted that during the period 1996 - 2006, production of through-hole PCB will decrease from 40% to less than 10%. During the same time frame, SMT will increase from 53% up to 66%. Direct chip attach (DCA) will grow from 7% to 24%.

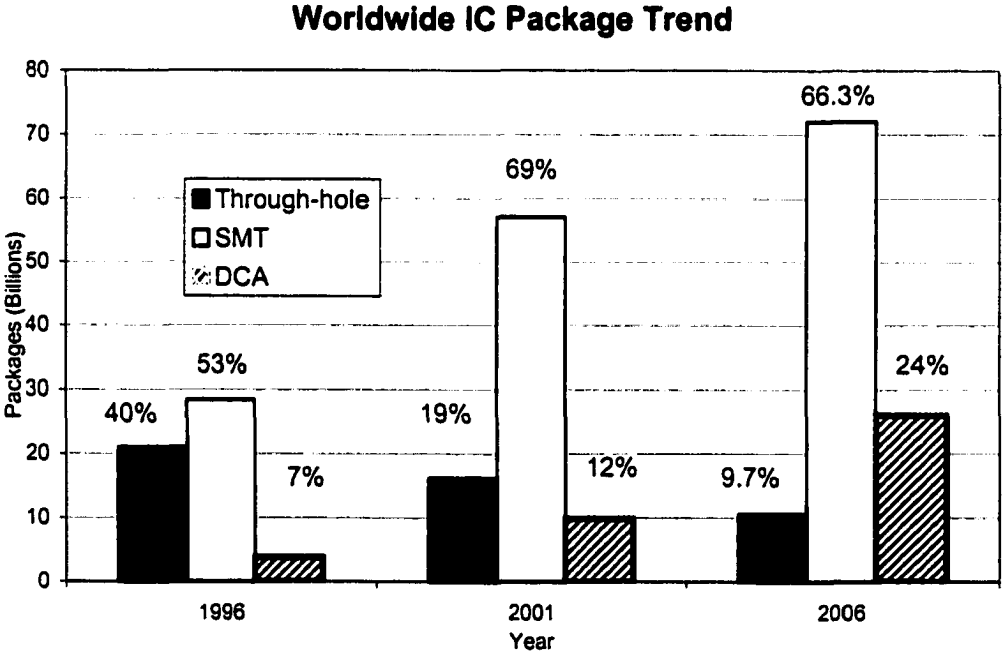


Figure 1-1 Worldwide IC package usage trend

1.1.1 Packaging for Through-hole Technology

DIP was the most common package for multi-lead through-hole components until the early 1980s. The standard DIP pitch (distance between the center of two adjacent leads) is 2.5 mm (100 mil). The most common lead or input/output (I/O) number for the DIP package is 8, 14, 16, 24, or 40 [Landers, et al., 1994]. Another through-hole package designed for high pin count is PGA. The pitch of PGA ranges from 2.5 mm (100 mil) to

Reproduced with permission of the copyright owner. Further reproduction prohibited without permission.

1.25 mm (50 mil), and the number of I/O is normally larger than 50.

As the products get smaller and more complex, the components get smaller and more complex. This requires high surface connection density such as 200 ~ 500 I/Os per square inch. Conventional peripheral through-hole packages are difficult to handle when average surface connection density is larger than 150 connections per square inch [Grasso, 1994]. This accounts for the trend in electronic packaging and interconnection away from through-hole technology and toward SMT.

1.1.2 Surface Mount Technology and Fine Pitch

Surface mount technology (SMT) can be defined as the placement and attachment of surface mount components directly onto a land or pad on the substrate via a solder joint. In contrast, conventional through-hole technology is where the lead of the component is connected to the substrate via a through-hole insertion and solder joint. Through-hole technology commonly uses the wave soldering process to connect IC leads electronically to the PCB while SMT uses reflow soldering.

SMT was first introduced in military and aerospace electronic applications during the mid - 1960s in order to achieve the highest electronic densities and performances. Typically, a board design with surface mount devices can be 20 to 60 percent smaller than the "same" board designed with plated through-hole components [Shaw and Devos, 1998]. Today SMT has been used in almost all types of electronic products from satellites to automobiles and computers to home appliances. [Capillo, 1990].

Pitch refers to the distance between the center of two adjacent leads. There are

Reproduced with permission of the copyright owner. Further reproduction prohibited without permission.

two definitions of fine pitch. One is defined by the Institute for Interconnecting and Packaging Electronic Circuits (IPC) as leads from 0.1 mm to 0.5 mm (4 - 20 mils) (SMC-TR-001). The other is proposed by a printed circuit board consortium calling itself the "October Group" as a pitch of 1.0 - 0.5 mm (40 - 20 mils), and ultra fine pitch for pitches of less than 0.5 mm (20 mils) [Hutchins, 1996]. The latter definition of fine pitch and ultra fine pitch has been popularly used, and will be used accordingly in this dissertation.

1.1.3 Packaging for Surface Mount Technology

IC packages for surface mount technology include SO, CC, QFP, and BGA. Small outline packages (SO or SOIC) typically occupy 30 - 50% less area and have 70 % less thickness than an equivalent DIP. The standard lead pitch of SO is 1.3 mm (50 mil). Chip carriers have two classes: the plastic leaded chip carrier (PLCC) and the ceramic leaded chip carrier (CLCC). The Joint Electronic Device Engineering Council (JEDEC) standardized the CC with a pitch of 1.3 mm (50 mil) and 1.0 mm (40 mil). The number of I/O generally ranges from 16 to 150. Comparing SO with CC, SO is more space efficient for I/O counts less than 20 while CC is more space efficient for I/O counts of 28 or more [Landers, et al., 1994].

With a growing need for denser packaging and higher pin count, surface mount technology (SMT) has evolved from standard SMT to fine pitch SMT and ultra fine pitch SMT. Packages for fine pitch and ultra-fine pitch SMT include QFP and BGA. For example, the use of fine pitch SMT components is expanding dramatically increasing from 12% in 1989 to 26% in 1991 [Grasso, 1994].

Reproduced with permission of the copyright owner. Further reproduction prohibited without permission.

QFP is a package with "gull wing" leads. Normally it has lead counts from 80 to 304 and pitches of 0.80 mm (31 mil), 0.63 mm (25 mil), and 0.5 mm (20 mil). QFP may be less expensive and easier to utilize compared to other packages and assembly technology today due to the high volume in use and the maturity of the technology. [Brathwaite, 1998].

The advent of mobile telephones, pagers, and notebook computers has brought interconnection miniaturization to new levels. These products typically require from 100 to 300 interconnections per square inch of PCB space - a significant increase to the 30 to 60 connections per square inch required by a desktop personal computer [Brathwaite, 1998]. These newer, stricter requirements have accelerated BGA to become one of the leading technologies.

The BGA package is a square or rectangular component, and its bottom has a series of solder balls on a particular input/output (I/O) grid pattern. BGA has the significant advantage of smaller physical size per I/O count over QFP. For example, a 208-pin QFP with 0.5 mm (20 mil) pitch has a density of 12.72 mm^3/lead; a 225-pin BGA with 1.27 mm (50 mil) pitch has a density of 6.85 mm^3/lead - a reduction of 46% [Lau, 1996]. Though BGA offers density, performance, and handling advantages compared to QFP, it is more expensive than QFP. For example, the 208-pin PQFP (Plastic Quad Flat Package) can be purchased for less than one penny per lead (about $1.80) - 30 to 50 percent lower than a comparable pin count BGA. BGA is considered cost effective when I/O counts are above 240 [Ewanich, 1997]. Therefore, BGA is an excellent package choice for pin-count larger than 256. BGA for surface mount assembly

Reproduced with permission of the copyright owner. Further reproduction prohibited without permission.

normally refers to a pitch level of 0.6 mm (25 mil) to 1.27 mm (50 mil). BGA with a pitch of less than 0.5 mm (20 mil) is called micro-BGA.

1.1.4 Direct Chip Attach

An emerging technology in electronics packaging that offers the greatest density is direct chip attach (DCA). DCA is defined as directly attaching the chip (without a package) on the printed circuit board (PCB) with any materials and methods. (Lau, et al. 1998). DCA includes flip chip (FC) and chip on board (COB).

COB is where the IC chip is mounted directly to the surface, usually using a conductive epoxy. The electrical interconnection is made by wire bonding the chip to the PCB. The chip and wire bond patterns are encapsulated with a polymer to protect the wire bonds. However, because of the cost and infrastructure in supplying the known good die (KGD) and the cost and availability of the corresponding fine line (2 mil) and spacing printed circuit board, this process has not achieved widespread use. Instead, a class of new packaging technology called chip scale packaging (CSP) has appeared (Lau, et al. 1998).

CSP is defined as packaged ICs where the footprint of the package is no more than 20 percent of the area of the original die size, and directly surface mountable (IPC J-STD-012). CSP such as micro-BGA can be considered an intermediate step between BGA and DCA.

Flip chip is perhaps the most efficient assembly process. In the flip chip assembly, the IC chip, which has solder balls bonded to the interconnection terminals, is flipped to

Reproduced with permission of the copyright owner. Further reproduction prohibited without permission.

face down and is mounted directly to the PCB. This assembly process is also called C4 (controlled collapse chip connect), which was introduced by IBM in 1964. The popularly used term "flip chip" now includes the assembly of CSPs. Solder bumps used in FC are 100 ~ 250 μm in diameter and 50 ~ 200 μm high. Table 1-1 summaries the evolution of electronic packaging.

Table 1-1 Evolution of electronics packaging

Board level Assembly	Through-hole technology	SMT		DCA	
		Traditional	Fine Pitch	Flip Chip	COB
Package type	DIP PGA	SO CC	QFP BGA	CSP mBGA	Bare chip wire bond
Pitch (mm)	DIP (2.5) PGA (1.27~2.5)	SO (1.27) CC (1.0~1.27)	QFP (0.3~0.8) BGA(0.5~1.27)	0.2 ~ 0.5	-
Application		Satellite, Automobile, Airplanes, Desktop computer	Mobil phone, Notebook computer	Digital cameras, Mobil phone	Calculator, Watches, Portable consumer
Years	1970s	1980s	1990s	2000	
No. of I/O	<150	100 ~ 200	200 ~ 500	>300	>300

1.2 Effects of High Density Packaging on SMT Manufacturing Process

These high-density packages have created a tremendous impact on board-level assembly. Surface mount assembly processes include screen/stencil printing, pick and place, solder reflow, and inspection and test. Fine pitch assembly challenges all of processes and materials. Lau (1994) overviewed the economics, design, material process,

Reproduced with permission of the copyright owner. Further reproduction prohibited without permission.

equipment, quality, and reliability issues of fine pitch assembly. Among these, one of the main challenges continues to be the solder paste stencil printing process and, specifically, controlling the amount of solder paste deposited.

In the late 1980s, research results showed that 65% of all surface mount defects were attributed to the printing process. That figure (for traditional SMT assembly) dropped to 16% in 1994 due to the hard work of many researchers and engineers and engineering innovation [Hall, 1997]. For fine pitch SMT assembly, Clouthier (1999) reported that it is well documented that 52 to 71 percent of SMT defects can be attributed to faults in screen/stencil printing. Brathwaite (1998) stated that: defect levels for 0.65 mm (25 mil) pitch QFPs are 50 to 200 defects per million (DPM); for 0.3 mm (12 mil) pitches defect levels can be as much as an order of magnitude greater. Therefore, the solder paste stencil printing process is still not completely understood.

1.3 Screen Printing vs. Stencil Printing

Screen printing has been the dominant method of thick film deposition because of its low cost. Screen printing roots come from the ancient Chinese art of reproducing paintings. It was first used in electronics during World War II to facilitate the mass production of electronic circuits. [Riemer, 1988]. At that time it was only used to paste conductors. In the 1950's, it was used on plastics, which were parts of radios and TVs, for printing nameplates and instructions. With the occurrence of SMT during the mid- 1960s, screen printing technology began to be widely used to paste conductors, resistors, dielectrics, solder paste, and solder masks.

Reproduced with permission of the copyright owner. Further reproduction prohibited without permission.

The schematic of the screen printing process is shown in Figure 1-2. The screen is supported by the emulsion in the openings. The squeegee pushes down on the screen, causing the screen to come into contact with the pad over the substrate. When the squeegee is moved along the screen surface, it pushes the paste through the openings, which covers the desired areas of the substrate. Screens count on a snap-off distance and the tension of the screen to cause the screen to peel out of the ink after the squeegee has gone by.

With the growing need for denser packaging, screen printing has been refined to yield high resolution prints with various types of thick film inks. Table 1-2 shows industry capability for fine line screen printing [Holden, 1998]. Data indicates that 5 - 10 mil lines and spaces can be mass produced in industry. Some companies can print 3 - 4 mil lines and spaces. Only a few companies have the capability to print 2 mil lines and spaces. This is done in the laboratory and has not been proven for production volumes.

Smaller powder (in the range of a few microns to submicrons) or low viscosity paste is required during screen printing. In addition, thick prints are difficult. These limitations make it difficult to print solder paste using screens with smaller pitch and higher lead count requirements. The main reasons are that solder pastes contain larger particles (in the range of approximately 75 μm to a few microns) and are generally higher in viscosity than thick film inks. Solder paste printing on 1.27 mm (50 mil) pitch pads

Reproduced with permission of the copyright owner. Further reproduction prohibited without permission.

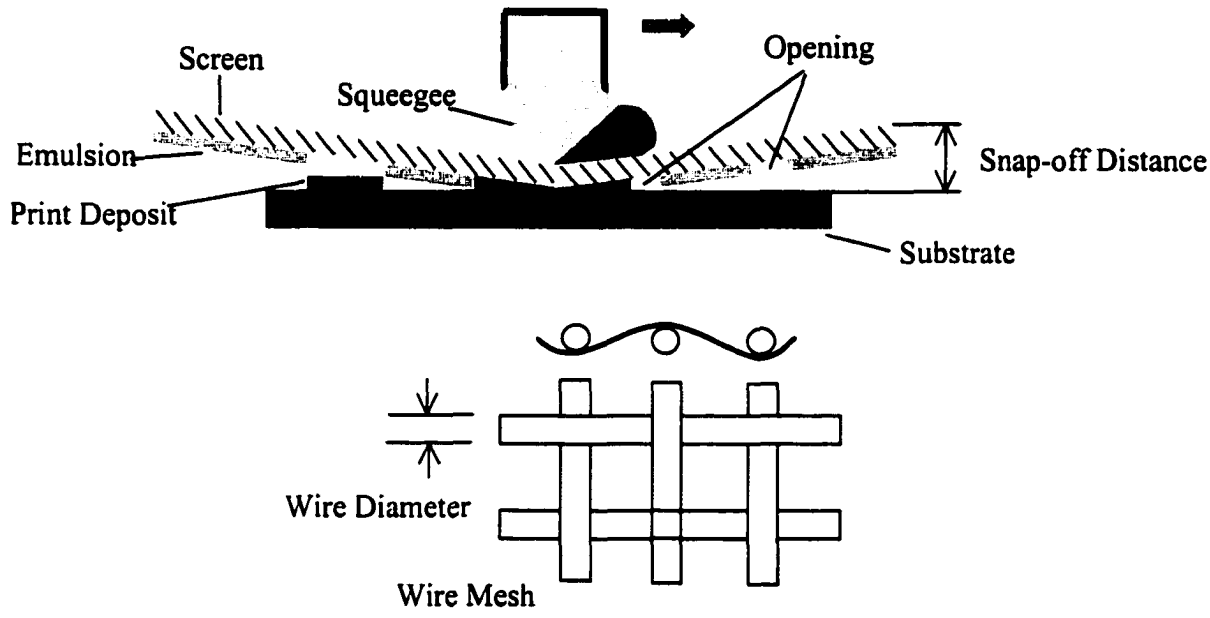


Figure 1-2 Schematic diagram of the screen printing process

Table 1-2 Industry capability for fine line screen printing

Feature	Conventional	Advanced	Leading Edge	State of the Art
Line width (mil)	6	4	3	2
Spacing width (mil)	7	4	3	2

Reproduced with permission of the copyright owner. Further reproduction prohibited without permission.

was easily performed using thick film screens. Today most PCBs contain fine pitch components or ultra-fine pitch components. For example, some PCMIA cards have 0.4 mm (16 mil) pitch components. This trend to smaller pitch and higher lead count has removed the screen from the solder paste printing process and has placed demanding performance criteria on the metal mask stencil. [Coleman, 1997].

Stencil printing was first used to deposit solder paste at IBM Austin in November 1983. [Voss, 1989]. Since then stencil printing has become the dominant method for solder paste deposition. The advantages of stencils are that they have a longer life, can be any size, can use any powder size, and are more robust during printing than screens. The disadvantages of stencils are that they require longer time to produce, have a high cost, provide no gasketing (may smear), and make it difficult to print long lines. Therefore, screens and stencils have their different application areas. Generally thick film uses screens, while SMT solder uses stencils.

There are many variables that affect SMT printing and many experiments in industry have been done to evaluate the process. Because of the complexity of the printing process, and the difficulty of measuring some process variables such as solder paste viscosity and deformed squeegee angle, it is difficult to understand the process by only using experimental data. Therefore, an analytical approach is necessary to understand the mechanisms of the stencil printing process.

1.4 Objectives of Research

The following objectives are proposed for this research project:

Reproduced with permission of the copyright owner. Further reproduction prohibited without permission.

1) Develop an analytical model to explain the mechanisms of the stencil printing process.
2) Identify the critical process variables based on the model.
3) Validate the model by designing and conducting an experiment.
4) Optimize the stencil printing process.

1.5 Limitations of Research

The following limitations exist in order to simplify model development:

1) The solder paste is assumed to be a Newtonian fluid.
2) There is no leakage under the squeegee.
3) The solder paste does not slip on the stencil surface.
4) There is no paste stick at the sidewall of the aperture.

Further explanations of these assumptions will be made in Chapters 3 and 5.

Reproduced with permission of the copyright owner. Further reproduction prohibited without permission.

2 Literature Review

2.1 The Stencil Printing Process

The stencil printing process can be divided into three stages: the paste travel stage (Stage I), the paste deposition stage (Stage II), and the paste release stage (Stage III). In stage I, the squeegee forces the paste roll in front of the squeegee and generates a high pressure. In stage II, the high pressure injects the paste into the stencil aperture. In stage III, the stencil releases, and paste is left on the pad of the PCB. A schematic of the stencil printing process is shown in Figure 2-1.

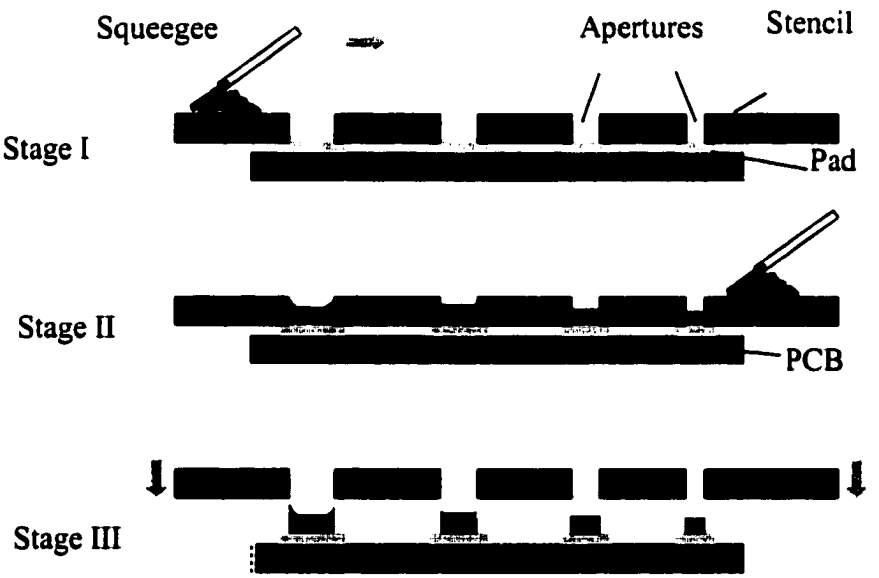


Figure 2-1 Schematic of the stencil printing process

Reproduced with permission of the copyright owner. Further reproduction prohibited without permission.

The components of a stencil printing process include the printer, the substrate, the stencil, the squeegee, the solder paste, and the process parameters. The detailed variables of the above six components that influence the printing process are summarized in Figure 2-2. Since there are many independent variables, an analysis is necessary to determine the critical input variables that affect the output variables. Here the output variables are the volume and its deviation from target volume of deposited solder paste, the area and its deviation from target area of solder paste deposited, and the thickness and its deviation from target thickness of solder paste deposited. Control of the correct volume of paste on the board is essential in order to avoid solder bridges (too much solder paste), and open solder joints (insufficient solder paste). If applied to BGA and FCOB, thickness control is also important to attain low defect levels. Because of the complexity of the printing process, the difficulty of measuring some process variables such as deformed squeegee angle, the constantly changing component technology and new solder paste introduction, the stencil printing process is still not completely understood.

Many experimental investigations on the relationships between the input variables and the output variables have been carried out. The huge empirical database, as a result of experiments, has played an important role in guiding the industry to implement the stencil printing process. Among them, two experimental phenomena have been difficult to understand. One is that increasing stencil thickness does not always increase the thickness of paste deposited (Fujiuchi and Toriyama, 1994; Whitmore, et al., 1997). The other is that perpendicular apertures (longer side of the apertures perpendicular to the squeegee travel direction) print thicker paste deposits than parallel apertures of the same size (Mannan, et al., 1994; Markstein, 1997).

Reproduced with permission of the copyright owner. Further reproduction prohibited without permission.

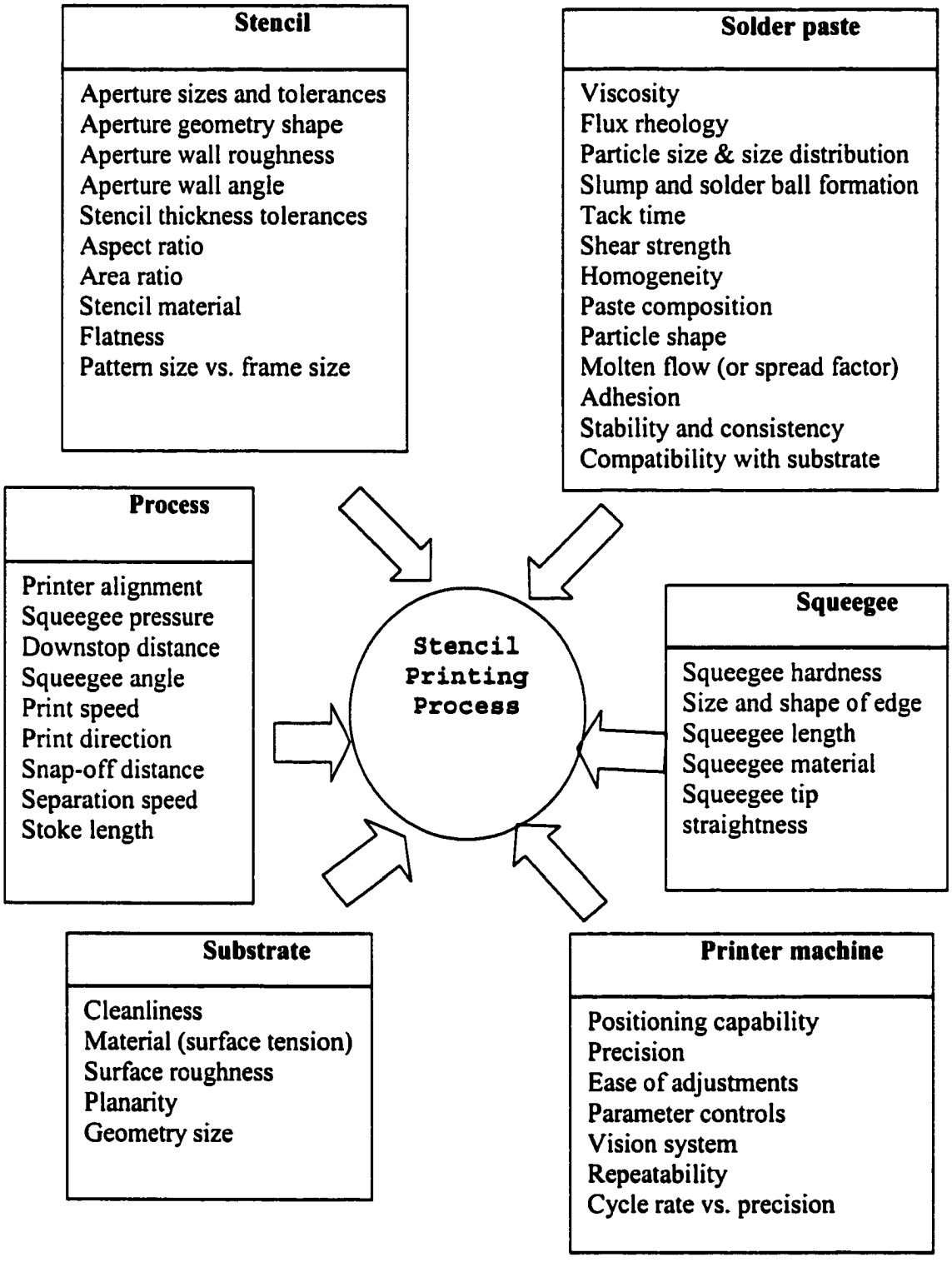


Figure 2-2 Factors that influence the stencil printing process

Reproduced with permission of the copyright owner. Further reproduction prohibited without permission.

2.2 *Experimental Work on Stencil Printing*

2.2.1 Effects of the Stencil

The stencil is a thin foil with small apertures. Brass, stainless steel, alloy 42, and molybdenum are typical materials used for stencil foil. Stencils are commonly manufactured by chemical etching or laser cutting processes.

Brass was the primary stencil material used in the 1980s. Stainless steel was the most common material in the 1990s. The switch to stainless steel occurred in the late 1980s because fine pitch technology required an increase in stencil durability. Stainless steel stencils are more difficult to etch than brass. Molybdenum is another stencil material but has limited popularity because of its cost and difficulty to etch. The advantage of molybdenum is that it has great wear resistance.

The most common manufacturing techniques used to produce stencils are chemical etching and laser cutting. Chemical etching requires four general steps: generate artwork, transfer the image onto metal foil, etch the image into the foil, and mount it in a frame. Etch factor is an important quality index during chemical etching. The etch factor is defined as the ratio of the vertical etch depth to the lateral etch depth. The factor is dependent on the process and stencil thickness (Morris and Wojcik, 1994). In the laser cutting process, a pulsating laser is used to vaporize the metal in small increments. It generates a substantial heat affected zone and a scalloping edge around each aperture. The roughness of the sidewall of the aperture and tolerance of the aperture size are two important quality indexes for stencils made this way. Generally, chemical etching can

Reproduced with permission of the copyright owner. Further reproduction prohibited without permission.

provide a smoother aperture while tight tolerance of the aperture size can be more easily controlled by laser cutting process.

Ideally, the length (L) and width (W) of the aperture and the thickness (T) of the stencil determine the volume of the solder paste deposited, and the thickness of the stencil determines the thickness of the solder deposited. However, this is not always true. Fujiuchi and Toriyama (1994) reported that the bump volume with a stencil thickness of 60 μm is larger than that of a stencil thickness of 80 μm. Whitmore, et al. (1997) found that increasing stencil thickness does not necessarily lead to thicker deposits. Thus one key question is how to determine the stencil thickness to maximize the solder volume for different aperture sizes. Aspect ratio and area ratio are recommended as important stencil design guides in determining the maximum stencil foil thickness in industry. The aspect ratio is defined as the width of the aperture divided by the height of the aperture (or the thickness of the stencil). The area ratio is the ratio of the area of the aperture opening to the area of the sidewall of the aperture. Different recommendations have been published. For example, Wilson and Bloomfield (1995) suggested the optimal aspect ratio of 1.25. Coleman (1996) recommended larger than 1.5 for the aspect ratio and larger than .66 for the area ratio. Markstein (1997) proposed the generally accepted aspect ratio should be larger than 1.5 (1.8 for chemically etched stencils and 1.2 for electropolished laser-cut and electroformed stencils).

Empirical observations show that perpendicular apertures print higher than parallel apertures. Markstein (1997) reported that deposited paste thickness was about 6% greater when the aperture length was oriented parallel to the squeegee blade than when apertures were oriented perpendicular to the squeegee. However, interior angle or

Reproduced with permission of the copyright owner. Further reproduction prohibited without permission.

polygon geometry had no effect on paste deposition, and aperture sidewall taper had a noticeable difference in print quality when near-square sidewalls were used (Monghan, et al. 1995).

2.2.2 Effects of the Solder Paste

The solder paste plays a critical role in determining stencil print quality. Generally, solder paste with fine particles, high viscosity, high yield point, high thixotropy and minimal slump tend to perform well (Morris and Wojcik, 1991).

Paste rheology is a very important variable in predicting the printing behavior of the solder paste. Good rheology solder paste has the tendency to flow when stressed by the squeegee and the tendency to keep the printed columns from slumping once the stencil is lifted. Viscosity and thixotropic properties are the two most important parameters of paste rheology. Solder paste particle size, metal load, and flux/vehicle rheology are the main elements that affect paste rheology.

A solder paste is specified by the maximum and minimum ball sizes comprising the paste. A typical designation like -325/+500 means that the solder alloy particles pass through a 325 mesh screen but cannot pass through a 500 mesh screen (which means the diameter of solder particle size is between 0.0254mm and 0.0432mm). For details see ASTM B-214, *Test for Sieve Analysis of Granular Metal Powers.* Hwang (1989a) recommended the diameter of the largest particle should be less than one-third the smallest dimension of the stencil. Xiao, et al. (1993) suggested that the maximum powder size allowed is approximately 1/7 of the typical aperture width. Although a fine powder is required for good printability, powder that is too fine is a detriment to the rheological

Reproduced with permission of the copyright owner. Further reproduction prohibited without permission.

property. This is because small particles have more surface area, which demands more flux than usual to remove all the oxides present on the particle's surface (Danielsson, 1995).

Metal load is not only an important variable that influences paste rheology but also a critical variable in determining the deposited volume and thickness after reflow. The metal load is defined as the percentage of solder paste solids content. A metal load of 90.5 to 91% seems to be the optimum for most properties (Xiao, et al. 1993). The vehicle of the solder paste is primarily a carrier for the solder paste and provides the desirable rheology essential for printing. The function of fluxes is to clean the surfaces to be joined, to clean the surface of the solder powder, and to maintain cleanliness during reflow. Common flux types include rosin (R), rosin mildly active (RMA), rosin active (RA), synthetic activated (SA), and other additives (OA) (Hwang, 1989b).

2.2.3 Effects of the Process Variables

Squeegee pressure: Proper squeegee pressure should be set properly to achieve a clean wipe of the stencil. Too much pressure on the squeegee will cause the prints to smear and may damage the stencil, while too little squeegee pressure will cause the solder to skip and provide insufficient wetting (Lau, 1994).

Squeegee angle: A squeegee angle of 45° is most commonly used in industry. Lideen and Dahl (1994) reported that the 129 durometer squeegee at 45°, the composite squeegee at 45°, and the metal squeegee at 60° have proven to be the best angles for both ultra fine pitch and other larger pitch printing because these angles gave the most

Reproduced with permission of the copyright owner. Further reproduction prohibited without permission.

consistent print and the volume of the print was closest to the designed volume.

Print speed: There are conflicting experimental results concerning print speed. Mannan, et al. (1994) found a linear rise in paste height with squeegee velocity during stencil printing. Wilson and Bloomfield (1995) reported that no noticeable deterioration in print height occurred in print speeds from 25 mm per second to nearly 200 mm per second. Lau (1994) noted that the squeegee speed depends on the viscosity of the paste.

Snap-off distance: The snap-off distance is the distance between the bottom of the stencil and the substrate. Usually, stencil printing is on-contact, which means the snap-off distance is zero. Wilson and Bloomfield (1995) found that a small snap-off distance helps paste release from ultra fine pitch apertures.

Separation speed: Opinions differ regarding the separation speed function. Whitmore et al. (1997) suggested that the separation speed is critical for paste release. However, Ekere, et al. (1993) studied the stencil/substrate separation speed based on experiments, and concluded that the speed of separation does not significantly affect the number of printing defects for some solders whereas for others a very low value of separation speed results in more defects. Sahay, et al. (1995) presented an analytical model for the release process that implies the separation speed is not an important parameter for print quality.

2.2.4 Effects of the Squeegee

A metal squeegee is commonly used in stencil printing because it provides more consistent paste prints than a polyurethane squeegee. However a polyurethane squeegee has advantages in step-stencil printing. A step-stencil is a stencil that has sections that are

Reproduced with permission of the copyright owner. Further reproduction prohibited without permission.

different thicknesses. The durometer of a polyurethane squeegee is the measure of its hardness, which means the ability of the blade to resist bending during printing. Durometer is measured on the Shore A scale. The higher the durometer, the greater the blade rigidity. Generally, a hardness of 60 to 85 is suitable for screen printing, and a hardness of 80 to 100 is good for stencil printing.

2.2.5 Effects of the Substrate

For good print definition (especially with fine-pitch), the pad surface of the PCB must be smooth and flat to permit the stencil to seal against the board and to prevent paste from spreading toward adjacent lands, forming bridging.

The most common surface finish of PCBs is hot-air solder leveling (HASL). During manufacture, the board is dipped into a bath of molten solder and an air knife, i.e., a blast of compressed air, removes the excess. The resulting surface is highly solderable and sufficiently smooth for printing at millimeter pitches and above (Hobby, 1999). However, the dome of the pad (uneven finish on pad surface) from HASL can affect the fine pitch solder paste printing (Trinite, 1999). Therefore, other surface finishes including immersion deposition are receiving attention more recently. Generally, boards with immersion silver have a better surface in flatness than boards with HASL. A comparison of different board finishes was made by Seto, et al. (1999) and Bratin, et al. (1999). No reports on the effects of board finish seem to have been published yet.

Reproduced with permission of the copyright owner. Further reproduction prohibited without permission.

2.2.6 Effects of the Printing Machine

Board and stencil alignment is very important since badly aligned prints may result in the formation of bridges of paste. In fine pitch printing, a vision-alignment system is essential.

2.3 Theoretical Work on the Stencil Printing Process

2.3.1 Rheological Behavior

An understanding of the rheological behavior of solder paste is essential in investigating flow characteristics in stencil printing. Before discussing rheological behavior, other related concepts are discussed. Shear stress is defined as the force (F) to move one parallel plate relative to another divided by the area (A) between the plates. The unit of shear stress is a Pascal. Shear rate is defined as the rate of motion of two parallel plates (V) divided by the distance separating the plates (y). The unit of shear rate is one sec^{-1}. The viscosity is defined as the ratio of shear stress to shear rate. The viscosity shows the tendency of fluids to flow. The higher the viscosity of the fluid, the greater the resistance to flow. Rheology is the study of the flow and deformation of materials (White, 1991). Instead of looking at viscosity as a single condition, rheology studies the entire shear stress/shear rate curve.

Most common fluids such as water and air are Newtonian fluids. The characteristics of a Newtonian fluid are that it is homogeneous, isotropic, and has a constant viscosity.

Reproduced with permission of the copyright owner. Further reproduction prohibited without permission.

However, many fluids are non-Newtonian because their viscosity depends on the shear rate. For example, the viscosity of pseudoplastic fluids (shear-thinning) decrease with an increase of shear rate, or their shear stresses increase much more slowly than that of Newtonian fluids with an increase of shear rate. Dilatant fluids (shear-thickening) behave the opposite to pseudoplastic fluids; their viscosities increase with increasing shear rate. Bingham fluids behave as solids before the shear stress exceeds its yield point (threshold shear stress) and flow at a constant viscosity after that point. Another common rheological property of some non-Newtonian fluids is thixotropy. Thixotropic fluids behave with time-dependent flow, which means that their viscosity changes over time. The relationships between shear stress and shear rate for different fluids are shown in Figure 2-3. The relationships between viscosity and shear rate are shown in Figure 2-4 (Hwang, 1989).

Solder pastes are normally formulated to be pseudoplastic and thixotropic. The pseudoplastic characteristic is desirable during printing. It permits the paste transfer through the apertures and allows for faster stencil release during printing because of its low viscosity under the shear rate of printing. Once the shear rate drops after the stencil is released from the deposits, the viscosity becomes high, which minimizes spreading and thus solder bridging.

The viscosity of solder paste also changes as a function of temperature. When the temperature increases, the viscosity decreases. In addition, solvent evaporation will cause viscosity to increase.

Reproduced with permission of the copyright owner. Further reproduction prohibited without permission.

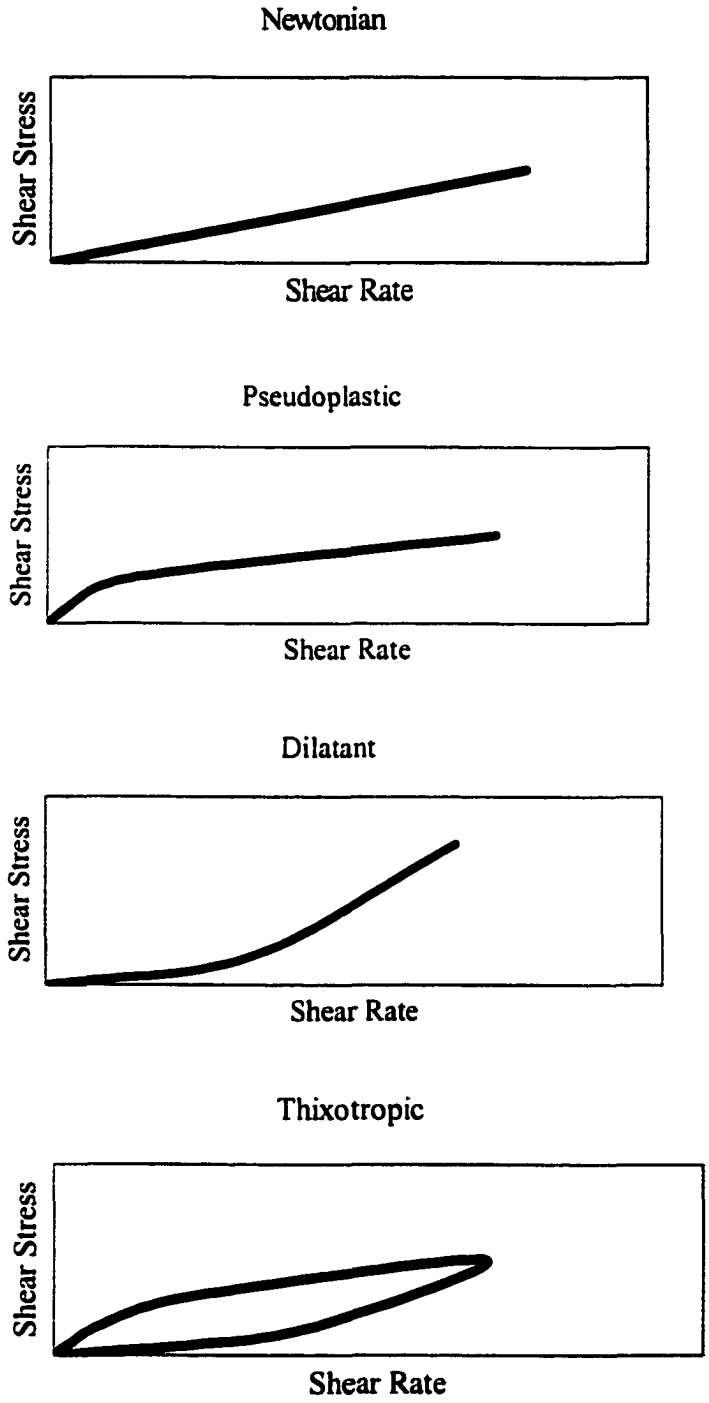


Figure 2-3 Shear stress vs. shear rate for different fluids

Reproduced with permission of the copyright owner. Further reproduction prohibited without permission.

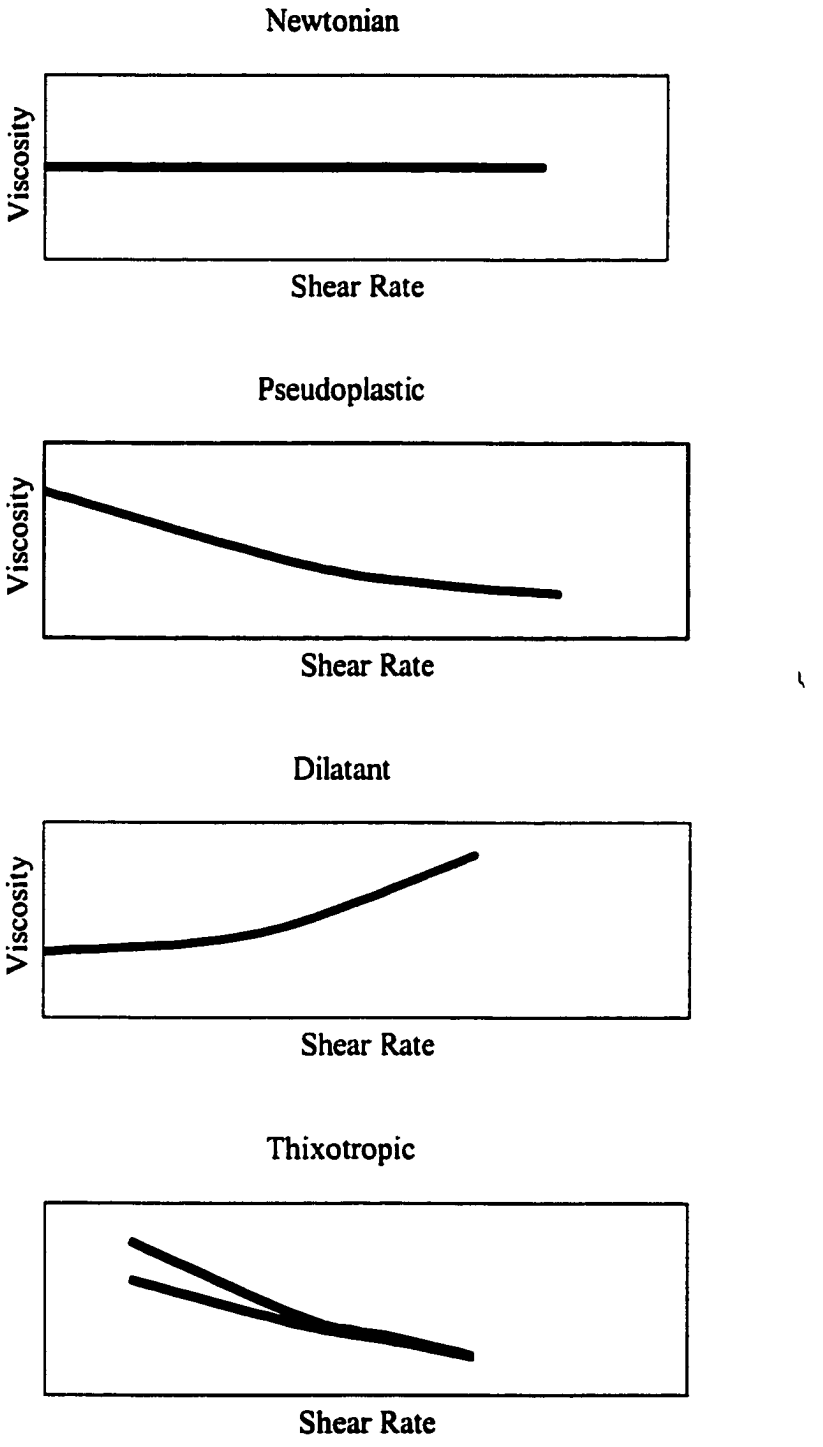


Figure 2-4 Viscosity vs. shear rate for different fluids

Reproduced with permission of the copyright owner. Further reproduction prohibited without permission.

2.3.2 Streamline Pattern of Paste in Front of the Squeegee

In studying the screen printing process, Riemer (1987, 1988, 1989) presented a streamline function ψ derived from Taylor's solution of Stokes equation as follow:

$$\psi = rV[B\sin\varphi + C\varphi\cos\varphi + D\varphi\sin\varphi] \quad (2\text{-}1)$$

where

r, φ = Cylindrical coordinates (radius and phase)

V = Squeegee speed

α = Angle between squeegee and screen surface

$B = -\alpha^2/(\alpha^2 - \sin^2\alpha)$

$C = \sin^2\alpha/(\alpha^2 - \sin^2\alpha)$

$D = (\alpha - \sin\alpha\cos\alpha)/(\alpha^2 - \sin^2\alpha)$

Hanrahan, et al (1992) described a numerical model of solder paste flow with a free surface in stencil printing. The model was developed using the finite element CFD software package, Fidap. They achieved the same results as Riemer. Owczarek and Howland (1990a, 1990b) refined the streamline pattern by considering the deformation of the squeegee.

It should be noted that the streamline of the Riemer's model is in reference to the coordinate system that is fixed with the squeegee. In the original screen printing process, the screen is in motion and the squeegee is at rest. Riemer's model was correct for that situation. However, in most commercial applications of screen printing and stencil printing, printers operate with the screen or stencil at rest and the squeegee in motion. In

Reproduced with permission of the copyright owner. Further reproduction prohibited without permission.

this case, the reference system of the streamline is attached to the moving squeegee.

It is important to determine the pressure at the surface of the screen/stencil. In his screen printing process model, Riemer [1988a, 1988b] treated the ink roll in front of the squeegee as a pump generating high hydrostatic pressure close to the squeegee edge to inject ink into the screen meshes. The pressure generated at the squeegee and screen surface is described as follow:

$$p_{squeegee} = [2\alpha \sin\alpha/(\alpha^2 - \sin^2\alpha)]\eta V(1/r) \approx (5/\sin^2\alpha)\eta V(1/r) \quad (2\text{-}2)$$

$$p_{screen} = [2 \sin^2\alpha/(\alpha^2 - \sin^2\alpha)]\eta V(1/r) \approx (4.5/\sin^2\alpha)\eta V(1/r) \quad (2\text{-}3)$$

where

r = distance from contact point between squeegee and screen

α = squeegee attack angle

V = Squeegee speed

η = ink viscosity

From equations (2-2) and (2-3), it can be seen that the pressure is proportional to squeegee speed, V, and viscosity, η, and inversely proportional to $\sin^2\alpha$.

Owczarek and Howland (1990a, 1990b) analyzed squeegee deformation. Their conclusions were that the angles of squeegees during printing decrease from the undeformed angle of 45 degrees by about 20 degrees for hard squeegees (90 shore A) and by 30 - 40 degrees for soft squeegees (60 shore A). Therefore, α in equations (2-2) and (2-3) should be the angle of the deformed squeegee.

Reproduced with permission of the copyright owner. Further reproduction prohibited without permission.

2.3.3 Aperture Filling Process

Riemer (1988a, 1988b) modeled the screen as many pipes and the flow in each pipe as Hagen-Poiseuille flow. Ekere and Lo (1991) pointed out Riemer's model is invalid due to three assumptions that do not apply to the screen printing process: 1) the screen is a perfectly flexible matrix of isolated capillaries oriented normal to the screen's surface and the flow in each capillary is described by Hagen-Poiseuille flow; 2) the continuity of flow is maintained between the ink in the ink roll and within and passing through the screen, and 3) Poiseuille's flow assumes circular cross-sectioned capillary tubes of infinite length. Owczarek and Holland (1990a, 1990b) derived the relationship between the deposited dry paste thickness and the ratio of the paste flow speed under the squeegee to the squeegee speed.

Two experimental results cannot be explained well. One is that increasing stencil thickness does not increase the thickness of the paste deposited. [Fujiuchi and Toriyama, 1994; Whitmore, et al., 1997]. The other is that perpendicular apertures (longer side of the apertures perpendicular to the squeegee travel direction) print higher than parallel. [Mannan et al. 1994, Monaghan, et al. 1995].

Until this research, no model could explain the first phenomenon. Conflicting opinions exist for the second phenomenon. Mannan et al (1994) theorized that the differences in paste height between perpendicular and parallel apertures are due to the different pressures underneath the squeegee in the two cases. They suggested that the viscoelastic nature of the paste played an important part in creating the large pressure difference. Miric's (1995) opinion is that perpendicular apertures will be more readily released from solder paste deposits than parallel apertures.

Reproduced with permission of the copyright owner. Further reproduction prohibited without permission.

A fine pitch stencil printing process model using a Taguchi - Neural network method was developed. [Li, et al., 1996]. Six design parameters were selected to analyze the printing process: squeegee material, pad material, snap-off distance, squeegee pressure, squeegee angle, and squeegee speed. It was reported that this model was in excellent agreement with experiment results, and it could be used to predict the average solder paste height and the solder paste height variation. But the reasons why the six design parameters determine the paste height and height variation are still unclear in this model.

2.3.4 Release Process

A simple model based on the fluid flow through ducts to determine the amount of material possibly sticking to the wall of the stencil aperture was proposed [Sahay, et al., 1995]. The print quality is defined as the ratio of the printed volume to the aperture volume in the model. However, the assumption of no slip at the wall when calculating velocity in this model may be incorrect; Mannan et al. (1995) pointed out that wall slip is a well-documented phenomenon and plays an important role in aperture emptying for solder paste. Studies of shear stress at a solder paste/stencil interface were done by Head, et al. (1994) and Mannan, et al. (1995).

Currie and Ekere (1998) studied the release process of the paste from the stencil apertures by considering two factors: 1) the tack strength between the paste and the substrate or land, and 2) the strength with which the paste adheres to the sidewall of the aperture. For good paste transfer, the adhesive forces of the paste on the substrate should always be greater than those at the aperture walls. They concluded that theoretical

Reproduced with permission of the copyright owner. Further reproduction prohibited without permission.

analysis shows that the critical separation speed for solder paste is about 2.4 mm/s, and the values determined experimentally were approximately 3 mm/s. Therefore separation speeds below 3 mm/s are recommended to minimize the incidence of skipping. For Currie and Ekere's work, one disadvantage is that they did not consider the effects of aperture size and stencil thickness.

Ekere, et al. (1993) studied the stencil/substrate separation speed based on experiments, and concluded that the speed of separation does not significantly affect the number of printing defects for some solders whereas for others a very low value of separation speed results in more defects.

2.4 Summary

The solder paste stencil printing process is quite complex. Many experiments have been performed in industry and universities. However, the mechanism of the printing process is still not well understood. Critical process variables have not been clearly identified yet. Further, two experimental phenomena have not been explained very well. One is that increasing stencil thickness does not increase the thickness of the paste deposited. The other is that perpendicular apertures (longer side of the apertures perpendicular to the squeegee travel direction) print higher than parallel apertures.

Reproduced with permission of the copyright owner. Further reproduction prohibited without permission.

3 Modeling of the Solder Paste Stencil Deposition Process

Solder paste can be considered as a kind of fluid, so it cannot be represented by a single concentrated mass located at a fixed center of gravity. In this study, the following assumptions are made:

- The solder paste is a Newtonian fluid. This assumption is questionable because solder paste exhibits pseudoplasticity (or shear-thinning) and thixotropy. However, modeling the solder paste as a non-Newtonian fluid makes it difficult to derive an analytical solution. In addition, the rheological behavior of the solder paste depends on its composition and manufacturer. Not only do different solder paste types have different rheological properties, but also some similar solder types made by different manufacturers also have different rheologies. Detailed discussions are found in Hwang (1989b) and Ekere and Lo (1991). Relaxation of the Newtonian assumption will be discussed in future research.
- The flow is incompressible.
- There is no leakage under the squeegee.
- This is a two dimensional problem.
- The inertia term is negligible in the momentum equation. This assumption is reasonable because the viscosity of solder paste is very high (about 1000 kcps) so that its Reynolds number is very low ($< 10^{-5}$). For so small a Reynolds number, Stokes' creeping-flow theory can be used effectively.

Reproduced with permission of the copyright owner. Further reproduction prohibited without permission.

- The paste does not slip on the stencil surface. It should be noted that the no-slip condition is assumed only at the stencil surface with respect to the paste travel stage (stage I). Slip at the aperture wall at the stencil release stage (stage III) is a well-documented phenomenon (Mannan, et al., 1995).

3.1 Nomenclature

ARR	Area ratio
ASR	Aspect ratio
D	Distance of the paste extending from the tip of the squeegee in the direction of travel
H	Thickness of the stencil
L	Length of the rectangular aperture or the slit
P	Paste pressure
R	Radius of the circular aperture
S	Squeegee speed
T	the total filling time
TR	Transfer ratio
U	Squeegee speed
V	Total deposited volume
W	Width of the rectangular aperture or the slit
r	Distance from contact point between squeegee and screen, also used for position vector in cylindrical coordinates.
t	the instantaneous filling time

Reproduced with permission of the copyright owner. Further reproduction prohibited without permission.

$\mathbf{v}$	Paste velocity (vector)
α	Squeegee actual attack angle
η	Paste viscosity
ρ	Density of the paste
∇	Gradient operator
∇^2	Laplacian operator
ψ	Stream function
f(Q)	Paste quantity factor

3.2 The Hydrodynamics of the Paste Travel Process

Based on the stated assumptions, the paste travel process can be modeled as creeping flow described by Stokes' equation:

$$\nabla P = \eta \nabla^2 \mathbf{v} \tag{3-1}$$

As shown in Figure 3-1, solder paste is bounded by the squeegee and the stencil. The squeegee and the stencil meet at an angle α, which is the squeegee angle. The squeegee moves at a velocity U and the stencil is at rest.

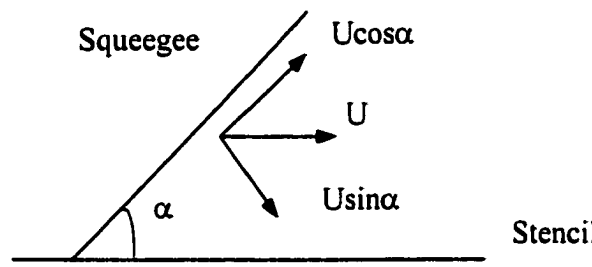


Figure 3-1 Flow between the squeegee and the stencil

Reproduced with permission of the copyright owner. Further reproduction prohibited without permission.

The problem is easiest to solve in the cylindrical coordinate system. The stream function, $\psi(r, \theta)$, for a planar flow in cylindrical coordinates is defined as (Deen, 1998)

$$v_r = (1/r)\partial\psi/\partial\theta \qquad v_\theta = -\partial\psi/\partial r \tag{3-2}$$

The stream function form of Stokes' equation is

$$\nabla^4\psi = 0 \tag{3-3}$$

$$\nabla^4 = \nabla^2(\nabla^2) \quad \nabla^2 = (1/r)\partial(r\partial/\partial r)/\partial r + (1/r^2)\partial^2/\partial\theta^2$$

The no-slip and no-penetration conditions at the squeegee ($\theta=\alpha$) and the stencil ($\theta=0$) are expressed as

$$v_r(r, \alpha) = U\cos\alpha \qquad v_\theta(r, \alpha) = -U\sin\alpha \tag{3-4}$$

$$v_r(r, 0) = 0 \qquad v_\theta(r, 0) = 0 \tag{3-5}$$

Using Eq. (3-2), these boundary conditions are written in terms of ψ as

$$\partial\psi/\partial\theta(r, \alpha) = Ur\cos\alpha \qquad \partial\psi/\partial r(r, \alpha) = U\sin\alpha \tag{3-6}$$

$$\partial\psi/\partial\theta(r, 0) = 0 \qquad \partial\psi/\partial r(r, 0) = 0 \tag{3-7}$$

Examining the boundary conditions in Eq. (3-6), it appears the solution may be of the form

$$\psi = rf(\theta) \tag{3-8}$$

Substituting Eq. (3-8) in Eq. (3-3),

$$d^4f/d\theta^4 + 2\,d^2f/d\theta^2 + f = 0 \tag{3-9}$$

The general solution for Eq. (3-9) is

$$f(\theta) = A\cos\theta + B\sin\theta + C\theta\cos\theta + D\theta\sin\theta \tag{3-10}$$

where A, B, C, and D are constants.

Using these boundary conditions to evaluate the constants in Eq. (3-10), we obtain

Reproduced with permission of the copyright owner. Further reproduction prohibited without permission.

$A = 0$

$B = -C = U\sin^2\alpha/(\sin^2\alpha - \alpha^2)$

$D = U(\sin\alpha\cos\alpha - \alpha)/(\sin^2\alpha - \alpha^2)$

The stream function is found to be

$$\psi(r, \theta) = Ur[\sin^2\alpha\sin\theta - (\sin^2\alpha)\theta\cos\theta + (\sin\alpha\cos\alpha - \alpha)\theta\sin\theta]/(\sin^2\alpha - \alpha^2) \quad (3\text{-}11)$$

Riemer's (1988a,b) result was

$$\psi(r, \theta) = Ur[\alpha^2\sin\theta - (\sin^2\alpha)\theta\cos\theta + (\sin\alpha\cos\alpha - \alpha)\theta\sin\theta]/(\sin^2\alpha - \alpha^2) \quad (3\text{-}12)$$

as a result of modeling the squeegee as fixed and the stencil moving toward the squeegee with a velocity U.

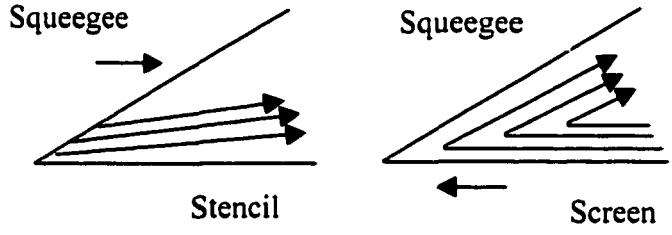


Figure 3-2 Streamline (a: the model; b: Riemer's model)

The comparison of the two model's streamlines is shown in Figure 3-2. It should be noted that the difference between the two streamlines is that they are in different reference frames. Specifically, the proposed model's streamline is visualized on the stencil if one considers the stencil to be at rest and the squeegee to be in motion in the direction away from the stencil/squeegee contact point. Riemer's flow pattern is visualized on the squeegee when the squeegee is at rest and the screen moves toward the screen/squeegee contact point. The physical interpretations of the two models are the

Reproduced with permission of the copyright owner. Further reproduction prohibited without permission.

same. Since most stencil printing and screen printing involves a stencil or screen at rest and a squeegee moving, the model developed here more accurately represent the stencil/screen printing process. The velocity components are

$$v_r = U[\sin^2\alpha\cos\theta - \sin^2\alpha(\cos\theta - \theta\sin\theta)+(\sin\alpha\cos\alpha - \alpha)(\sin\theta + \theta\cos\theta]/(\sin^2\alpha - \alpha^2) \quad (3\text{-}13a)$$

$$v_\theta = -U[\sin^2\alpha\sin\theta - \sin^2\alpha\ \theta\cos\theta + (\sin\alpha\cos\alpha - \alpha)\theta\sin\theta]/(\sin^2\alpha - \alpha^2) \quad (3\text{-}13b)$$

The r component in Eq. (3-1) is

$$\partial P/\partial r = 2(\eta U/r^2)[\sin^2\alpha\cos\theta - (\sin\alpha\cos\alpha - \alpha)\sin\theta]/(\sin^2\alpha - \alpha^2)$$

At the stencil surface ($\theta = 0$),

$$\partial P/\partial r|_{(\theta = 0)} = 2(\eta U/r^2)\sin^2\alpha/(\sin^2\alpha - \alpha^2) \quad (3\text{-}14)$$

The pressure P at the stencil surface is

$$P = \int_0^r \partial P/\partial r|_{(\theta = 0)}\, dr = 2(\eta U/r)\sin^2\alpha/(\alpha^2 - \sin^2\alpha) \quad (3\text{-}15)$$

The shear stress in the solder paste at the stencil surface is

$$\tau_{\theta r}|_{(\theta = 0)} = (2\eta U/r)(\sin\alpha\cos\alpha - \alpha)/(\sin^2\alpha - \alpha^2) \quad (3\text{-}16)$$

where r = Distance from the contact point between squeegee and stencil.

The obtained shear stress and pressure in the solder paste at the stencil surface agree with the results of Riemer (1988a, b). Eqs. (3-15) and (3-16) show that the shear stress and pressure of the solder paste at the stencil surface are proportional to the squeegee speed and paste viscosity, inversely proportional to distance from the vicinity of the squeegee, and a function of the squeegee angle. Since solder paste is a pseudoplastic (shear-thinning) fluid, the viscosity decreases with an increase in shear rate. This characteristic is desirable in the stencil printing process. Therefore, high shear stress is required during the aperture filling process. Table 3-1 compares the pressure and the shear stress at the stencil surface with different squeegee angles.

Reproduced with permission of the copyright owner. Further reproduction prohibited without permission.

Table 3-1 Pressure and shear stress vs. squeegee angle

Squeegee Angle	Pressure at the stencil surface	Stress at the stencil surface
60°	$4.33\eta U/r$	$3.54\eta U/r$
45°	$8.55\eta U/r$	$4.88\eta U/r$
30°	$20.7\eta U/r$	$7.5\eta U/r$

3.3 The Aperture Filling Process

It should be noted that the aperture filling process could not be modeled as Poiseuille flow, which assumes capillary tubes of infinite length. In the stencil printing process, the stencil is only a thin foil.

Roscoe (1949) studied the flow of highly viscous fluid through an aperture in a thin plate. He obtained a relationship between the rate of flow per unit time Q and pressure difference between the two sides. His results are

Flow through a circular aperture: $Q = PR^3/(3\eta)$ (3-17)

Flow through a slit (L>>W): $Q = \pi PLW^2/(32\eta)$ (3-18)

Considering the symmetry of a rectangle aperture, flow rate Q through a rectangle aperture should be

$$Q = \pi PL^2W^2/(32\eta(L+W)) \quad (3\text{-}19)$$

Substituting Eq. (3-15) in Eqs. (3-17), (3-18), and (3-19) yields

Circular aperture: $Q = 0.67\,(UR^3/r)f(\alpha)$ (3-20)

Slit: $Q = 0.2\,[ULW^2/r]\,f(\alpha)$ (3-21)

Rectangle aperture: $Q = 0.2\,[UL^2W^2/((L+W)r)]\,f(\alpha)$ (3-22)

Where $f(\alpha) = \sin^2\alpha/(\alpha^2 - \sin^2\alpha)$

Reproduced with permission of the copyright owner. Further reproduction prohibited without permission.

Total deposited volume (V) is

$$V = \int_0^T Q dt = \int_0^D Q/U dr \tag{3-23}$$

where

T = the total filling time = D/U

dt = the instantaneous filling time = dr/U

By substituting Eqs. (3-20), (3-21), and (3-22) into Eq. (3-23), the total volume is determined to be:

through a circular aperture: $V = 0.67\ R^3\ f(\alpha)f(Q)$ (3-24)

through a slit: $V = 0.2\ [LW^2]\ f(\alpha)f(Q)$ (3-25)

through a rectangular aperture: $V = 0.2\ [L^2W^2/(L+W)]\ f(\alpha)f(Q)$ (3-26)

where $f(Q) = \int_0^D (1/r)dr$ (3-27)

f(Q) is a paste quantity factor that increases with paste quantity in front of the squeegee. Equation (3-27) shows that f(Q) will be infinite when $r \rightarrow 0$, which indicates that the paste pressure in Equation (3-15) increases to an extremely high value in the vicinity of the squeegee edge. However, in an actual printing situation, paste pressure is limited by the capability of the paste to transfer shear stresses at high shear rates, and also by the quality of the seal between the squeegee and the stencil. In order to generate a high pressure to inject the paste into the aperture, stencil planarity, PCB board planarity, and squeegee parallelism must be precisely controlled.

Equations (3-24) and (3-25) show that the solder volume that can be deposited is independent of the thickness of the stencil. It relates to the actual attack angle and aperture size. It should be noted that this holds true as long as the deposited volume is less than the aperture volume. If the deposited volume is larger than the aperture volume,

Reproduced with permission of the copyright owner. Further reproduction prohibited without permission.

the squeegee will scoop the excess paste. In the actual situation, the volume of paste deposited when a thicker stencil is used may be less than the volume of paste deposited when a thinner stencil is used because more paste may stick to the wall of the thicker stencil.

3.4 Paste Transfer Ratio vs. Aspect Ratio

As defined in Section 2.2.1, the area ratio (ARR) is:

For a circular aperture: $ARR = \pi R^2/(2\pi RH) = R/(2H)$ (3-28)

For a rectangle aperture: $ARR = LW/[2(L+W)H]$ (3-29)

The aspect ratio (ASR) is $ASR = W/H$ (3-30)

Define transfer ratio (TR) as the deposition volume divided by the aperture volume. Substituting Eqs. (3-24), (3-25), and (3-26) as the deposited volume yields

For the circular aperture: $TR = 0.42\ f(\alpha)f(Q)ARR$ (3-31)

For the rectangle aperture: $TR = 0.4\ f(\alpha)f(Q)ARR$ (3-32)

For the slit: $TR = 0.2\ f(\alpha)f(Q)ASR$ (3-33)

Equations (3-31) and (3-32) show that the transfer ratio is proportional to the area ratio. But the conclusion that the transfer ratio is proportional to the aspect ratio can be drawn only if the length L of a rectangle aperture is much larger than its width W (L>>W). In addition, it is difficult to determine the width of a circular aperture in Eq. (3-30). Therefore, the area ratio is recommended as an indicator for choosing the stencil thickness. This is consistent with Coleman's (1996) experience.

f(Q) is mainly determined by the seal condition between the squeegee and the stencil. If the squeegee angle is fixed and f(Q) is assumed to be constant (unknown), the

Reproduced with permission of the copyright owner. Further reproduction prohibited without permission.

relationship between the transfer ratio and the area ratio will be:

TR = C * ARR ARR < a critical value

TR = 1 ARR > a critical value

Where C is a constant.

The critical point is where the deposited solder paste volume equals the aperture volume and no excess paste is scooped. According to industry experience and our experiment [Pan, et al., 1999a], the critical point is between 0.6 to 0.7. The maximum stencil thickness can be determined by the critical value.

For a circular aperture: $H_{max} < 0.7\sim0.8\ R$

For a rectangle aperture: $H_{max} < 0.7\sim0.8\ LW/(L+W)$

3.5 Printing Perpendicular vs. Parallel Apertures

As mentioned previously, a perpendicular aperture prints higher than a parallel aperture. Two possible explanations have been proposed. One is less paste is scooped in a perpendicular aperture than a parallel one. The other is the difference in pressure that occurs under the squeegee in the two kinds of apertures. Mannan, et al. (1994) analyzed the static deformation and dynamic deformation of the squeegee and concluded that a perpendicular aperture will be scooped more than a parallel aperture. Then they deduced that the differences in paste height are due to the different pressures underneath the squeegee in the two cases.

The pressure difference between a perpendicular aperture and a parallel aperture can be explained as follows. From the analysis in Section 3.3, the paste deposited volume is proportional to the paste pressure and the highest pressure of paste occurs in the

Reproduced with permission of the copyright owner. Further reproduction prohibited without permission.

vicinity of the squeegee edge. It should be noted that these conclusions are derived based on the assumption that there is no paste leakage under the squeegee, i.e. the paste speed at the contact point is zero. However, when the squeegee is over the aperture, there is normal velocity of paste through the aperture under the squeegee as shown in Figure 3-3. In this case the normal velocity is constant because of no inertia term. Since the normal velocity occurs, the paste pressure above the aperture would drastically decrease. In other words, the highest paste pressure occurs at the edge of the aperture or when the squeegee just reaches the aperture. A perpendicular aperture has a longer side than a parallel aperture at that time. This is why a perpendicular aperture prints higher.

Reproduced with permission of the copyright owner. Further reproduction prohibited without permission.

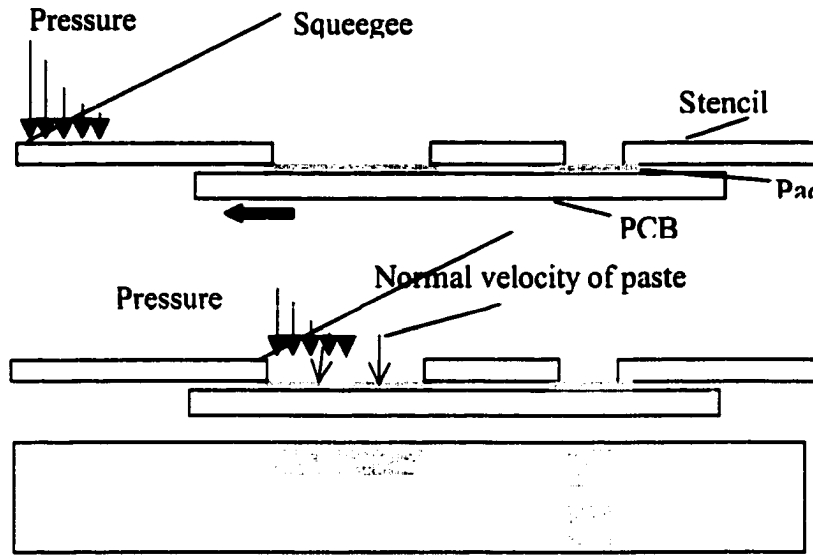


Figure 3-3 Aperture filling mechanism

Reproduced with permission of the copyright owner. Further reproduction prohibited without permission.

3.6 Summary

An analytical model has been developed for the deposition process of stencil printing. The following conclusions are made:

1) Aperture opening size and paste pressure generated determine the amount of solder paste deposited. The volume of paste deposited is independent of the stencil thickness when the deposited volume is less than the aperture volume. Area ratio is recommended as a main indicator for determining the thickness of a stencil.

2) α in Equations (3-24) and (3-26) is the actual attack angle. It is determined by the squeegee angle, the squeegee pressure, and the squeegee hardness. The smaller is α, the more paste is deposited.

- From the model, the squeegee angle should have a significant effect in adjusting the volume of deposited paste. However, most squeegee holders used in industry do not have the ability to adjust the angle.
- The higher the squeegee pressure (smaller α), the more paste is deposited. But if the squeegee pressure is too high, stencil deformation will result leading to paste leakage under the squeegee and different pressures along the squeegee blade. So a too high squeegee pressure leads to unsatisfactory print quality. In addition, the high squeegee pressure can destroy the stencil or decrease the stencil life. Proper squeegee pressure should be set high enough for a clean wipe of the stencil.
- The higher the squeegee hardness, the more robust are the paste deposits due to keeping α constant. This is why industry generally chooses a metal squeegee for solder paste printing.

Reproduced with permission of the copyright owner. Further reproduction prohibited without permission.

3) A perpendicular aperture prints higher than a parallel aperture. One way to avoid the difference between a perpendicular aperture and a parallel aperture may be to design 45 degrees and 135 degrees apertures with respect to the squeegee, or to design the parallel aperture slightly bigger relative to the perpendicular aperture.

4) Stencil planarity, PCB board planarity, and squeegee parallelism are required to generate the high pressure required to inject the paste into the aperture.

Reproduced with permission of the copyright owner. Further reproduction prohibited without permission.

4 Description of Experimental Procedure

4.1 Description of the Experiment

The goal of this experiment is to determine which are the critical variables that control the amount of solder paste deposited, to validate the model, and to determine the critical ARR value. Based on the model in Chapter 3, the previous studies in Chapter 2, and discussions with the engineers at Visteon, an Enterprise of Ford Motor Co., six variables were selected for study in this experiment. They are stencil thickness, aperture size, aperture shape, board finish, solder paste type, and print speed. The response variables are the volume, area, and height of solder paste deposited, which were measured by an in-line fully automatic laser-based 3-D solder paste inspection system. Table 4-1 summarizes the variables and their levels for the experiment. Table 4-2 shows the aperture size of the stencils. Table 4-3 compares the solder paste characteristics of Type 3 and Type 4.

The stencils used for the experiment were laser-cut from stainless steel. Two stencil thicknesses were selected. One is 0.1 mm (4 mil) and the other was 0.15 mm (6 mil). Both stencils had the same pattern, which included three aperture groups:

Group 1: regular rectangular (QFP) apertures with the widths of 0.38 mm (15 mil), 0.32 mm (12 mil), 0.25 mm (10 mil), 0.2 mm (8 mil), and 0.15 mm (6 mil). Each width had 102 pads in the "parallel to squeegee travel" orientation and 102 pads in the "perpendicular to squeegee travel" orientation. A total of 1020 pads were evaluated.

Reproduced with permission of the copyright owner. Further reproduction prohibited without permission.

Table 4-1 Input variables and their levels

Stencil thickness	0.1 mm (4 mil)	0.15mm (6 mil)
Solder paste type	Type 3	Type 4
Board finish	Immersion Ag	HASL*
Print speed	2 in/sec	8 in/sec
Aperture size	See Table 2	
Aperture shape	See Figure 2	

* HASL = Hot Air Solder Leveling.

Table 4-2 Aperture sizes of a stencil (unit: mil = 0.0254mm)

Pitch (mil)	30	25	20	16	12
QFP aperture width	15	12	10	8	6
QFP aperture length	80	70	60	50	40
BGA aperture diameter	15	12	10	8	6

Table 4-3 Solder paste specification

	Type 3	Type 4
Dimension	90-3-M10	90-4-M10
Viscosity @5rpm	1570 poise	1620 poise
Viscosity @30rpm	430 poise	480 poise
F.O.G.*	40/32 μm	27/24 μm
Alloy	Sn62/Pb36/Ag2	
Metal content	90%	
Flux type	No-clean LR 735	

* F.O.G. (Fineness of Grind) is a simple test to check for the largest particle/agglomerate size in a paste.

Reproduced with permission of the copyright owner. Further reproduction prohibited without permission.

Group 2: slant rectangular (QFP) apertures with the widths of 0.38 mm (15 mil), 0.32 mm (12 mil), 0.25 mm (10 mil), 0.2 mm (8 mil), and 0.15 mm (6 mil). Each width had 30 pads in the "45 degrees to squeegee travel" orientation and 30 pads in the "135 degrees to squeegee travel" orientation. A total of 300 pads were evaluated. Note that the distance of aperture-to-aperture is designed much larger than the pitch to make measurement feasible.

Group 3: circular (BGA) apertures with diameters of 0.38 mm (15 mil), 0.32 mm (12 mil), 0.25 mm (10 mil), 0.2 mm (8 mil), and 0.15 mm (6 mil). Each diameter had 216 pads. A total of 1080 pads were evaluated.

The test pattern was designed as a 3 × 3 Latin square so the variability due to the pad positions relative to the squeegee and squeegee travel direction was balanced. The test pattern is shown in Figure 4-1. It should be noted that the information about aperture size and shape in this design is confounded because they are all in a block. The other 4 factors: stencil thickness, board finish, solder type, and print speed were designed as a factorial design. Due to the time limit of the use of the printing machine in a production line, only one replication was selected. Thus a total of 16 boards (2-level 4 factors factorial design) were printed. The randomized 2^4 factorial design matrix is shown in Table 4-4.

Reproduced with permission of the copyright owner. Further reproduction prohibited without permission.

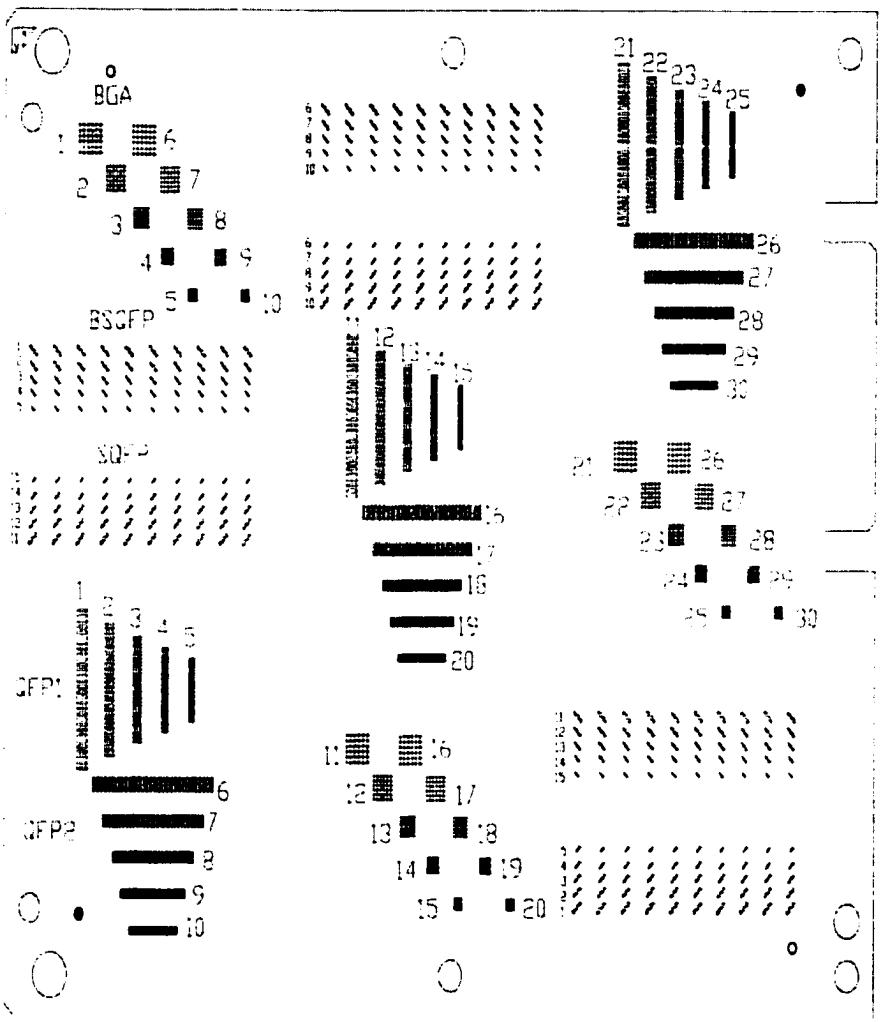


Figure 4-1 Test pattern of stencils and FR-4 boards

Reproduced with permission of the copyright owner. Further reproduction prohibited without permission.

Table 4-4 Randomized 2^4 factorial design matrix

Experimental sequence	Board finish + HASL - Silver	Stencil thickness (mils) - 4 + 6	Solder size (μm) - 23 + 42	Print speed (in/sec) - 2 + 8
1 (17)	-	-	-	+
2	+	-	-	-
3	-	+	+	+
4 (18)	-	-	-	-
5	-	-	+	+
6	-	+	+	-
7 (19)	+	+	+	+
8	+	-	+	-
9	+	+	-	-
10 (20)	-	-	+	-
11	-	+	-	+
12	+	+	+	-
13 (21)	+	+	-	+
14	+	-	-	+
15	-	+	-	-
16	+	-	+	+

Reproduced with permission of the copyright owner. Further reproduction prohibited without permission.

In order to generate comparative data on specified process variables, the remaining process variables were determined based on the engineer's knowledge and experience and limited to the values shown in Table 4-5.

The rheology of solder paste type 3 and type 4 is shown in Figure 4-2. In order to keep solder paste properties the same for each run, the paste was kneaded 3 times before printing. The reason is that the viscosity of solder paste may change after it was kneaded a different number of times. To get steady state results, each run printed three times and only the third print was measured because the results of the first two may be unstable. The third board of each run was measured right after it was printed since a long waiting time between print and measurement could cause the solvent of paste to evaporate and result in a lower amount when measured.

A fully automatic solder paste inspection system is currently used for inspection of 0.635 mm (25 mil) QFP components of automobile electronics products. Whether the inspection system is accurate enough to measure experimental results needs to be investigated first. The next section describes an experiment conducted to investigate the gauge repeatability and reproducibility of the inspection system.

Reproduced with permission of the copyright owner. Further reproduction prohibited without permission.

Table 4-5 Process variables

Printer	MPM AP HiE
Squeegee	8 inch metal squeegee blade with 45 degree
Squeegee pressure	8 lb
Down-stop distance	0.0835 inch
Snap-off distance	On-contact
Separation speed	Level 6 (about 0.6-0.9 mm/s)
Stencil mesh tension	28 N/cm

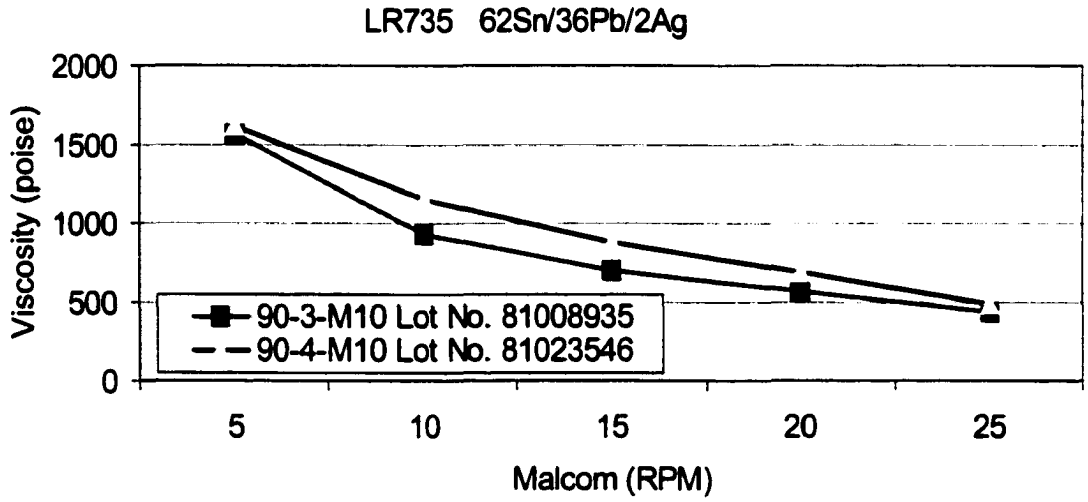


Figure 4-2 Rheology of Solder Paste Type 3 and Type 4

Reproduced with permission of the copyright owner. Further reproduction prohibited without permission.

4.2 Gauge Repeatability & Reproducibility Study for a 3-D Solder Paste Inspection System

4.2.1 Introduction

As the pitch of components decreases and tighter tolerances are required, more advanced measurement machines must be developed to meet the challenges. The purpose of a measurement machine is to provide data that accurately represent real product dimensions.

It should be noted that gauge repeatability & reproducibility in one range might not extend to other ranges since the variance might depend on the mean level of the measurement. For example, if a solder paste inspection system can measure volume of solder paste for 0.635 mm (25 mil) pitch within the required repeatability, it does not guarantee the system can measure the volume of solder paste for 0.3 mm (12 mil) pitch within the required repeatability. A fully automatic laser-based 3-D triangulation solder paste inspection system is currently used for inspection of 0.635mm (25mil) pitch QFP components of automobile electronics products. This section presents an investigation of whether the present system can be used successfully for measuring 0.4 mm and 0.3mm pitch QFPs and BGAs.

4.2.2 Gauge Accuracy, Repeatability, and Reproducibility

Measurements typically act as random variables, the behavior of which can be

Reproduced with permission of the copyright owner. Further reproduction prohibited without permission.

summarized by a mean (μ) and variance (σ). It is well known that the measured data includes the variation of the product and the variation of the measurement machine.

$$\mu_{total} = \mu_{product} + \mu_{measurement}$$

$$\sigma^2_{total} = \sigma^2_{product} + \sigma^2_{measurement}$$

where μ_{total} is the observed average of a set of measurements; $\mu_{product}$ is the true mean of the measured product; $\mu_{measurement}$ is the measurement system bias (e.g. gauge accuracy); σ^2_{total} is the overall variance; $\sigma^2_{product}$ is the variance of the measured product; and $\sigma^2_{measurement}$ is the variance caused by the measurement system and measurement procedures.

Gauge repeatability is defined as the measurement variation caused by a measurement system measuring the same dimension many times using the same measurement methodology. Gauge reproducibility is the measurement variation obtained by different operators measuring the same dimension. For fully-automated measurement systems requiring no operators, gauge reproducibility might be ignored although sometimes it may be used to characterize variation associated with different parts of the machine or difference machines. The machine-to-machine reproducibility can be evaluated by the degree of correlation. Melendez (1999) suggested that the reproducibility component could be evaluated by changing time, board alignment or fixturing, or board orientation.

A proper measurement system should be unbiased and have sufficient capability to detect variation in the product, which requires that $\mu_{measurement}$ be close to 0, and that the ratio of $\sigma^2_{measurement}$ to $\sigma^2_{product}$ be small enough. Gauge accuracy is achieved by

Reproduced with permission of the copyright owner. Further reproduction prohibited without permission.

calibrating the measurement system to a traceable reference standard.

The objective of a gauge repeatability & reproducibility analysis is to identify and quantify the sources of the measurement variability. Generally, the sources of the measurement variation include 1) instrument variation, 2) measurement process variation, 3) operator related variation, 4) variation among test samples, 5) environmental fluctuations [Haider, et al., 1995].

4.2.3 Absolute Measurement & Relative Measurement

The measurement system performance parameters (accuracy, repeatability & reproducibility) can be evaluated in two ways. One is called "absolute measurement" in which the measurement system is calibrated to a traceable reference standard such as one set by the National Institute of Standards and Technology (NIST). The resulting data is verified against the absolute values. This process is normally done by the manufacturers of measurement systems. All performance parameters can be obtained by this method.

The method commonly used in production is "relative measurement," which assumes the average of a number of performed measurements as the nominal value. In this way, gauge repeatability & reproducibility can be evaluated, but not accurately since the true values are not known (the average of the measured data may be biased).

4.2.4 Analysis Method

One classical and simple way to analyze the gauge capability is to use X-bar and R charts [Montgomery and Runger, 1993a, 1993b, Haider, et al., 1995]. Precision-to-

Reproduced with permission of the copyright owner. Further reproduction prohibited without permission.

tolerance (P/T) ratio is commonly used as an index of gauge capability. The P/T ratio is defined as the ratio of $6\sigma_{measurement}$ to the total tolerance range (the difference between the upper and lower limits of the specified tolerance). Generally, a value of P/T of 0.1 or less means it is a proper gauge. However, Montgomery and Runger (1993) point out that there are dangers in relying too much on the P/T ratio as they may be made arbitrarily small by increasing the width of the specification range. They recommend using the ratio of $\sigma_{measurement}$ to $\sigma_{product}$ or $\sigma_{measurement}$ to σ_{total} as a gauge capability index. This method presupposes a reasonable statistics background to design and analyze the experiments.

The ratio of $\sigma_{measurement}$ to the mean of the measured value is proposed to be a gauge repeatability index. Since the deviation of a set of measurements normally depends on the mean level of the measured value, the index is reasonable and satisfies engineering requirements. Using this index, analysis of the measurement repeatability for an automated measurement system is simple and easy. It should be noted that the difference between the above three methods is that different indexes are used to evaluate the gauge repeatability and reproducibility.

4.2.5 Triangulation Principle

The inspection system uses laser triangulation to measure solder paste height, area, and volume. Laser triangulation is considered the most effective method for high speed and high resolution 3-D SMT inspection [Svetkoff, et al. 1987]. Double triangulation techniques can reduce the shadow effects present in single triangulation. A double triangulation system is shown in Figure 4-3. The laser beam is swept across solder

Reproduced with permission of the copyright owner. Further reproduction prohibited without permission.

deposits and height reference points on a printed circuit board (PCB). The light scattered from the solder deposits is captured by two Position Sensitive Devices (PSD). As the deposit height changes by ΔH, the light reflected on the PSDs moves ΔD as indicated. The two images are analyzed and the height profile of the deposit is calculated. The measurement system has resolution settings of 18 μm, 25 μm, and 36 μm, which can be selected depending on the smallest lead pitch in the PCB.

Warpage of PCBs may have significant influence on the measurement accuracy and capability since the warpage will result in uncertainty of the reference height of the PCB. The volume and height of the solder deposits become smaller as the lead pitch is decreased. The volume measurement of small deposits may be more sensitive to the warpage. Though most warpage of PCBs can be eliminated by a proper clamping mechanism, minimizing the influence of the remaining warpage is necessary. In this measurement system, up to 10 local reference heights close to the solder paste deposit to be measured can be selected. From these local reference heights, the "virtual" exact reference height at the solder paste deposit is calculated. Figure 4-4 shows board warpage with local reference heights and solder pad.

Reproduced with permission of the copyright owner. Further reproduction prohibited without permission.

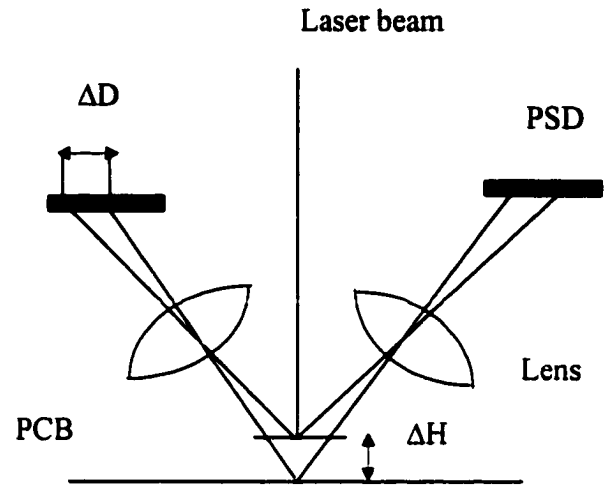


Figure 4-3 Laser triangulation

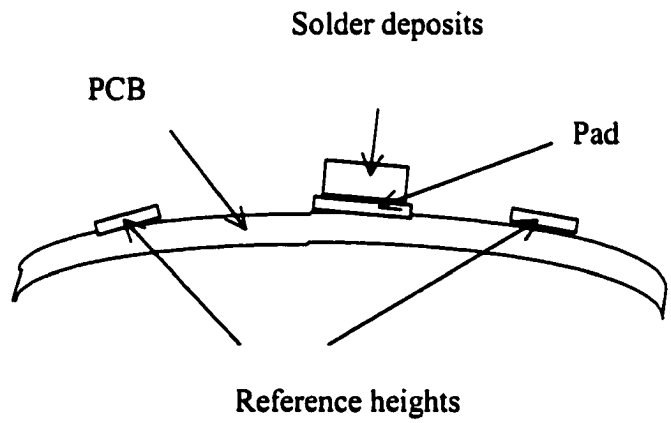


Figure 4-4 Board warpage with local reference heights and solder pad

Reproduced with permission of the copyright owner. Further reproduction prohibited without permission.

4.2.6 Gauge Repeatability Analysis of a 3-D Solder Paste Inspection System

A fully automatic laser-based 3-D triangulation solder paste inspection system is currently used for inspection of 0.635mm (25mil) pitch QFP components of automobile electronics products. As the pitch of QFP components decreases and the use of BGA components increases, the gauge repeatability of the inspection system must be reevaluated since the repeatability may relate to the mean level of measured value.

An experiment was conducted to investigate whether the system can be used successfully for measuring 0.4 mm (16 mil) and 0.3mm (12 mil) pitch QFPs and BGAs. A test board shown in Figure 4-1 featuring 0.76 mm (30 mil), 0.6 mm (25 mil), 0.5 mm (20 mil), 0.4 mm (16 mil), and 0.3 mm (12 mil) pitch QFP and BGA was designed. A total of 2,400 pads were on the board. In solder paste inspection, volume, area, and height of the solder paste deposited are considered important measurements. After stencil printing, the volume, area, and average height of solder paste deposited on all pads were measured by the 3-D inspection system 10 times. Therefore, a total of 72,000 data points were obtained for each board.

As mentioned in Section 4.2.4, gauge repeatability is defined as the scatter of standard variation of a set of measurements with respect to its average. The data manipulation for the repeatability test was performed on an Excel spreadsheet. The mean and standard deviation of a set of measurements on each pad were calculated. An X-Y chart of mean and standard deviation was then plotted. If all scattered points were below a line with a slope of 0.05, it meant the repeatability of the machine was less than 5%.

The repeatability chart of solder deposit volume is shown in Figure 4-5. The

Reproduced with permission of the copyright owner. Further reproduction prohibited without permission.

results indicated that there were three outliers and the repeatability was larger than 5% when mean volume was small. A microscope was used to measure the volumes of the three outlier deposits and it was found that the volumes measured by the inspection system were much lower than they should have been and the results were uncertain. After investigating and consulting the manufacturer of the inspection system, it was concluded that the uncertainty of these three deposit volumes might be due to improper reference point selection. Note that the reference points were automatically determined by the inspection system.

The repeatability charts of solder deposit area and average height are shown in Figure 4-6 and Figure 4-7. Figures 4-5, 4-6 and 4-7 show that the repeatability becomes unacceptable when the mean values are very small. After removing all data of the 0.3 mm (12 mil) and 0.4 mm (16 mil) pitch BGAs and the three outliers, the repeatability of volume, area, and average height are shown in Figures 4-8, 4-9, and 4-10. Results indicate that the system is capable of measuring the volume and area down to 0.3 mm (12 mil) pitch QFPs and 0.5 mm (20 mil) pitch BGAs within the repeatability of 5%, while the repeatability of height for all deposits is within 18% and for the majority of the pads is within 5%. It was observed that the heights of most 0.4 mm and 0.3 mm pitch BGAs measured by the system were zero. These pads were checked then by a microscope and it was found that there were solder deposits although some pads only had several solder particles. It was concluded that the system may consider all solder deposits lower than

Reproduced with permission of the copyright owner. Further reproduction prohibited without permission.

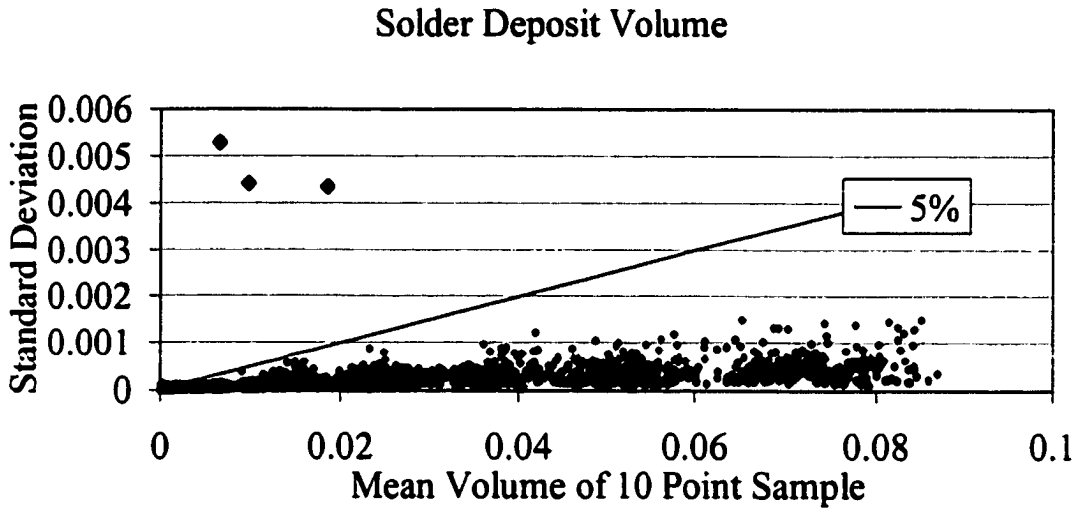


Figure 4-5 Repeatability of the Solder Deposit Volume

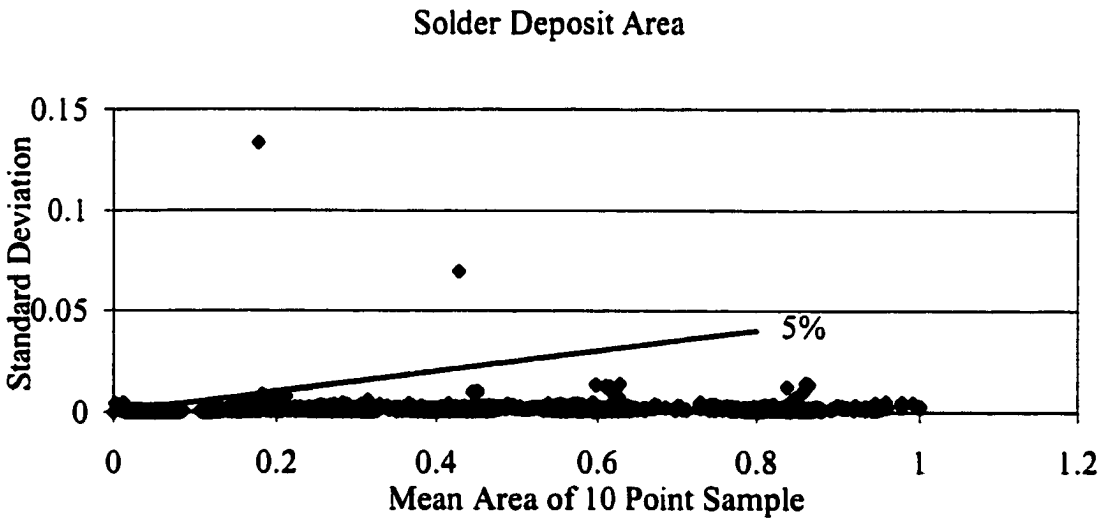


Figure 4-6 Repeatability of the Solder Deposit Area

Reproduced with permission of the copyright owner. Further reproduction prohibited without permission.

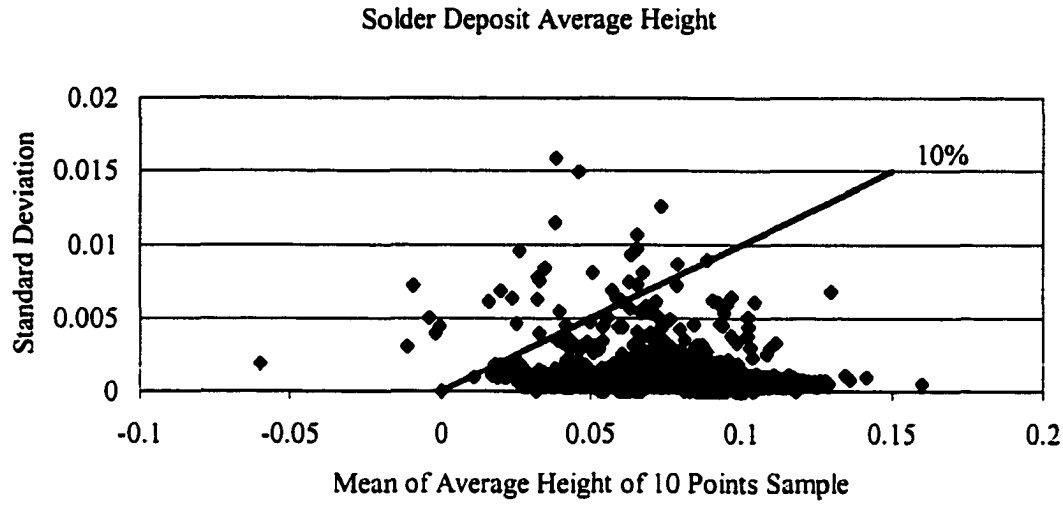


Figure 4-7 Repeatability of the Solder Deposit Average Height

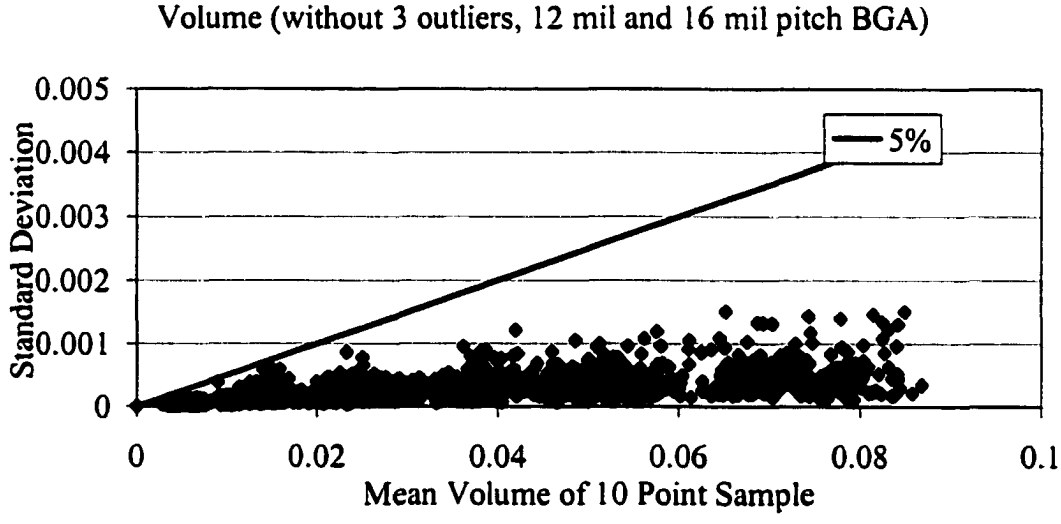


Figure 4-8 Repeatability of the Solder Deposit Volume

Reproduced with permission of the copyright owner. Further reproduction prohibited without permission.

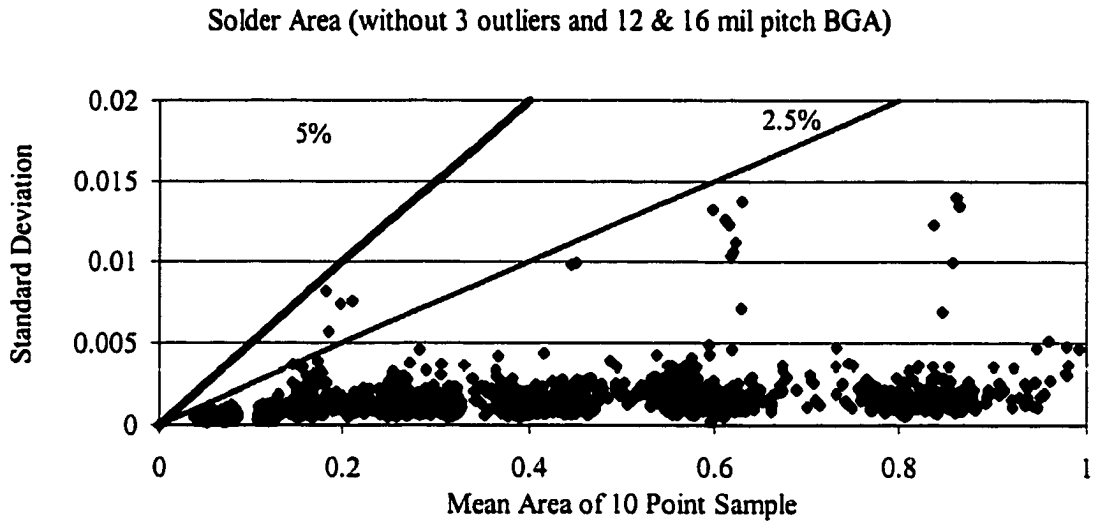


Figure 4-9 Repeatability of the Solder Deposit Area

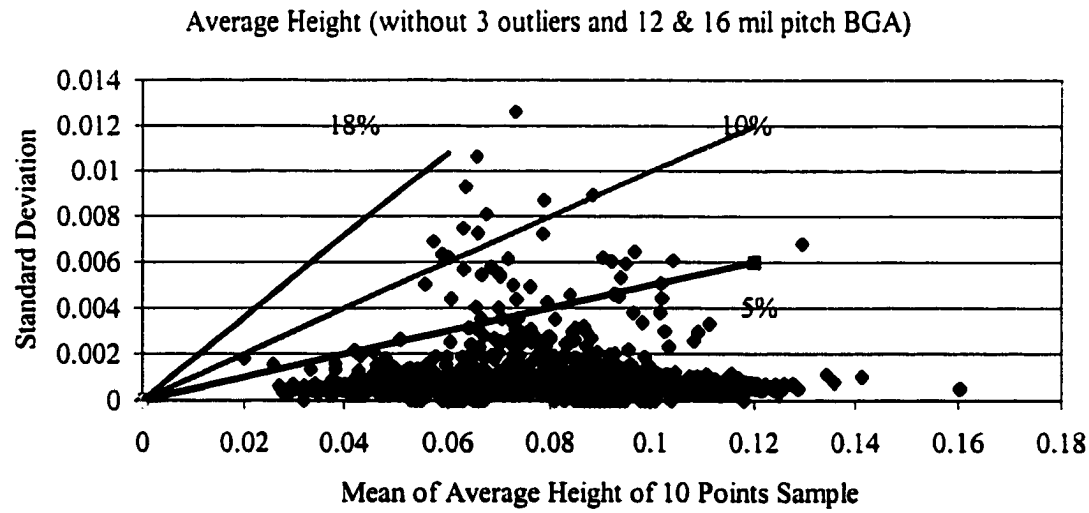


Figure 4-10 Repeatability of the Solder Deposit Average Height

Reproduced with permission of the copyright owner. Further reproduction prohibited without permission.

0.025 mm (1 mil) as zero. Therefore, the inspection system may be capable of measuring 0.4 mm and 0.3 mm pitch BGAs if more solder was deposited at the pads.

4.2.7 Conclusions

A method to estimate the repeatability of an automatic measurement system is discussed. A 3-D solder paste inspection system is analyzed and the results show that the system is capable of measuring solder deposits higher than 0.025 mm (1 mil) with repeatability of 5% for volume and area measurement and with repeatability of 5% for average height of the majority of pads and 18% for all pads. In addition, there are requirements in board design necessary to ensure the reference points for measurements can be specified close enough to the pads. These requirements depend on the measurement machine. For the machine in question, solder volume and area are better parameters to measure than solder height.

Reproduced with permission of the copyright owner. Further reproduction prohibited without permission.

5 Analysis and Discussion of Results

5.1 Residual check

Before analysis of variance (ANOVA), the adequacy of the model should be investigated. The adequacy of the model consists of the normality assumption, uniform variance, and independence of errors. The check of the normality assumption usually uses the normal probability plot. Figure 5-1 is the normal probability plot for the solder deposited volume of QFP. If the normality assumption is satisfied, the plot in Figure 5-1 will resemble a straight line. The general impression from examining the plot is that the line has heavy tails. So the plot is not completely normal. Fortunately, the F test is robust to the normality assumption in the fixed effects analysis of variance. The check of the uniform variance uses the plot of residual versus predicted value. The plot of residual versus predicted for the solder deposited volume of QFP is shown in Figure 5-2, which indicates that the uniform variance assumption is valid. The plot of residual versus experimental sequence is used to check the assumption of independence of errors. Figure 5-3 shows the plot of residual versus experimental sequence. There is no reason to suspect any violation of the independence assumption.

Reproduced with permission of the copyright owner. Further reproduction prohibited without permission.

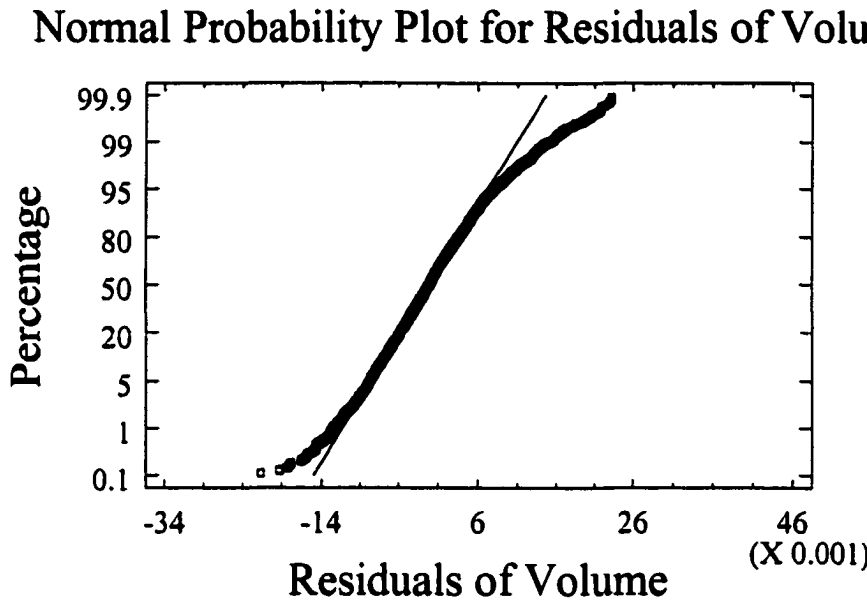


Figure 5-1 Normal probability plot for residuals of QFP solder deposited volume

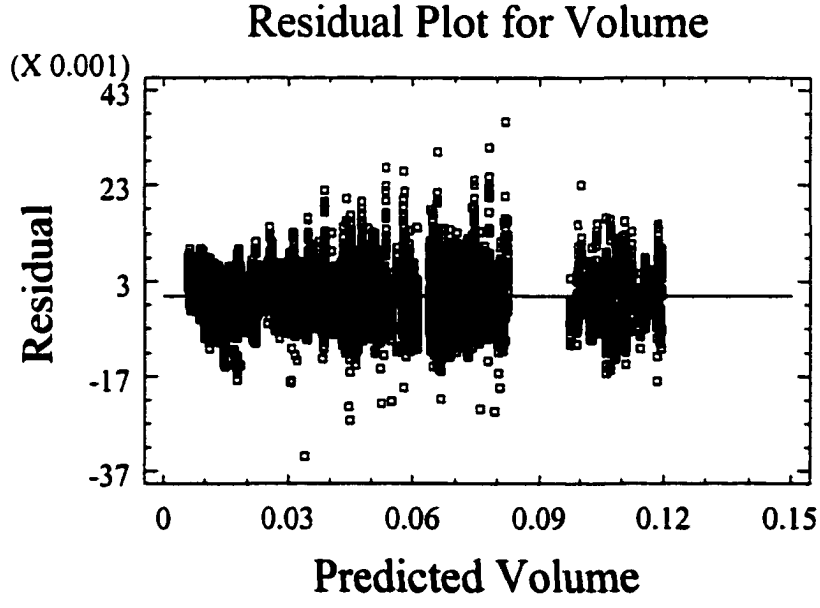


Figure 5-2 Plot of residual versus predicted values for solder deposited volume of QFP

Reproduced with permission of the copyright owner. Further reproduction prohibited without permission.

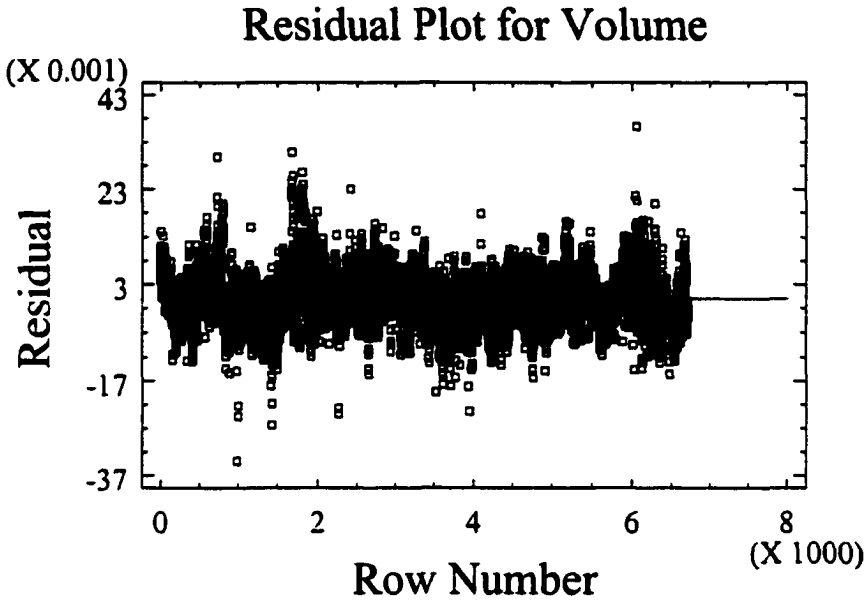


Figure 5-3 Plot of residual versus experimental sequence for QFP solder deposited volume

Reproduced with permission of the copyright owner. Further reproduction prohibited without permission.

It should be pointed out that the plots of residual versus all variables should also be checked. The residual versus pitch (or aperture width), stencil thickness, aperture shape, board finish, solder type, and print speed are shown in Figure 5-4, Figure 5-5, Figure 5-6, Figure 5-7, Figure 5-8, and Figure 5-9, respectively. The plot in Figure 5-4 indicate mild inequality of variance, with larger pitch having larger variance. The problem, however, is not severe enough to have a dramatic impact on the analysis and conclusions.

The assumption checks for the solder deposited volume of BGA are shown in Figure 5-10 to Figure 5-17. These plots do not reveal anything particularly troublesome with regard to the analysis and conclusions.

Another note is that data of BGA 0.3mm (12 mil) pitch and 0.4mm (16 mil) pitch and the three outliers caused by the measurement systems were removed before the analysis of variance. The removal of these outliers is justified in Section 4.2.6.

Reproduced with permission of the copyright owner. Further reproduction prohibited without permission.

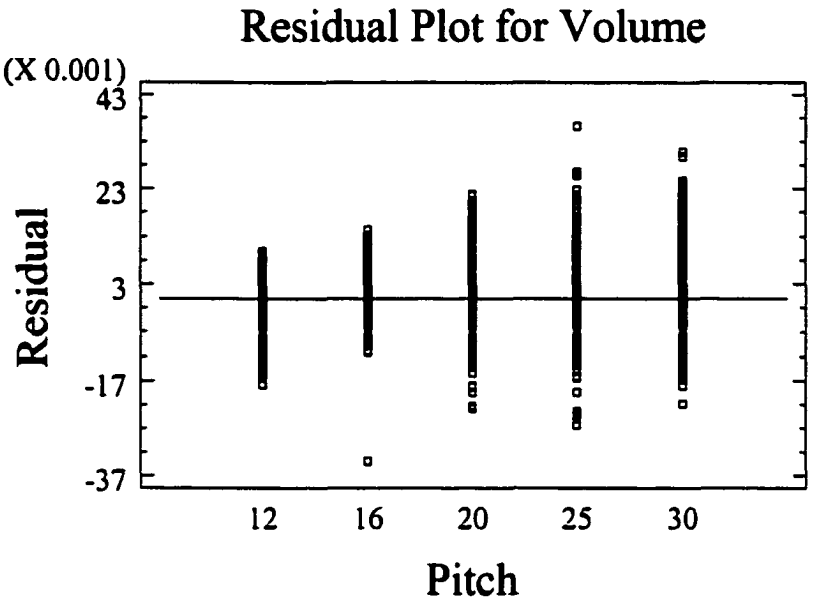


Figure 5-4 Plot of residual versus pitch (aperture width) for QFP solder deposited volume

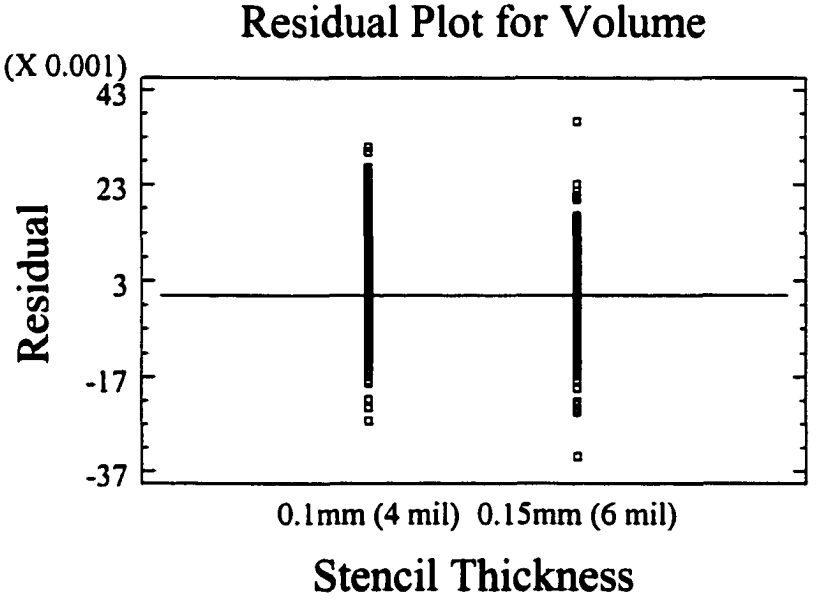


Figure 5-5 Plot of residual versus stencil thickness for QFP solder deposited volume

Reproduced with permission of the copyright owner. Further reproduction prohibited without permission.

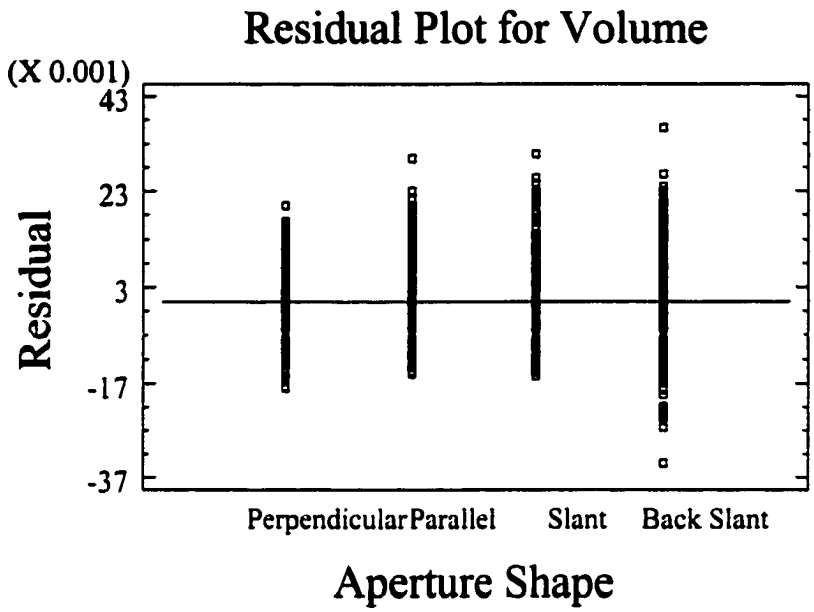


Figure 5-6 Plot of residual versus aperture shape for QFP solder deposited volume

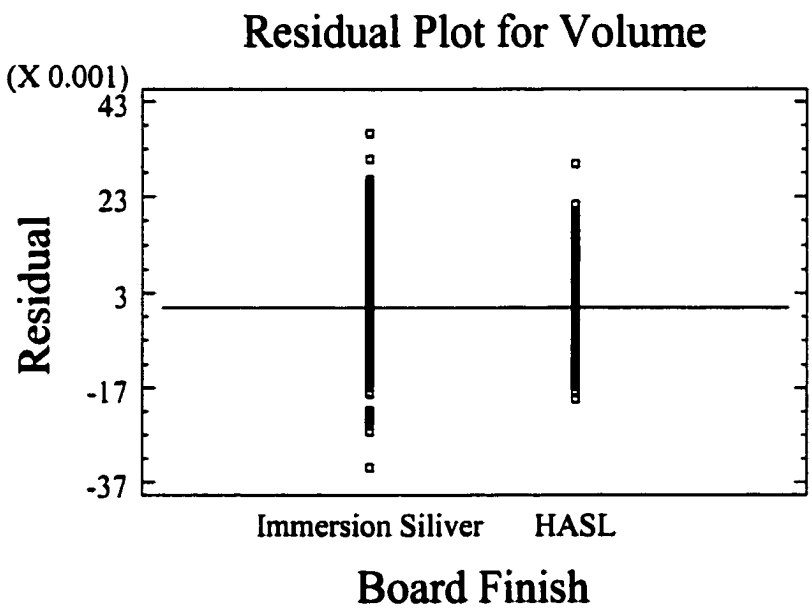


Figure 5-7 Plot of residual versus board finish for QFP solder deposited volume

Reproduced with permission of the copyright owner. Further reproduction prohibited without permission.

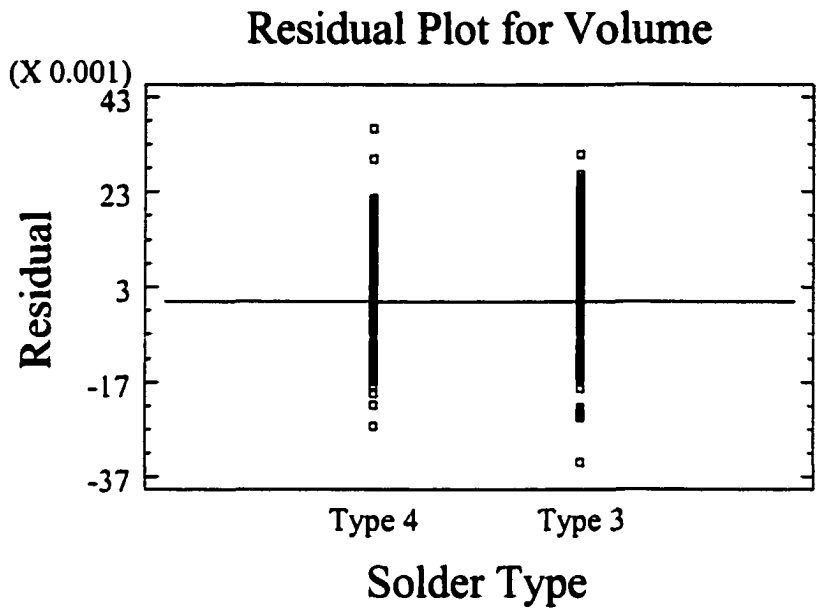


Figure 5-8 Plot of residual versus solder type for QFP solder deposited volume

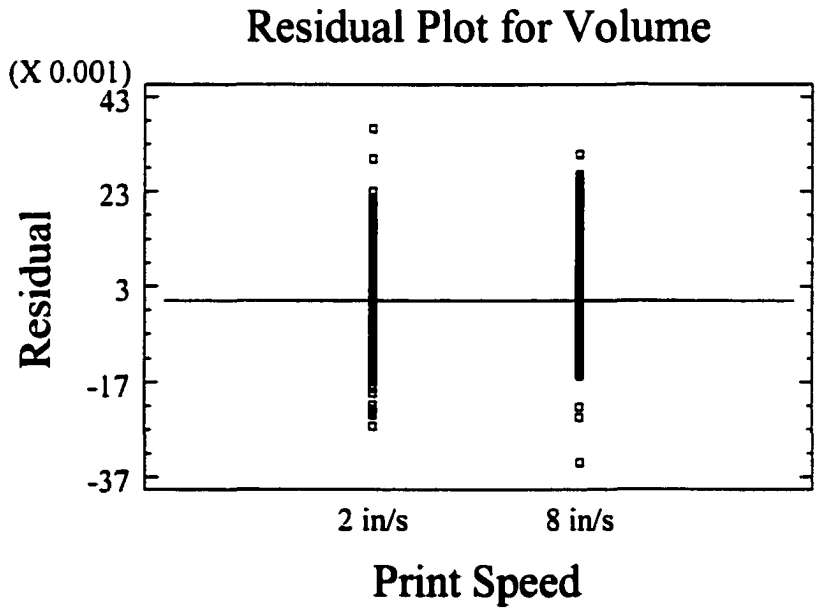


Figure 5-9 Plot of residual versus print speed for QFP solder deposited volume

Reproduced with permission of the copyright owner. Further reproduction prohibited without permission.

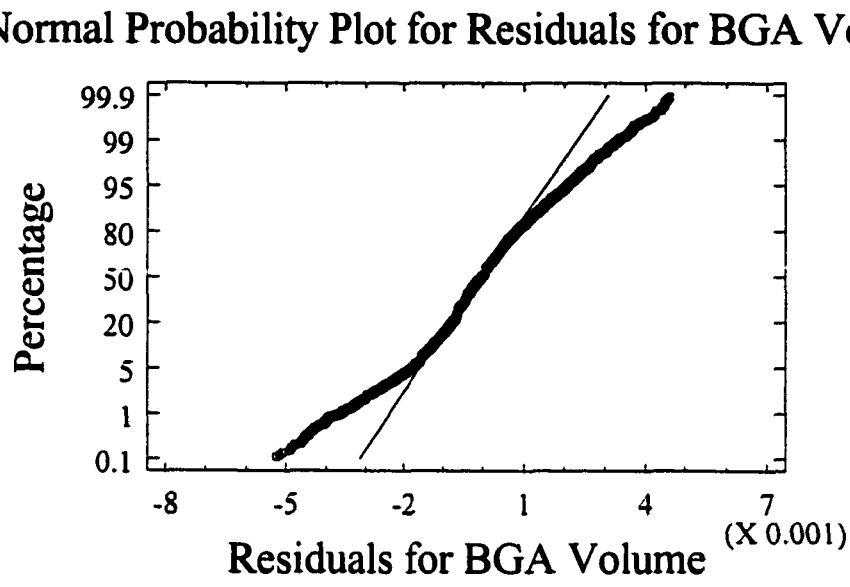


Figure 5-10 Normal probability plot for residuals of BGA solder deposited volume

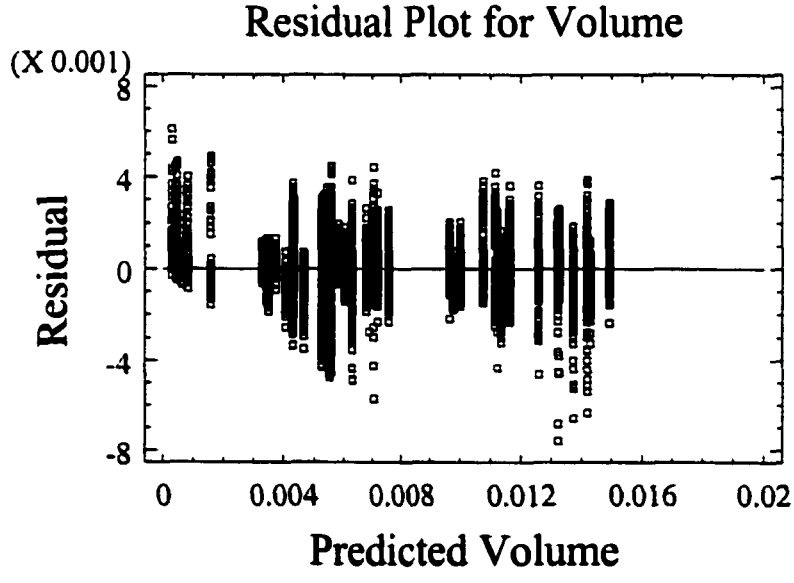


Figure 5-11 Plot of residual versus predicted values for solder deposited volume of BGA

Reproduced with permission of the copyright owner. Further reproduction prohibited without permission.

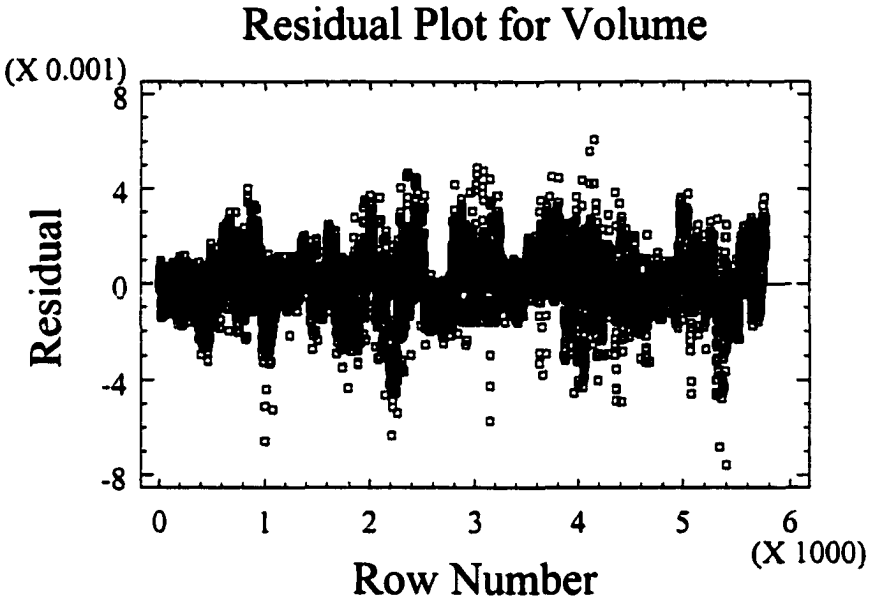


Figure 5-12 Plot of residual versus experimental sequence for BGA solder deposited volume

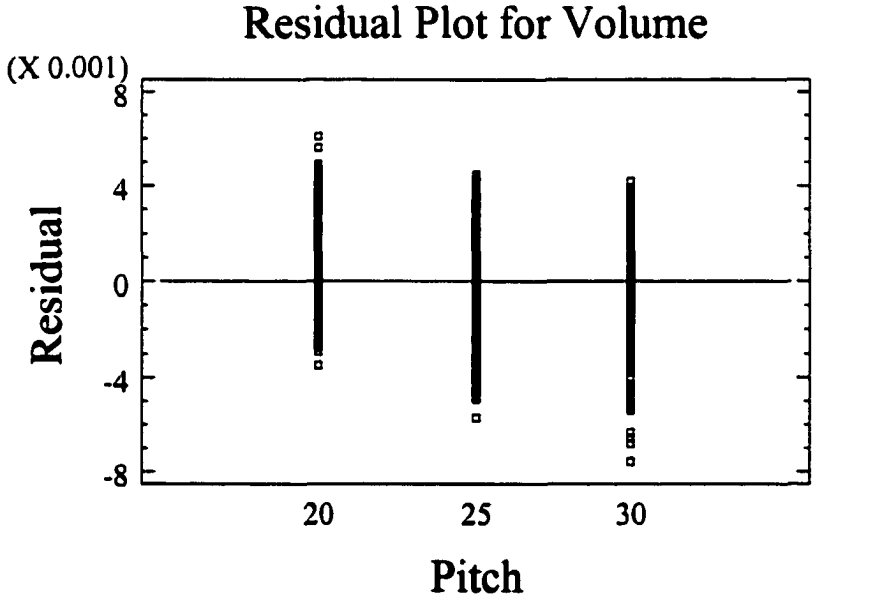


Figure 5-13 Plot of residual versus pitch (aperture width) for BGA solder deposited volume

Reproduced with permission of the copyright owner. Further reproduction prohibited without permission.

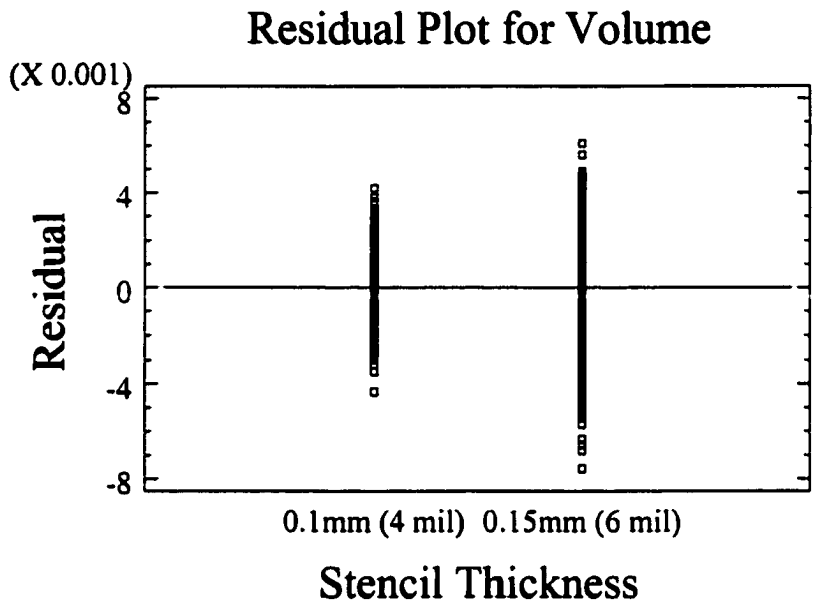


Figure 5-14 Plot of residual versus stencil thickness for BGA solder deposited volume

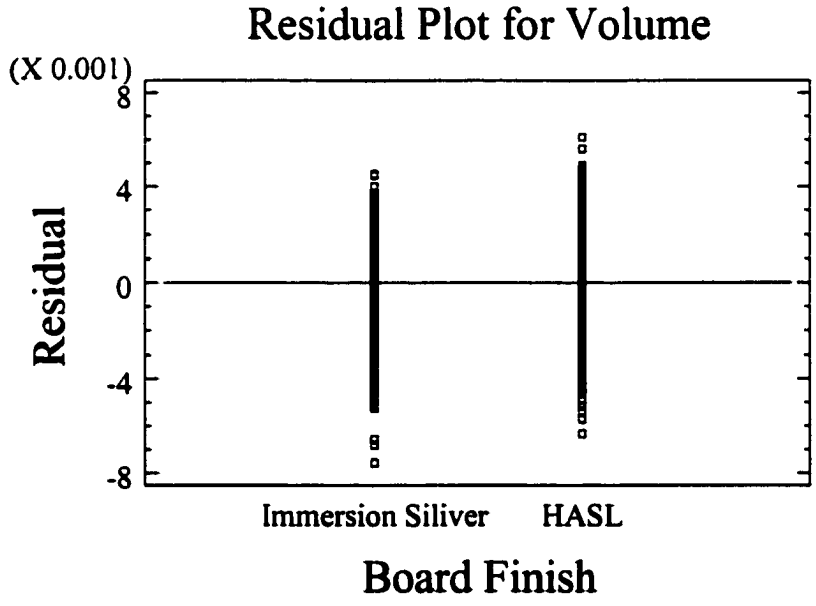


Figure 5-15 Plot of residual versus board finish for BGA solder deposited volume

Reproduced with permission of the copyright owner. Further reproduction prohibited without permission.

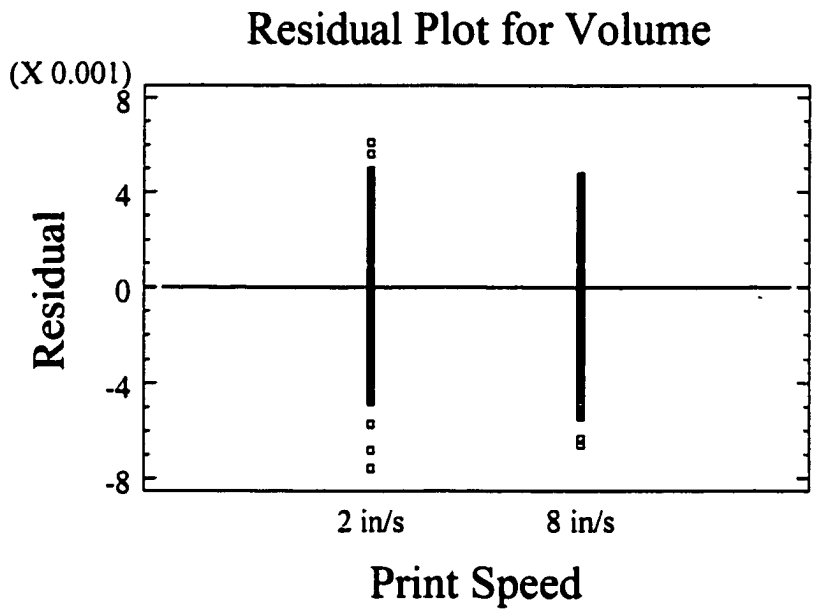


Figure 5-16 Plot of residual versus print speed for BGA solder deposited volume

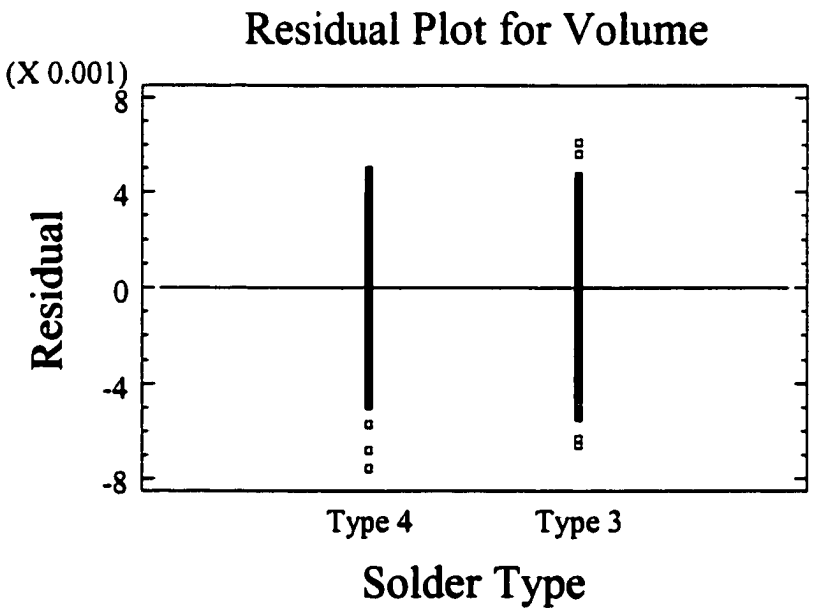


Figure 5-17 Plot of residual versus solder type for BGA solder deposited volume

Reproduced with permission of the copyright owner. Further reproduction prohibited without permission.

5.2 Analysis of the Data

5.2.1 Effects of Aperture Size and Stencil Thickness

The data were analyzed using Analysis of Variance (ANOVA). The ANOVA Table for the volume of solder paste deposited for QFP apertures is shown in Table 5-1. It shows that aperture size (pitch) and stencil thickness have statistically significant effects on the volume of solder deposited. It is intuitivly clear that a bigger aperture will result in more volume than a smaller one. One may think that a thicker stencil will deposit more volume than a thinner one as well. However, this is not always true. The interaction plot of QFP aperture size and stencil thickness in Figure 5-18 shows that the 0.1 mm (4 mil) stencil deposited more volume than the 0.15 mm (6 mil) stencil at the 0.3 mm (12 mil) pitch level. The ANOVA Table for the volume of solder paste deposited for BGA apertures is shown in Table 5-2. The interaction plot of BGA aperture size and stencil thickness in Figure 5-19 shows that the 0.1 mm (4 mil) stencil deposited more volume than the 0.15 mm (6 mil) stencil at the 0.5 mm (20 mil) pitch and 0.635 mm (25 mil) pitch level. Similar experimental results were reported by Fujiuchi and Toriyama (1994). They found that the bump volume with a stencil thickness of 60 μm was larger than that of a stencil thickness of 80 μm.

Reproduced with permission of the copyright owner. Further reproduction prohibited without permission.

Table 5-1 ANOVA for QFP solder deposited volume

Source	Sum of Squares	Df	Mean Square	F-Ratio
Main effect				
A:Pitch	4.77883	4	1.19471	40964.5
B:Stencil Thickness	0.542481	1	0.542481	18600.7
C:Aperture Shape	0.0174194	3	0.00580648	199.09
D:Board Finish	0.0057145	1	0.00571457	195.94
E:Solder Type	0.0001592	1	0.000159239	5.46
F:Print Speed	0.0056206	1	0.00562065	192.72
Interactions				
AB	0.364078	4	0.0910194	3120.90
AC	0.0098917	12	0.000824316	28.26
AD	0.0048905	4	0.00122264	41.92
AE	0.0003570	4	0.000089251	3.06
AF	0.0009143	4	0.000228578	7.84
BC	0.0267863	3	0.00892875	306.15
BD	0.0000281	1	0.000028188	0.97
BE	0.0128406	1	0.0128406	440.28
BF	0.0140634	1	0.0140634	482.21
CD	0.0024322	3	0.000810743	27.80
CE	0.0016842	3	0.000561407	19.25
CF	0.0037196	3	0.00123988	42.51
DE	0.0080697	1	0.00806978	276.70
DF	0.0017877	1	0.00178774	61.30
EF	0.0223297	1	0.0223297	765.65
Residual	0.194294	6662	0.000029164	
Total (Corrected)	6.01839	6719		

Reproduced with permission of the copyright owner. Further reproduction prohibited without permission.

Table 5-2 ANOVA for BGA solder volume

Source	Sum of Squares	Df	Mean Square	F-Ratio
Main Effects				
A:Pitch	0.0965794	2	0.0482897	28506.03
B:Stencil Thickness	0.000286738	1	0.000286738	169.27
C:Board Finish	0.000812605	1	0.000812605	479.69
D:Print Speed	0.0000336707	1	0.0000336707	19.88
E: Solder Type	0.0000108915	1	0.0000108915	6.43
Interactions				
AB	0.00990379	2	0.0049519	2923.17
AC	0.00016399	2	0.0000819951	48.40
AD	0.0000157014	2	0.0000078506	4.63
AE	0.000100836	2	0.000050418	29.76
BC	9.89627E-9	1	9.89627E-9	0.01
BD	9.85175E-7	1	9.85175E-7	0.58
BE	0.000355628	1	0.000355628	209.93
CD	0.000175921	1	0.000175921	103.85
CE	0.000120655	1	0.000120655	71.22
DE	0.000428299	1	0.000428299	252.83
Residual	0.00972196	5739	0.0000016940	
Total (Corrected)	0.118711	5759		

Reproduced with permission of the copyright owner. Further reproduction prohibited without permission.

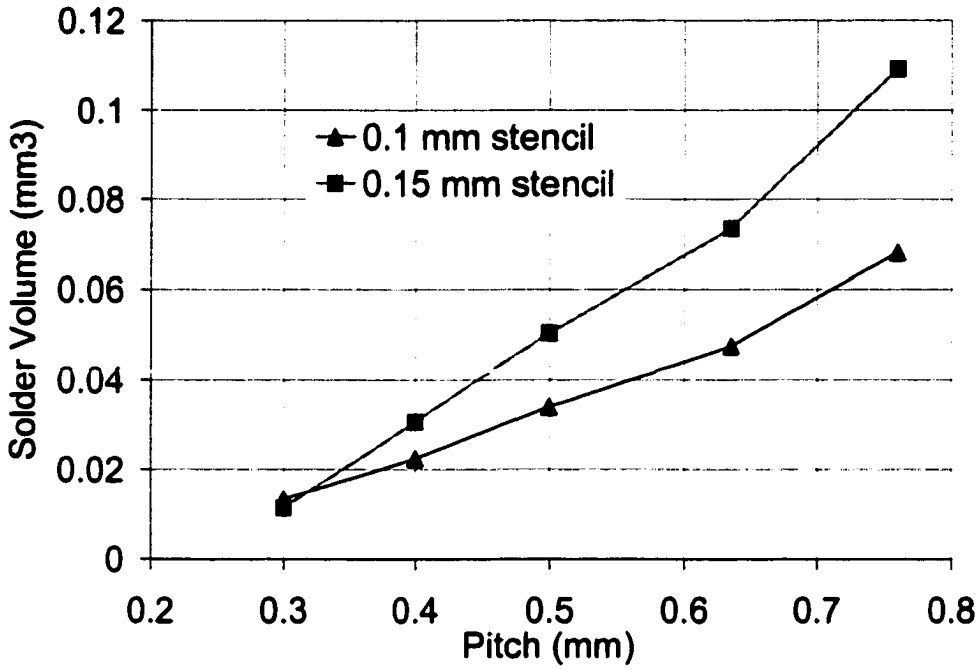


Figure 5-18 Interaction plot of QFP aperture size and stencil thickness

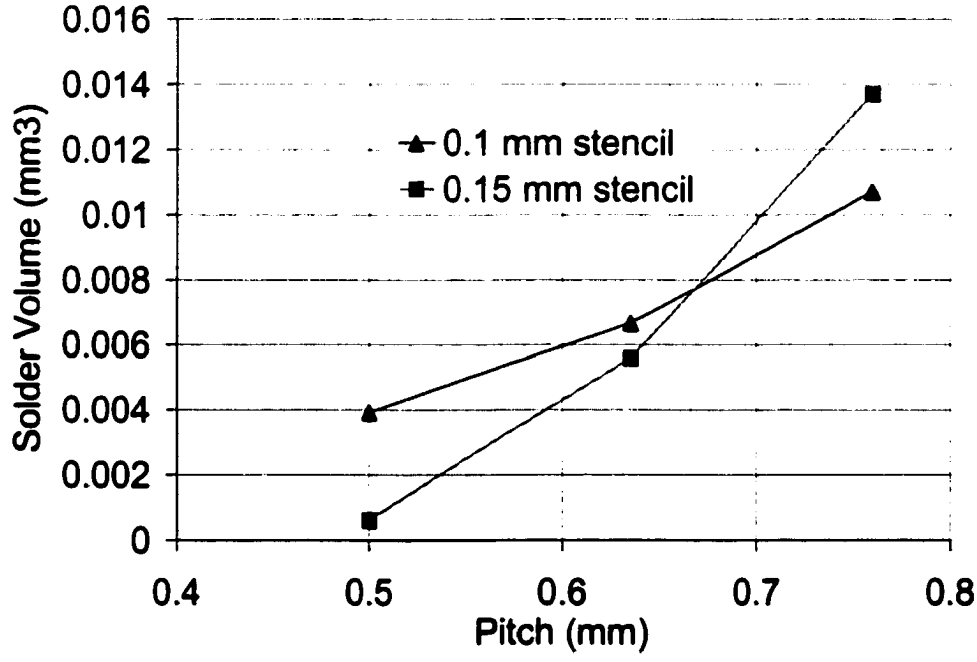


Figure 5-19 Interaction plot of BGA aperture size and stencil thickness

Reproduced with permission of the copyright owner. Further reproduction prohibited without permission.

Another analysis was performed using transfer ratio as the response variable. The ANOVA Table for transfer ratio of QFP apertures is shown in Table 5-3, and that of BGA apertures in Table 5-4. The results indicate that pitch (aperture size) and stencil thickness are still the critical variables since they have larger F-ratios. The interaction plot of QFP shown in Figure 5-20 illustrates that the transfer ratio of the 0.15 mm (6 mil) stencil increases as the pitch increases, while the transfer ratio of the 0.1 mm (4 mil) stencil remains constant as the pitch increases. The interaction of BGA in Figure 5-21 illustrates that the transfer ratio of the 0.15 mm (6 mil) stencil increases rapidly as the pitch increases, while that of the 0.1 mm (4 mil) stencil increases slowly as the pitch increases.

The relationship between transfer ratio and area ratio is shown in Figure 5-22. The calculation of area ratio and aperture volume is shown in Table 5-5. When AAR is larger than 0.6, the transfer ratio is a constant at about 0.9. When AAR is less than 0.6, the transfer ratio is proportional to the area aspect ratio. The difference between the model and experimental results can be explained by 2 facters. The first is that part of the paste is deposited outside of the pads of the PCB due to misalignment between the stencil and the PCB (the stencil apertures are designed the same size as the pad sizes of the PCB). The second is that part of the paste sticks to the inside of the stencil apertures. It was found that if the area ratio of BGA apertures equals that of QFP apertures, the two transfer ratios are also equal. That indicates that the relationship between transfer ratio and area ratio is independent of the aperture shape, at least for the two shapes considered.

Reproduced with permission of the copyright owner. Further reproduction prohibited without permission.

Table 5-3 ANOVA for QFP solder transfer ratio

Source	Sum of Squares	Df	Mean Square	F-Ratio
Main Effects				
A:Pitch	45.1981	4	11.2995	760.07
B:Stencil Thickness	8.72832	1	8.72832	587.11
C:Aperture Shape	3.8069	3	1.26897	85.36
D:Board Finish	1.12135	1	1.12135	75.43
E:Solder Type	0.163262	1	0.163262	10.98
F:Print Speed	4.11505	1	4.11505	276.80
Interactions				
AB	38.2819	4	9.57047	643.76
AC	2.05473	12	0.171228	11.52
AD	1.31444	4	0.328611	22.10
AE	0.169955	4	0.042488	2.86
AF	0.0960456	4	0.024011	1.62
BC	10.6912	3	3.56375	239.72
BD	0.34692	1	0.34692	23.34
BE	5.70317	1	5.70317	383.63
BF	6.96443	1	6.96443	468.46
CD	2.79318	3	0.931059	62.63
CE	1.16527	3	0.388423	26.13
CF	1.74029	3	0.580097	39.02
DE	4.14786	1	4.14786	279.01
DF	2.03097	1	2.03097	136.61
EF	9.25192	1	9.25192	622.33
Residual	99.0406	6662	0.014866	
Total (Corrected)	248.926	6719		

Reproduced with permission of the copyright owner. Further reproduction prohibited without permission.

Table 5-4 ANOVA for BGA solder transfer ratio

Source	Sum of Squares	Df	Mean Square	F-Ratio
Main Effects				
A:Pitch	217.495	2	108.748	5514.1
B:Stencil Thickness	259.224	1	259.224	13144.
C:Board Finish	8.79144	1	8.79144	445.78
D:Print Speed	0.294222	1	0.294222	14.92
E: Solder Type	0.0078316	1	0.00783164	0.40
Interactions				
AB	77.5489	2	38.7744	1966.0
AC	1.00898	2	0.504492	25.58
AD	0.158414	2	0.0792071	4.02
AE	0.791194	2	0.395597	20.06
BC	0.174292	1	0.174292	8.84
BD	0.0019776	1	0.00197768	0.10
BE	2.55086	1	2.55086	129.34
CD	1.73309	1	1.73309	87.88
CE	2.09363	1	2.09363	106.16
DE	6.17225	1	6.17225	312.97
Residual	113.182	5739	0.0197216	
Total (Corrected)	691.229	5759		

Reproduced with permission of the copyright owner. Further reproduction prohibited without permission.

Table 5-5 Area ratio (AAR) and aperture volume

Aperture shape	Pitch (mils)	Aperture size (mils)		Stencil thickness H(mils)	AAR (BGA: R/2H; QFP: LW/[2(L+W)H])	Aperture Volume ($10^{-3}mm^{-3}$)
		Diameter				
BGA	12	6		4	0.375	1.853
				6	0.25	2.780
	16	8		4	0.5	3.295
				6	0.33	4.942
	20	10		4	0.625	5.148
				6	0.42	7.722
	25	12		4	0.75	7.413
				6	0.5	11.12
	30	15		4	0.94	11.58
				6	0.625	17.37
		W	L			
QFP	12	6	40	4	0.65	15.732
				6	0.43	23.597
	16	8	50	4	0.86	26.219
				6	0.57	39.329
	20	10	60	4	1.07	39.329
				6	0.71	58.993
	25	12	70	4	1.28	55.061
				6	0.85	82.591
	30	15	80	4	1.58	78.658
				6	1.05	117.987

Reproduced with permission of the copyright owner. Further reproduction prohibited without permission.

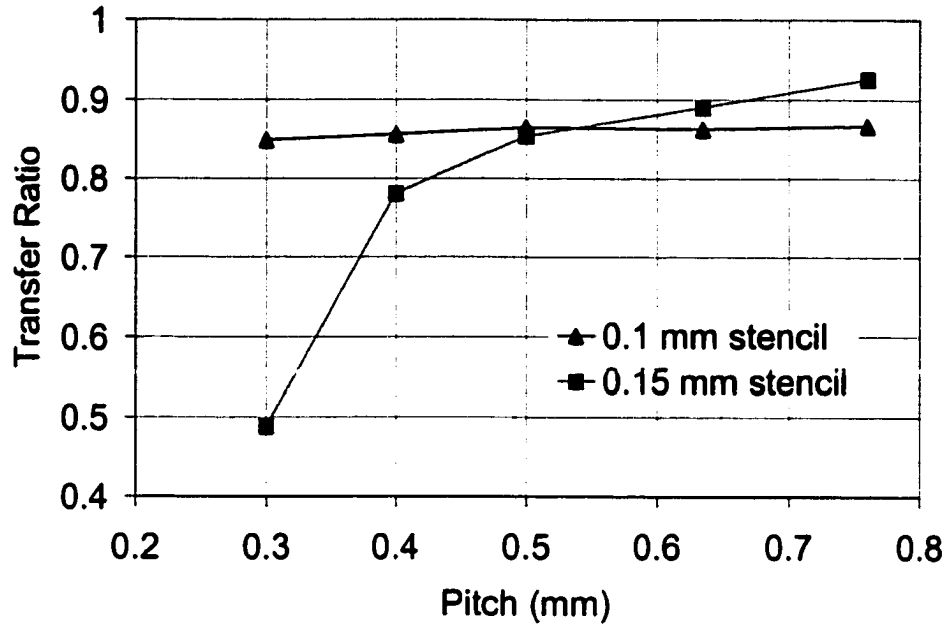


Figure 5-20 Transfer ratio vs. pitch for QFP apertures

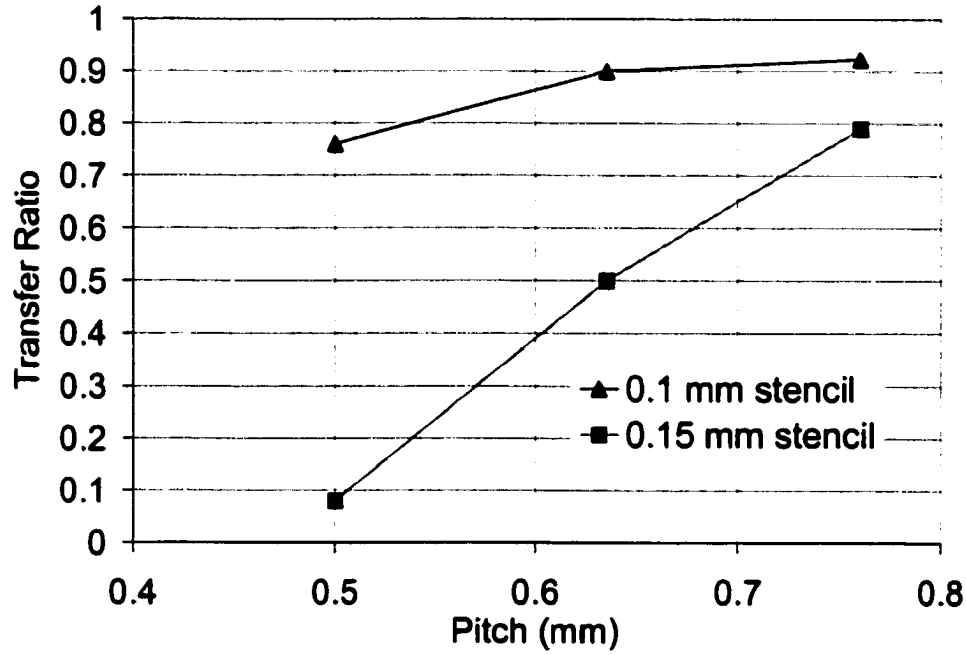


Figure 5-21 Transfer ratio vs. pitch for BGA apertures

Reproduced with permission of the copyright owner. Further reproduction prohibited without permission.

Figure 5-22 gives the critical area ratio of 0.6 when the squeegee attack angle is 45 degrees and the seal condition between the squeegee and the stencil is very good. The maximum stencil thickness for a specified aperture size can be calculated based on the critical area ratio. In industry, different guidelines have been published. For example, Wilson and Bloomfield (1995a, 1995b) suggested an optimal aspect ratio of 1.25. Coleman (1996) recommended larger than 1.5 for the aspect ratio and larger than .66 for the area ratio. Markstein (1997) proposed the generally accepted rule that the aspect ratio be larger than 1.5 (1.8 for chemically etched stencils and 1.2 for electropolished laser-cut and electroformed stencils). Here the aspect ratio is defined as the width of the aperture divided by the height of the aperture (or the thickness of the stencil). It should be pointed out that the critical area ratio depends on the squeegee attack angle and the seal condition between the squeegee and the stencil according to our model.

Stencil thickness has its lower bound also. Analysis shows that the area of solder deposits increases slightly as the stencil thickness decreases. It indicates that too thin a stencil could cause solder bridges. On the other hand, the decrease in stencil thickness results in a decrease of the aperture volume. The objective of solder deposition is to transfer a certain amount of solder paste to the PCB. Insufficient solder paste resulting from thinner stencils may cause solder opens. Therefore, a lower bound exists to achieve acceptable solder volume and area. In order to avoid solder bridges and solder opens, stencil thickness must be chosen larger than this lower bound.

The transfer ratio of the average experimental data in Figure 5-22 is smaller than that of the theoretical model. This is because the points in Figure 5-22 are the overall

Reproduced with permission of the copyright owner. Further reproduction prohibited without permission.

average of experimental data that have the same area ratio. Figure 5-23 shows that the average volume in solder paste deposited could be larger than aperture volume in some combinations of printing process variables. The points in each column in Figure 5-23 represent the average of the data that have the same area ratio in different experimental runs and different QFP aperture shapes. It was also found that some solder paste sticks to the aperture sidewall of the stencil when area ratio is less than 0.6. This is why almost all of the experimental points are less than the theoretical model predicts when the area ratio is less than 0.6. When the area ratio is greater than 0.6, a much smaller proportion of solder paste sticks to the sidewall.

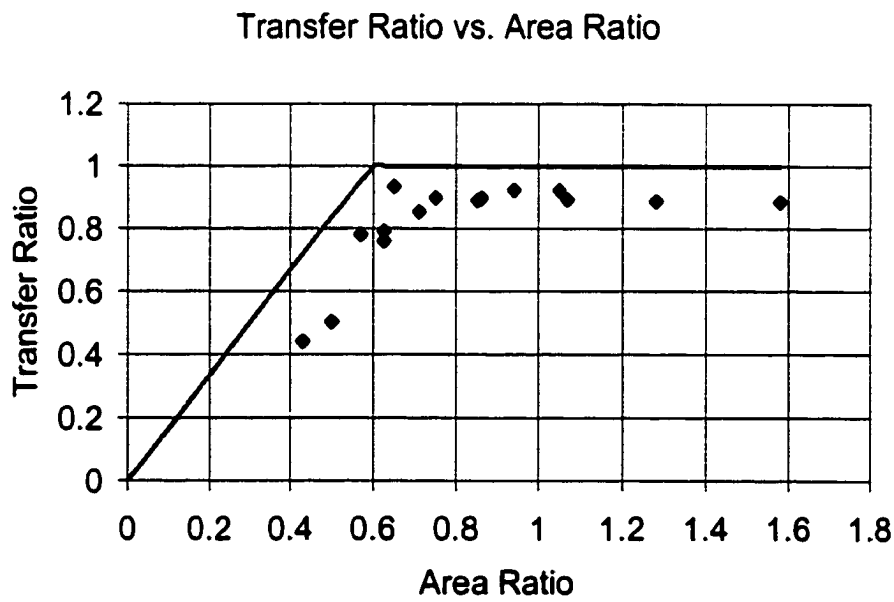


Figure 5-22 Comparison of the model and experimental results (points: the overall average of experimental data that have the same area ratio; line: model)

Reproduced with permission of the copyright owner. Further reproduction prohibited without permission.

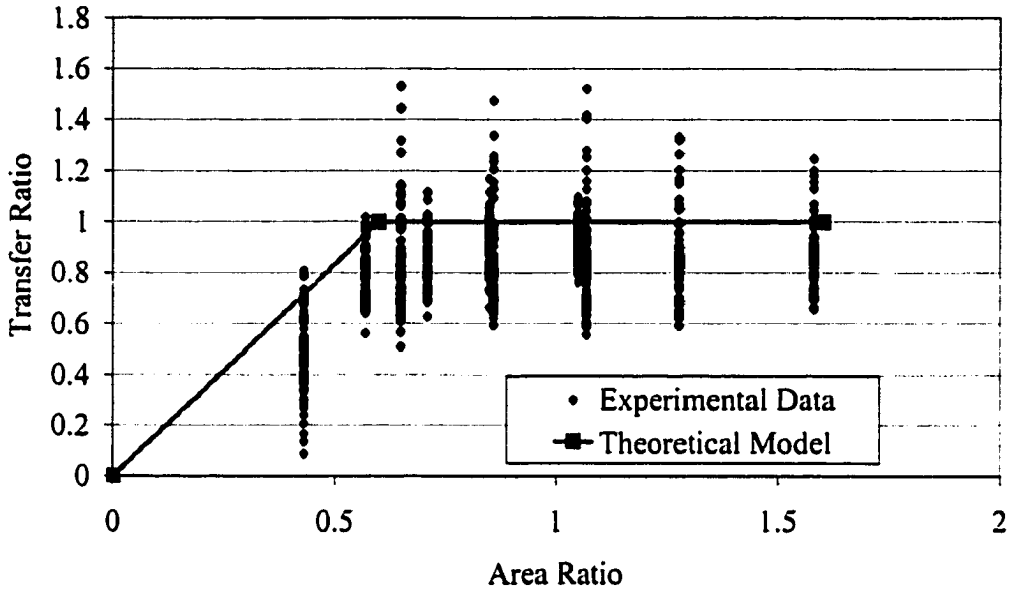


Figure 5-23 Comparison of the model and experimental results (points: the average of experimental data that have the same area ratio in different experimental runs and different QFP aperture shapes; line: model)

Reproduced with permission of the copyright owner. Further reproduction prohibited without permission.

5.2.2 Effects of Aperture Orientation

The plot of the mean of deposited solder volume versus aperture orientation is shown in Figure 5-24. It indicates that perpendicular apertures (longer side of the apertures perpendicular to the squeegee travel direction) deposit 8-9% more volume than parallel apertures, while the volume difference between slant apertures and back slant apertures is much smaller. The actual aperture sizes of the two stencils were measured by a microscope since the information of aperture shape was confounded in this experiment. It was found that the perpendicular apertures were slightly (about 3%) wider than the parallel apertures. There is no statistically significant difference between the slant aperture sizes and the back slant aperture sizes. Deducting the aperture size difference, perpendicular apertures print 5-6% more volume than parallel apertures. Analysis on the height of solder deposits draws the same conclusion. This is a well known experimental phenomena [Hannan, et al., 1994; Markstein, 1997]. It can be concluded that arranging the squeegee at 45 degrees with respect to the stencil apertures would decrease the variation of the height and volume of the solder deposits.

Reproduced with permission of the copyright owner. Further reproduction prohibited without permission.

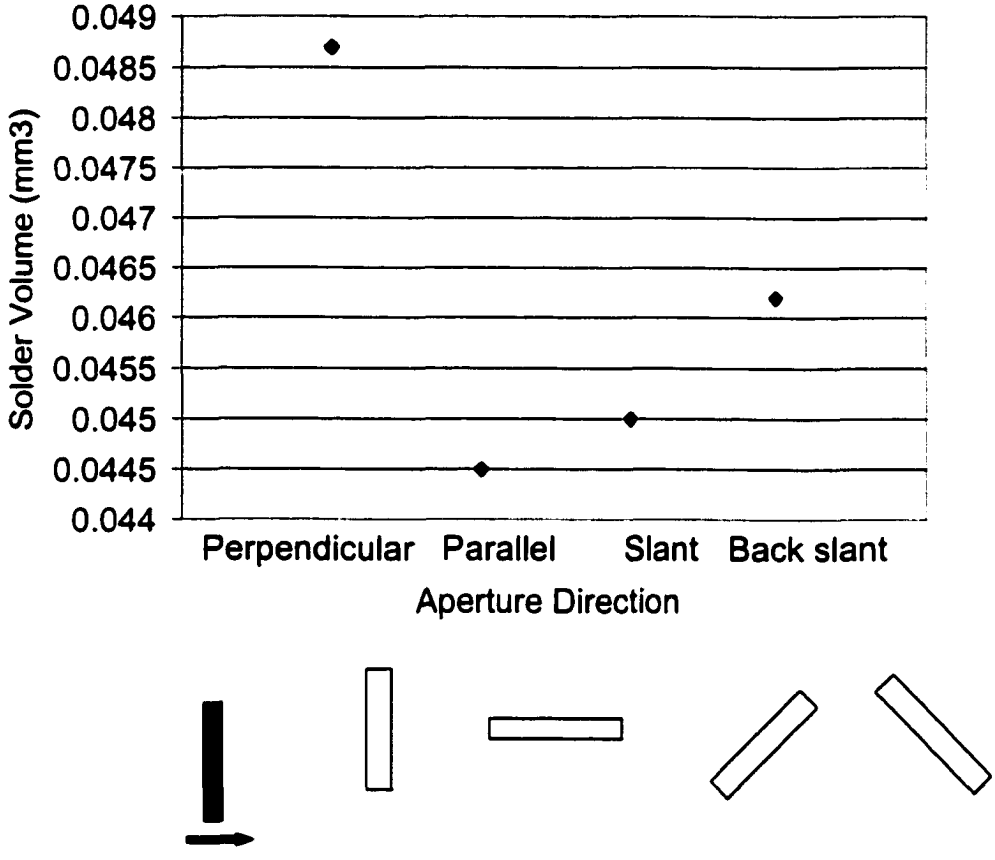


Figure 5-24 Solder volume vs. aperture orientation

Reproduced with permission of the copyright owner. Further reproduction prohibited without permission.

5.2.3 Effects of Solder Paste and Print Speed

The effect of print speed has confused many engineers because conflicting experimental results have been reported. Mannan, et al. (1994) found a linear rise in paste height with squeegee velocity during stencil printing. Wilson and Bloomfield (1995a, 1995b) reported no noticeable deterioration in print height in print speeds from 25 mm per second to approaching 200 mm per second.

The ANOVA analysis in Tables 5-5, 5-6, and 5-7 shows that a strong interaction exists between solder paste and print speed. The interaction plots of solder paste and print speed for QFP apertures and BGA apertures are shown in Figure 5-25 and Figure 5-26, respectively. They indicate that the transfer ratio of solder type 3 increases rapidly as the print speed increases while that of solder type 4 decreases slightly as the print speed increases. It can be concluded that the selection of optimal print speed should be based on solder paste type and that print speed could be used to adjust the volume, area, and height of solder deposits.

From the ANOVA tables, it seems that solder paste does not have a significant effect on the amount of solder paste deposited. From the interaction plots in Figure 5-25 and Figure 5-26, it is difficult to draw the conclusion that solder paste does not have a significant effect because a strong interaction exists between solder type and print speed. Further investigation should be conducted by selecting three levels of print speed.

Reproduced with permission of the copyright owner. Further reproduction prohibited without permission.

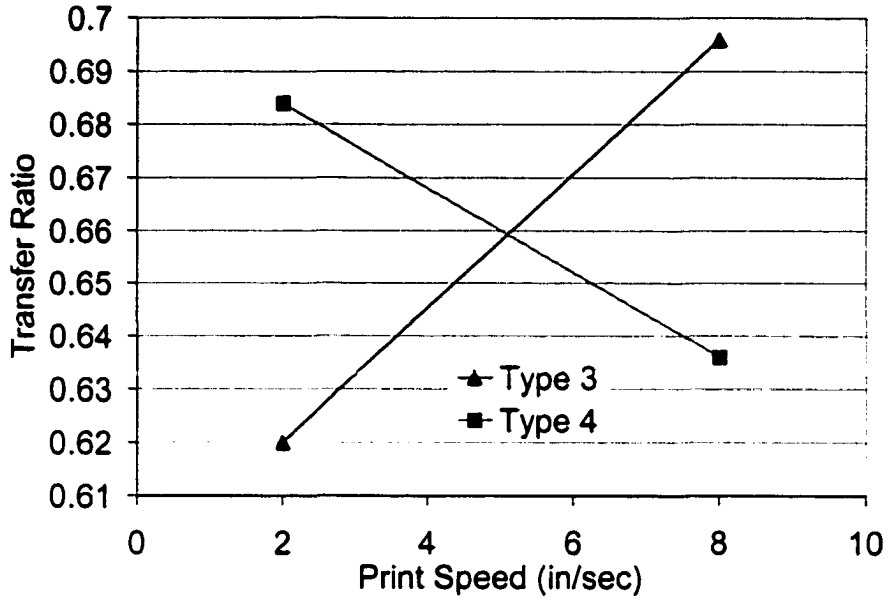


Figure 5-25 Interaction plot of solder type and print speed for QFP apertures

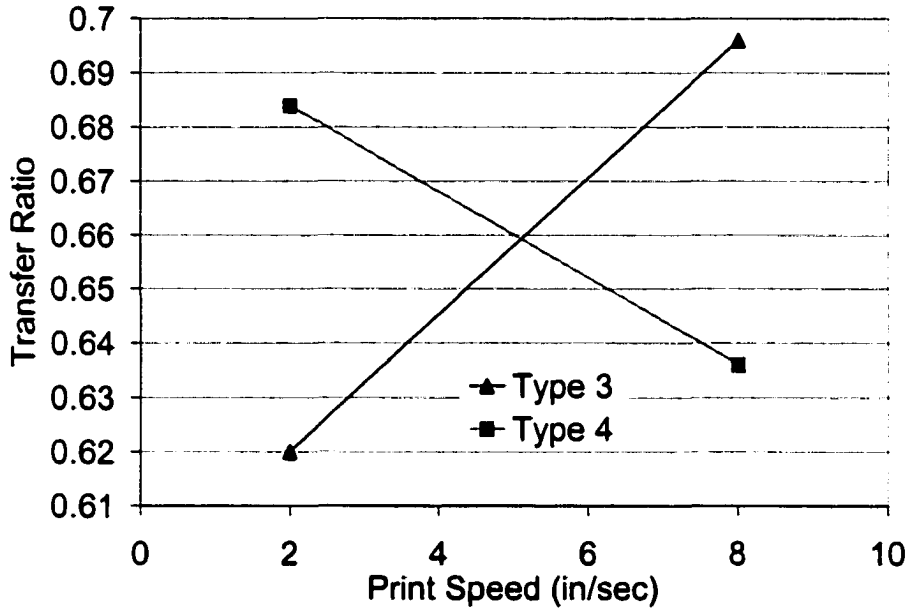


Figure 5-26 Interaction plot of solder type and print speed for BGA apertures

Reproduced with permission of the copyright owner. Further reproduction prohibited without permission.

This experimental phenomena may be explained as follows: the amount of solder paste deposited is determined by the aperture opening size and paste pressure generated. The paste pressure is proportional to the viscosity of solder paste times the print speed (Pan and Tonkay, 1999). Since solder paste is a non-Newtonian fluid, its viscosity changes with the change of shear rate. High print speeds result in a high shear rate so that the viscosity of the paste decreases. The result of the solder viscosity times the print speed depends on the solder rheology (the change in viscosity versus the shear rate). Different solder pastes have different rheologies. This is why an interaction exists between solder paste and print speed.

5.2.4 Effects of Board Finish

The relationship between the transfer ratio of deposited solder paste and the board finish for different pitches of QFP and for BGA are shown in Figure 5-27 and Figure 5-28, respectively. They indicate that more solder paste was deposited on HASL boards when the area of the aperture opening was small (all BGA apertures and 0.3 mm pitch QFP apertures) while more solder paste was deposited on silver boards when the area of the aperture opening was large (larger than 0.3 mm pitch QFP apertures).

One important consideration in board finish is flatness of the board surface. Generally, boards with immersion silver have a better surface flatness than boards with HASL. The area of solder paste deposited on HASL boards is found always slightly larger than that on silver boards. This may be due to the dome shape of HASL boards. The smooth surface with immersion silver allows the stencil to seal against the pad of the

Reproduced with permission of the copyright owner. Further reproduction prohibited without permission.

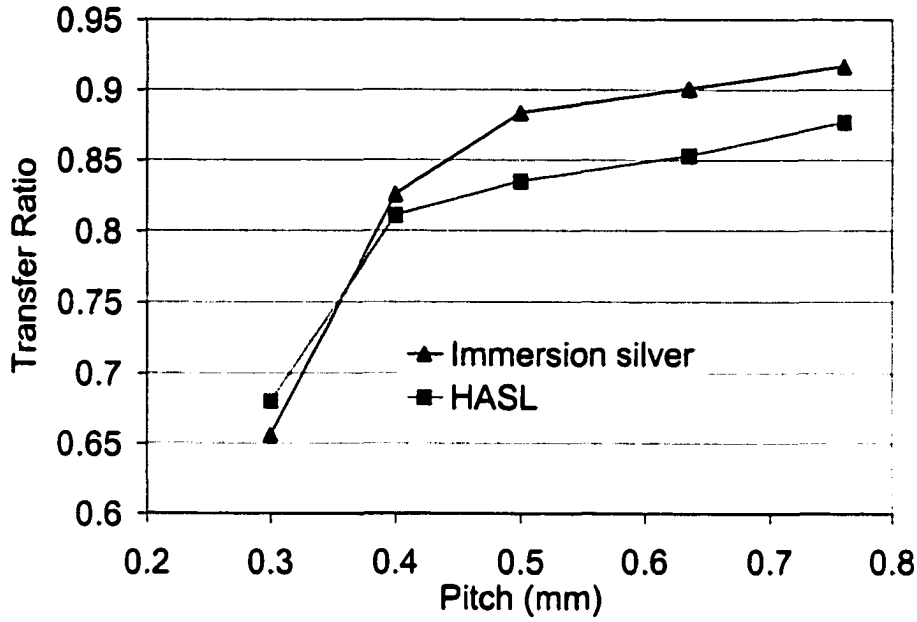


Figure 5-27 Transfer ratio vs. board finish for QFP apertures

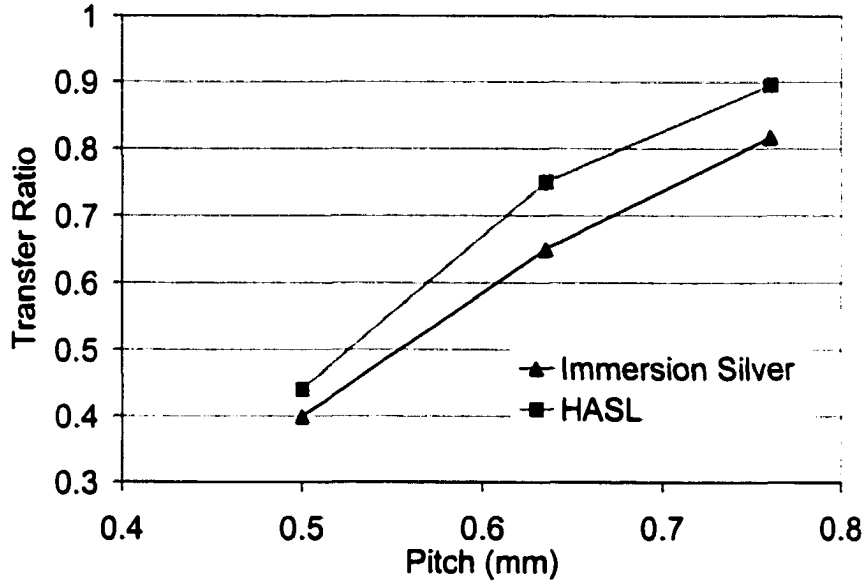


Figure 5-28 Transfer ratio vs. board finish for BGA apertures

Reproduced with permission of the copyright owner. Further reproduction prohibited without permission.

board and to prevent paste from forming solder bridging.

5.3 CONCLUSIONS

The following conclusions are drawn from our analysis:

1) The most critical process variables influencing the amount of solder paste deposited are aperture size and stencil thickness.
2) The transfer ratio is determined by the area ratio. Thicker stencils do not necessarily result in higher solder prints. An area ratio of larger than 0.6 is recommended for the selection of a proper stencil thickness.
3) A strong interaction between print speed and solder paste type indicates that a proper print speed should be selected depending on the solder paste type.
4) A perpendicular aperture prints higher and more volume than a parallel aperture. Aperture orientation of 45 degrees and 135 degrees with respect to the squeegee can decrease the variation of solder deposits.
5) Small apertures print more solder volume on HASL boards than that on immersion silver boards and big apertures print more solder volume on immersion silver boards than that on HASL boards.

Reproduced with permission of the copyright owner. Further reproduction prohibited without permission.

6 Conclusions and Future Research

6.1 Conclusions

Stencil printing is one of the most cost-effective solder paste deposition processes for surface mount assembly, chip scale packaging (CSP), ball grid array (BGA), and flip chip assembly. Though the technology is mature for traditional surface mount assembly (1.27 mm or 50 mil pitch level), it is still not completely understood for fine pitch surface mount assembly, chip scale packaging, ball grid array, and flip chip assembly. With the emergence of high-volume production of CSP and flip chip, stencil printing for these advanced packages becomes a hot research area.

The objectives of this research as presented in Chapter 1 can be summarized as follows:

1) Develop an analytical model to explain the mechanisms of the stencil printing process.
2) Identify the critical process variables based on the model.
3) Validate the model by designing and conducting an experiment.
4) Optimize the stencil printing process.

In order to reach the goals of the project, the research was divided into several phases. First, the process was modeled using fluid mechanics theory or transport process theory. Second, an experiment was designed to validate the model. Third, the

Reproduced with permission of the copyright owner. Further reproduction prohibited without permission.

measurement capability of an inspection system was evaluated in order to obtain data that accurately represent real product dimensions. Finally, the data were analyzed by ANOVA. The experimental results were found to be consistent with the model.

An analytical model has been developed for the deposition process of stencil printing. The model consists of two parts: the paste travel process and the aperture filling process. In the paste travel process, the stream function of solder paste was derived and the streamlines were drawn. The shear rate and pressure in the solder paste at the stencil surface were calculated. In the aperture filling process, the amount of solder paste that could be deposited into the stencil apertures was calculated. The results showed that aperture opening size and paste pressure generated by the squeegee travel determine the amount of solder paste deposited. The volume of paste deposited is independent of the stencil thickness when the deposited volume is less than the aperture volume. The relationship between paste transfer ratio and area ratio was then determined. Area ratio is recommended as a main indicator for determining the thickness of a stencil. The proper selection of squeegee pressure, squeegee angle, and squeegee hardness were also discussed. The model explained two experimental phenomena. One is that increasing stencil thickness does not always increase the thickness of paste deposited. The other is perpendicular apertures (longer side of the apertures perpendicular to the squeegee travel direction) print thicker paste deposits than parallel apertures. The model also shows that stencil planarity, PCB board planarity, and squeegee parallelism are required to generate the high pressure to inject the paste into the aperture.

A 3 x 3 Latin square experiment was designed and conducted to validate the

Reproduced with permission of the copyright owner. Further reproduction prohibited without permission.

model and optimize the stencil printing process. Six process variables were selected in the experiments and they were aperture size, aperture shape, board finish, solder paste type, print speed, and stencil thickness. The experimental results showed that the transfer ratio is determined by the area ratio and an area ratio of larger than 0.6 is recommended for the selection of a proper stencil thickness. The critical process variables influencing the amount of solder paste deposited are aperture size and stencil thickness. The experimental results were found to be consistent with the model. The experimental results also showed that a strong interaction exists between print speed and solder paste type. This infers that a proper print speed should be selected depending on the solder paste type. Small apertures print more solder volume on HASL boards than on immersion silver boards and big apertures print more solder volume on immersion silver boards than on HASL boards. Solder deposits on HASL boards cover more area than that on immersion silver boards. This infers that immersion silver boards are better in fine pitch printing.

The volume, area, and height of solder paste deposited were measured by a 3-D solder paste inspection system. In this study, a method to estimate the repeatability of a measurement system is discussed and the repeatability of the 3-D solder paste inspection system was analyzed.

6.2 Important Contributions

As a result of this research, the following important contributions have been made:

Reproduced with permission of the copyright owner. Further reproduction prohibited without permission.

1) An analytical model of the deposition process was proposed. The proposed model was validated by experiment.
2) Two experimental phenomena were explained. One is that increasing stencil thickness does not always increase the thickness of paste deposited. The other is that perpendicular apertures print higher than parallel apertures.
3) A method to estimate the repeatability of a measurement system is discussed.
4) The repeatability of a 3-D solder paste inspection system was analyzed.
5) The critical variables that influence the solder paste stencil printing process were identified.
6) Interactions between process variables were determined.
7) Since stencil printing can also be used for flip chip underfill deposition and conductor adhesive deposition, this study will accelerate the development and utilization of flip chip assembly.
8) By understanding the mechanism and process optimization of the solder paste printing process, this research will

- Improve surface mount assembly and flip chip yield
- Reduce defects
- Reduce rework
- Reduce labor cost for rework, inspection, and test
- Enhance time-to-market

Reproduced with permission of the copyright owner. Further reproduction prohibited without permission.

6.3 *Future Research*

There are many aspects of this research which could be explored further. In the modeling of the stencil printing process, solder paste is assumed to be a newtonian fluid. More rigorous models could be developed without the newtonian flow approximation. For example, modeling the solder paste as a power-law flow will be more accurate. However, analytical solution is difficult to obtain in a power-law model and simulation is necessary.

Another aspect is to calculate how much solder paste sticks to the inside of the stencil sidewall. This study involves the aperture filling process and the stencil release process. The mechanics of the stencil printer should be considered in the study. For example, Panasonic's stencil printer generates a small vibration during the release process. In theory, this will help the paste release from the stencil. Most other stencil printers do not use this vibration.

There are several other extensions that can be made to the experiments to investigate the effect of additional factors such as stencil release speed and squeegee angle, and more levels of the factors.

The stencil printing model developed in this study is applicable to flip chip underfill deposition and conductive adhesive deposition. Designing and conducting similar experiments in these areas are their possible enhancements.

Reproduced with permission of the copyright owner. Further reproduction prohibited without permission.

Bibliography

Austin, Benson M. (1969). "Thick-Film Screen Printing." *Solid State Technology*. June 1969, pp. 53 – 58.

Bacher, Rudolph J. (1986). "High Resolution Thick Film Printing." *Proceedings of the International Symposium on Microelectronics*. p. 576 – 581.

Brathwaite, Nicholas E. (1998). "CMs must Take the Technology Lead." *SMT*. Vol. 12, No.11, p.88-93.

Bratin, Peter; Pavlov, Michael; and Chalyt, Gene. (1999). "Evaluating Finishes Using SERA." *PC FAB*, Vol. 22, No. 5, pp. 30-37.

Capillo, Carmen. (1990). *Surface Mount Technology*. McGraw-Hill: New York.

Clouthier, Richard S. (1999). "The Complete Solder Paste Printing Processes." *Guide to Soldering & Printing, Special Supplement to SMT*. p. 6 - 8.

Coleman, William E. (1996). "Stencil Design for Advanced Packages." *SMT*. June 1996.

Currie, Mark A. and Ekere, N. N. (1998). "Stencil Printing's Aperture Emptying SubProcess." *Circuits Assembly*. November 1998, p. 40 - 51.

Danielsson, Hans. (1995). Surface Mount Technology with Fine Pitch Components: the Manufacturing Issues. New York, Chapman & Hall.

Deen, William M. (1998). *Analysis of Transport Phenomena*. New York: Oxford University Press.

Ekere, N. N. and Lo, E. K. (1991). "New Challenges in Solder Paste Printing." *Journal of Electronics Manufacturing*. Vol. 1, p. 29 - 40.

Ekere, N. N.; Ismail I.; Lo, E. K.; and Mannan, S. H. (1993). "Experimental Study of Stencil/Substrate Separation Speed in On-contact Solder Paste Printing for Reflow Soldering." *Journal of Electronics Manufacturing*. Vol. 3, p. 25 - 29.

Elias, Russell J. (1996), "Statistical Process Control for Semiconductor Metrology Systems." *Semiconductor International*, pp. 167-172, October 1996.

Ewanich, Jay. (1997). "BGA vs. QFP". *Advancing Packaging*, Sept./Oct. 1997, p.28-32.

Reproduced with permission of the copyright owner. Further reproduction prohibited without permission.

Fujiuchi, Shin'ichi and Toriyama, Kazushige. (1994). "Collective Screen Printing for Carrier Bump and SMT Pads." *Proceedings of IEEE/CPMT International Electronics Manufacturing Technology Symposium*. p. 109 - 112.

Grasso, James. (1994). "Electrical Test of Bare Fine Pitch Printed Circuit Boards." *Handbook of Fine Pitch Surface Mount Technology*. Edit by Lau, John H., New York, Van Nostrand Reinhold.

Haider, Syed E., Wang, Faa-Ching, Capps, John, and Price, Ron (1995), "Metrology Control for an Advanced 200 mm Sub-Micron Wafer Fab." *Proceedings of the 17th IEEE/CPMT International Electronics Manufacturing Technology Symposium*, Austin, TX, pp. 88-95, 1995.

Hall, Steve. (1997). "Efficiency Considerations in Electronics Assembly." *Circuit Assembly*. March 1997.

Hanrahan, T. F.; Monaghan, P. F.; and Babikian, R. D. (1992). "Modeling of a Solder Paste Flow with a Free Surface in Stencil Printing." *Advances in Electronic Packaging, Proceedings of the 1992 joint ASME/JSME conference on Electronic Packaging*. p. 587 - 592.

Holden, Happy. (1998). "Matching Printed Circuit Board Characteristics to Advanced Area-Array Component." *Advancing Microelectronics*, Vol. 25, No. 6, p. 18-19.

Hobby, Alen. (1999). "Step-by-Step SMT: Printing." *SMT*, Vol. 13, No, 4, p. 66-74.

Hutchins, Charles I. (1995). Mastering & Implementing BGA Technology. AEIC.

Hutchins, Charles I. (1996). Understanding and Using Surface Mount and Fine Pitch Technology - Including Ball Grid Array. SMTnet.

Hwang, Jennie S. (1989). *Solder Paste in Electronics Packaging*. New York, Van Nostrand Reinhold.

Lathrop, Richard R., Jr. (1997). "Solder Paste Print Qualification Using Laser Triangulation." *IEEE Transactions on Components, Hybrids, and Manufacturing Technology - Part C*. Vol. 20, No. 3, p. 174 - 182.

Lau, John H. (1994). *Handbook of Fine Pitch Surface Mount Technology*. New York, Van Nostrand Reinhold, Chapter 1.

Lau, John. (1996). *Flip Chip Technologies*, McGraw-Hill, New York.

Lau, John; Wong, C. P.; Prince, John L.; and Nakayama, Wataru. (1998). *Electronic Packaging Design, Materials, Process, and Reliability*. McGraw-Hill, New York.

Reproduced with permission of the copyright owner. Further reproduction prohibited without permission.

Landers, T. L.; Brown, W. D.; Fant, E. W.; Malstron, E. M.; Schmitt, N. M. (1994). *Electronics Manufacturing Processes*. Prentice Hall, New Jersey.

Li, Y.; Mahajan, R. L.; and Nikmanesh, N. (1996). "Fine Pitch Stencil Printing Process Modeling and Optimization." *Journal of Electronic Packaging*. Vol. 118, p. 1 - 6.

Lideen, Jamey D. and Dahl, Arthur O. (1994). "Printing Techniques for Fine Pitch Screen Printing." *Proceedings of the Technical Program - NEPCON West*. p. 1862 - 1877.

Mannan, S. H.; Ekere, N. N.; Ismail, I.; and Lo, E. K. (1994). "Squeegee Deformation Study in the Stencil Printing of Solder Pastes." *IEEE Transactions on Components, Hybrids, and Manufacturing Technology - Part A*, Vol. 17, No. 3, p. 470 - 475.

Mannan, S. H.; Ekere, N. N.; Ismail, I.; and Currie, M.A. (1995). "Flow Processes in Solder Paste During Stencil Printing for SMT Assembly." *Journal of Materials Science: Materials in Electronics*, Vol. 6, p. 34 - 42.

Markstein, Howard W. (1997). "Controlling the Variables in Stencil Printing." *Electronic Packaging & Production*. Vol. 37, No. 2, p. 48 - 56.

Melendez, Carlos A. (1999), "Characterizing and Controlling the Process." *SMT (Special supplement: Guide to Soldering & Printing)*, pp. 9-10, January 1999.

Miller, L. F. (1969). "Paste Transfer in the Screening Process." *Solid State Technology*, June 1969, p. 46– 52.

Miric, A. Z. (1995). "High Quality Solder Pastes: Printing and Soldering in the World of Fine Pitch." *Soldering & Surface Mount Technology*. No. 21. p. 26-29.

Moffatt, H.K. (1964). "Viscous and Resistive Eddies Near a Sharp Corner." *Journal of Fluid Mechanics*. Vol. 18, p. 1 -18.

Monaghan, K.; Head, L.; Sahay, C.; and Constable, J. (1995). "Analysis of the Effects of Interior Aperture Angle on Print Quality in Solder Paste Stenciling." *Materials Research Society Symposia Proceedings*. V. 390, p. 213 -218.

Montgomery, Douglas C. and Runger, George C. (1993a), "Gauge Capability and Designed Experiments. Part I: Basic methods." *Quality Engineering*, Vol. 6, No. 1, pp. 115-135.

Montgomery, Douglas C. and Runger, George C. (1993b), "Gauge Capability and Designed Experiments. Part II: Experimental Design Models and Variance Component Estimation." *Quality Engineering*, Vol. 6, No. 2, pp. 289-305, 1993.

Reproduced with permission of the copyright owner. Further reproduction prohibited without permission.

Montgomery, Douglas C. (1997). *Design and Analysis of Experiments (4th ed.).* John Wiley & Sons, New York.

Morris, John R. and Wojcik, Thaddeus. (1991). "Stencil Printing of Solder Paste for Fine Pitch Surface Mount Assembly." *IEEE Transactions on Components, Hybrids, and Manufacturing Technology.* Vol. 14, No. 3, p. 560 - 566.

Morris, John R. and Wojcik, Thaddeus. (1994). "Screen and Stencil Printing Technology for Fine-Pitch Assembly." *Handbook of Fine Pitch Surface Mount Assembly.* Edited by Lau, John H. New York, Van Nostrand Reinhold. Chapter 6.

Newsome, Robert. (1998). "Meeting the increasing Demands of Assembling Advanced Packages". *Electronic Packaging & Production.* January, 1998.

Owczarek, Jerzy A. and Howland, Frank L. (1990a). "A Study of the Off-contact Screen Printing Process -- Part I: Model of the Printing Process and Some Results Derived From Experiments." *IEEE Transactions on Components, Hybrids, and Manufacturing Technology.* Vol. 13, No. 2, p. 358 - 367.

Owczarek, Jerzy A. and Howland, Frank L. (1990b). "A study of the Off-contact Screen Printing Process -- Part II: Analysis of the Model of the Printing Process." *IEEE Transactions on Components, Hybrids, and Manufacturing Technology.* Vol. 13, No. 2, p. 368 - 375.

Pan, Jianbiao and Tonkay, Gregory (1999), "A Study of Solder Paste Deposition Process in the Stencil Printing." *Proceedings of the 1999 ASME International Mechanical Engineering Congress and Exposition: Electronics Manufacturing Issues,* Nashville, Tennessee, November 14-19, 1999, pp. 75-82.

Pan, Jianbiao; Gregory Tonkay, Robert Storer, Ron Sallade, and David Leandri (1999a), "Critical Variables of Solder Paste Stencil Printing for micro-BGA and Fine Pitch QFP." *Proceedings of the 24th IEEE/CPMT International Electronics Manufacturing Technology (IEMT) Symposium,* Austin, TX, October 18-20, 1999, pp. 94-101.

Pan, Jianbiao; Gregory Tonkay, Robert Storer, Ron Sallade, and David Leandri (1999b), "Gauge Repeatability & Reproducibility Study for a 3-D Solder Paste Inspection System." *Proceedings of the 1999 International Symposium of Microelectronics (IMAPS'99),* Chicago, Illinois, October 26-28, 1999, pp. 532-537.

Pan, Jianbiao; Gregory Tonkay, Robert Storer, Ron Sallade, and David Leandri (1999c), "Experimental Study of Solder Paste Stencil Printing for Fine Pitch and Ultra-Fine Pitch QFP and BGA." *Proceedings of 13th Conference with Industry: Competing in a Global Manufacturing Environment,* Lehigh University, May 24 & 25, 1999, pp. 59-66.

Reproduced with permission of the copyright owner. Further reproduction prohibited without permission.

Pan, Jianbiao; Tonkay, Gregory L.; and Quitero, Alejandro. (1998). "Screen Printing Process Design of Experiments for Fine Line Printing of Thick Film Ceramic Substrates." *Proceedings of IMAPS'98*, San Diego, CA. p. 264 - 269.

Parikh, Mayank R.; Quilty, William F, Jr.; and Gardiner, Keith M. (1991). "SPC ans setup analysis for screen printed thick films." *IEEE Transactions on Components, Hybrids, and Manufacturing Technology.* Vol. 14, No. 3, p. 493 – 498.

Riemer, Dietrich E. (1987). "The Shear and Flow Experience of Ink During Screen." *Proceedings of the International Symposium on Microelectronics (ISHM'87)*, p. 335-340.

Riemer, Dietrich E. (1988a). "Analytical Engineering Model of the Screen Printing Process: Part I." *Solid State Technology*, August 1988, p. 107 - 111.

Riemer, Dietrich E. (1988b). "Analytical Engineering Model of the Screen Printing Process: Part II." *Solid State Technology*, September 1988. p. 85 - 90.

Riemer, Dietrich E. (1989). "Screen Printing Process Theory." *Microelectronic Packaging Technology Materials and Processes.* Edited by Wei T. Shieh, ASM International.

Roscoe, R. (1949). "The Flow of Viscous Fluids Round Plane Obstacles." *Philosophical Magazine.* Vol. 40, No. 302, p. 338 - 351.

Sahay, C.; Head, L. M.; Shereen, R.; Dujari, P.; Constable, J. H.; and Westby, G. (1995). "Study of Print Release Process in Solder Paste Printing." *Journal of Electronic Packaging.* Vol. 117, p. 230 - 234.

Shaw, Robert and Devos, John. (1998). "Time for a PTH to SMT Conversion." *SMT.* Vol. 12, No.9, p.68-69.

Seto, P., Evans, J. and Bishop, S., (1999). "Analysis of the Palladium Finish." *SMT*, Vol. 13, No. 6, pp. 60-63.

Svetkoff, D. J., D. N. Smith, and B. L. Doss (1987), "Automatic Inspection of Component Board Using 3-D and Greyscale Vision." *Hybrid Circuits*, No. 13, May 1987.

Taylor, Greffrey. (1960). "Similarity Solutions of Hydrodynamic Problems." *Aeronautic and Astronautics.* Vol. 4, p. 21 - 28.

Trinite, George. (1999). "Importance of Board Planarity." *Guide to Soldering & Printing, Special Supplement to SMT.* p. 12-13.

Reproduced with permission of the copyright owner. Further reproduction prohibited without permission.

Vardaman, Jan. (1997). "What Does a CSP Cost." *Guide to Emerging Technologies, special supplement to Advanced Packaging.* July/August 1997, p. 3 – 4.

Vardaman, Jan (1998). "Market Drives and Trends for High I/O Packages", *Circuit Assembly*, Vol. 9, No. 2.

White, Frank M. (1991). *Viscous Fluid Flow*, 2nd edition, New York, McGraw-Hall.

Whitmore, Mark; Mackay, Colin; and Hobby, Alan. (1997). "Plastic Stencils for Bottom-Side Chip Attach." *Electronic Packaging & Production.* Vol. 37, No. 13, p. 68 - 72.

Wilson, Tony and Bloomfield, David. (1995). "An Optimistic Outlook for Ultra Fine Pitch (Part I)." *Electronic Production.* February 1995. p. 39 - 42.

Wilson, Tony and Bloomfield, David. (1995). "An Optimistic Outlook for Ultra Fine Pitch (Part II)." *Electronic Production.* March 1995. p. 83 - 86.

Xiao, M.; Lawless, K. J.; and Lee, N. -C. (1993). "Prospects of Solder Paste in the Ultra Fine Pitch Era." *Soldering & Surface Mount Technology.* No. 15. p. 4 – 13.

Reproduced with permission of the copyright owner. Further reproduction prohibited without permission.

Vita

Jianbiao Pan was born in Zhejiang province, P. R. China on February 28, 1968. He received his B.S. degree in Mechatronics from Xidian University, Xian, P. R. China in July 1990, and the M.S. degree in Manufacturing from Tsinghua University, Beijing, P. R. China in July 1996. During the period of August 1990 to August 1993, he worked in Changfeng Industry Group as a Mechanical Engineer and Project Director. He is pursuing the Ph.D. degree in Department of Industrial and Manufacturing Systems Engineering at Lehigh University, with an expected date of completion in May 2000. He has received many awards during studying and working including Outstanding Student Scholarship from Xidian University and Tsinghua University, Fellowship from Lehigh University, Innovation and Invention Prize, and Third Award for Best Paper from Changfeng Industry Group, and First Prize for Student Poster from IMAPS Keystone Chapter.

Jianbiao Pan's research interests are in modeling and process optimization of electronics manufacturing processes, quality control, CAD/CAPP/CAM, and mechanical design and analysis. His dissertation is on Modeling and Process Optimization of Solder Paste Stencil Printing for Fine Pitch Surface Mount Assembly under guidance by Professor Gregory L. Tonkay. He has developed an integrated CAPP/CAM system for automobile transmission shafts at Tangshan Gear Plant, China, a joint venture of Toyota. He designed a precision adjuster using AutoCAD and directed several projects involved in electro-mechanical product design, manufacture, and assembly. He has published 8

Reproduced with permission of the copyright owner. Further reproduction prohibited without permission.

technical papers in journals and international conferences. He is a member of IEEE, SME, and IMAPS. He was the chair of SME Lehigh University Student Chapter in 1997-1998 and received the Outstanding Student Officer Award from SME Region 3 in 1998.

Reproduced with permission of the copyright owner. Further reproduction prohibited without permission.